Extremely Large Aperture Array (ELAA) Communications: Foundations, Research Advances and Challenges

SICONG YE [1] (Member, IEEE), MING XIAO [1] (Senior Member, IEEE),
MAN-WAI KWAN[2] (Senior Member, IEEE), ZHENG MA [3] (Member, IEEE),
YONGMING HUANG [4] (Senior Member, IEEE), GEORGE KARAGIANNIDIS [5,6] (Fellow, IEEE),
AND PINGZHI FAN [3] (Life Fellow, IEEE)

(Invited Paper)

[1]Division of Information Science and Engineering, KTH Royal Institute of Technology, 100 44 Stockholm, Sweden
[2]Stockholm Research Center, Huawei Technologies Sweden AB, 164 40 Kista, Sweden
[3]Provincial Key Laboratory of Information Coding and Transmission, Southwest Jiaotong University, Chengdu 611756, China
[4]National Mobile Communication Research Laboratory, School of Information Science and Engineering, Southeast University, Nanjing 210096, China
[5]Department of Electrical and Computer Engineering, Aristotle University of Thessaloniki, 54124 Thessaloniki, Greece
[6]Artificial Intelligence and Cyber Systems Research Center, Lebanese American University, Beirut 03797751, Lebanon

CORRESPONDING AUTHOR: M. XIAO (e-mail: mingx@kth.se)

ABSTRACT Extremely large aperture array (ELAA) represents a paradigm shift in wireless antenna systems, poised to redefine the capabilities of future networks, particularly in the era of the sixth generation (6G) networks. The integration of multiple-input multiple-output (MIMO) technology with an unprecedented scale of antenna arrays enables transformative potential for enhancing spectral efficiency, increasing coverage, and enabling new applications. This paper provides a comprehensive overview of ELAA, delving into fundamental concepts, state-of-the-art technologies, and practical applications. We commence by presenting the fundamentals of ELAA technology, focusing on the various architectural categories and two fundamental properties of communication in the near-field region of ELAA, namely spherical wave propagation and channel spatial non-stationarity. We then illustrate the phenomenon of finite beam depth in the near field before presenting general distance boundaries based on various criteria and conducting a comprehensive performance analysis of this technology. Subsequently, in light of the distinctive electromagnetic characteristics of ELAA, we will examine the practical challenges that have emerged, including channel estimation, beamforming design, and the practical hardware issues that have arisen. Subsequently, we examine the diverse applications of ELAA across various domains, emphasizing its transformative potential in fields such as physical layer security, communication and sensing, and wireless power and information transfer. Finally, the paper concludes by outlining several promising avenues for future research and exploration within the realm of ELAA. These avenues are identified as areas ripe for investigation and innovation.

INDEX TERMS Extremely large aperture array, extremely large-scale multiple-input-multiple-output, near-field communication, channel modelling, signal processing.

I. INTRODUCTION

A. BACKGROUND

THE FIFTH generation (5G) of mobile communications represents a transformational leap in telecommunications technologies, driven by the growing demands and challenges of our increasingly connected world (people and devices). Building on the foundations laid by previous generations of mobile communications, from 1G to 4G, 5G has played a pivotal role in shaping mobile communications, with 4G in particular introducing mobile Internet applications. However, the explosive growth of data-intensive applications such as video streaming, Internet of Things (IoT) devices, and augmented reality (AR) has exposed the limitations of 4G mobile networks. As a result, 5G networks are poised to deliver on the promise of ubiquitous connectivity with unprecedented speeds, low latency and reliability. The potential use cases for 5G, including enhanced mobile broadband (eMBB), massive machine type communications (mMTC), and ultra-reliable low latency communications (URLLC), have been extensively studied [1]. With the maturity and imminent commercialization of 5G, the development of sixth-generation (6G) mobile networks has received considerable attention. Research into 6G mobile networks, as envisaged in initiatives such as International Mobile Telecommunications 2030 (IMT-2030) and Network 2030, has been included in the agenda to meet the demands of the intelligent information society expected by 2030 [2], [3].

In 2023, the IMT Body agreed on a draft of a new Recommendation entitled "Framework and overall objectives for the future development of IMT for 2030 and beyond". This document serves as the basis for standardization efforts to develop the next generation of IMT standards. It defines six deployment scenarios, including three extensions of IMT-2020 in 5G - immersive communication, massive communication, and hyper-reliable & low-latency communication - and three new scenarios: ubiquitous connectivity, AI and communication, and integrated sensing and communication (ISAC). 6G mobile networks are expected to enable breakthrough applications such as holographic video and digital twins. Achieving these advances requires extensive research to develop new wireless technologies that meet the Key Performance Indicators (KPIs) established for 6G, which represent a significant leap in network capabilities compared to 5G. The capabilities of IMT-2030 are detailed, including nine enhanced capabilities and six new capabilities. For example, connection density is expected to increase tenfold and latency is expected to drop to as low as 0.1ms. Leveraging the benefits of multiple-input, multiple-output (MIMO) technology is critical to meeting these stringent requirements, such as improved spectrum efficiency, reliability and connection density.

B. BASICS OF MULTI-ANTENNA TECHNOLOGY

Cooper's Law, named after wireless researcher Martin Cooper, encapsulates the exponential growth of wireless voice and data communications over several decades [4].

Three primary methods are typically employed to improve the efficiency of wireless networks: denser access point deployment, increased spectrum allocation, and improved spectral efficiency. While future wireless systems are expected to utilize denser access points and new spectral bands, maximizing spectral efficiency within existing bandwidth allocations remains critical. Multiple-input multiple-output (MIMO) technology offers a promising way to increase spectral efficiency to meet the growing demand for wireless connectivity.

The integration of multiple antennas at both the transmitter and receiver introduces a paradigm shift and provides several advantages over traditional single-antenna systems. These benefits can be broadly categorized into three main aspects: beamforming gain, spatial multiplexing, and spatial diversity.

1) BEAMFORMING GAIN

Historically, wireless telegraphy systems paved the way for modern telecommunications by enabling long-distance communication without physical wires. These systems relied on electromagnetic wave propagation principles and specialized equipment like antennas, transmitters, and receivers. The classical Friis' transmission formula [5] provides insights into received power (P_r) in free space for single-input, single-output (SISO) antenna systems:

$$P_r = \frac{G_t G_r \lambda^2}{(4\pi d)^2} P_t, \tag{1}$$

where P_t, G_t, G_r, λ, and d denote transmit power, antenna gains for transmitter and receiver, wavelength, and distance between antennas, respectively. Beamforming gain involves the strategic manipulation of transmitted signals to concentrate energy in specific directions, thereby improving signal strength and reception quality. Multiple antennas accomplish this by aggregating transmitted signals, similar to the emission from a single "virtual" antenna with high directivity, with an antenna gain M times greater than that of individual antennas.

Consider a uniform linear array (ULA), shown in Fig. 1(a), consisting of $M = 7$ isotropic antennas equally spaced along a straight line. When all antennas transmit simultaneously, each emitted signal component radiates similarly to the single-antenna case. Consequently, there is a superposition of M signal components at each spatial point, with different transmission paths causing different time delays. In the far-field region, where the propagation distance greatly exceeds the antenna spacing, beamforming concentrates signals in specific directions, thereby increasing the received signal power. This beamforming gain offers the potential to achieve SNR M times higher than single-antenna scenarios while maintaining the same transmit power.

2) SPATIAL MULTIPLEXING

Spatial multiplexing revolutionizes wireless communications by transmitting multiple independent data streams
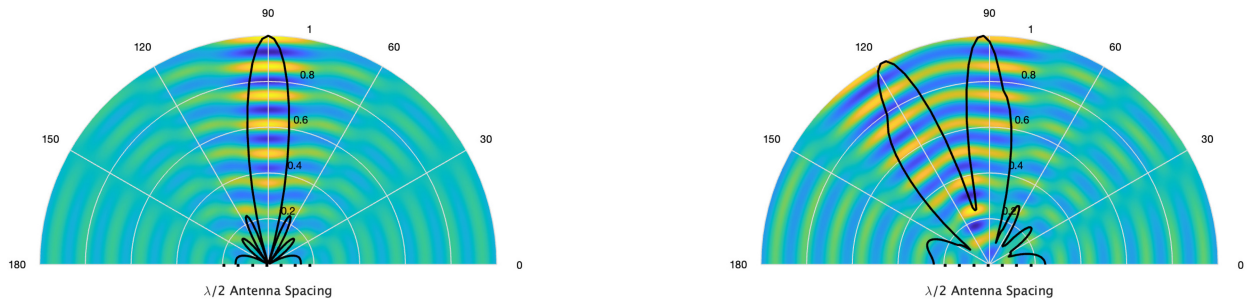
(a) The beam pattern and signal power in different directions and at different distances.

(b) The beam pattern and signal power of spatial multiplexing where two user equipment (UEs) are served at direction 90° and 120°.

FIGURE 1. The beam pattern and signal power in difference directions and at different distances from $M = 7$ isotropic antennas..

simultaneously over the same frequency band. Unlike traditional methods that allocate non-overlapping time-frequency resources to multiplex users, spatial multiplexing uses spatial dimensions to differentiate between users. With multiple antennas, each signal can have different spatial directivity, minimizing interference between users located outside of each other's main lobe. This technique allows multiple users to efficiently share time and frequency resources, increasing data rates linearly with the number of users.

In Fig. 1(b), two users situated at 90° and 120° illustrate spatial multiplexing. Optimizing beamforming maximizes the SINR by balancing signal strength and interference reduction, ensuring reliable communication.

3) SPATIAL DIVERSITY

Multiple antennas significantly improve the reliability of communication systems by mitigating the fading effects of multipath propagation. Spatial diversity uses the spatial separation between antennas to provide redundant paths for signal transmission, thereby improving link robustness. By adjusting antenna configurations and exploiting the differences in fading experienced by each antenna, spatial diversity improves communications reliability in challenging environments. The use of spatial diversity continuously mitigates the effects of fading, ensuring reliable communications.

C. EXTREMELY LARGE APERTURE ARRAY

Among many others, massive multiple-input, multiple-output (mMIMO) is one of the key technologies that has been integrated into 5G wireless networks. mMIMO involves deploying a large number of antennas at the base station, allowing for simultaneous communication with multiple users by spatially multiplexing their signals. This technology significantly enhances the spectral efficiency and capacity of 5G networks, enabling faster data rates and improved network performance. mMIMO in 5G leverages advanced signal processing and beamforming to achieve better signal quality and coverage, making it a crucial component in meeting the demands of high-speed mobile broadband and the IoT applications.

To further improve performance in various 6G use cases, researchers are exploring the feasibility of increasing the number of antenna arrays. First, mMIMO systems in which antenna arrays are equipped with a large number of antennas at both the transmitter and receiver side hold promise for transmitting multiple parallel data streams thanks to multiplexing gain and beamforming gain. In particular, the spatial resolution of an array is not determined by the number of antennas, but by the array aperture. Thus, it is generally advantageous to spread the antennas rather than to place an extremely large number of antennas in a compact space where the antenna spacing is less than the order of the wavelength. Second, high frequency bands such as millimeter wave (mmWave) and terahertz (THz) can provide abundant spectral resources to support high data rates. It is worth noting that antenna size is inversely proportional to frequency. Therefore, the use of high frequency bands allows more antennas to be used in arrays. Systems with a large number of antenna elements, often in the order of thousands or more, are often referred to as extremely large aperture array (ELAA) [6], [7], also known as extra-large massive MIMO (XL-MIMO) in the literature. As defined in [6], an ELAA consists of hundreds of distributed BS antennas that jointly and coherently serve a large number of distributed users.

D. RELATED ARTICLES

In the field of ELAA technologies, a wealth of related studies has been published. These works explore various aspects from fundamental principles to advanced applications. A comparative summary of these articles, highlighting their contributions and limitations, is provided in Table 1. A comprehensive understanding of existing research on ELAA is important for contextualizing our work and identifying gaps and areas for further work. Several studies have focused on Holographic MIMO (HMIMO) communications [8], [9], [10], [11], [12], providing detailed overviews of the latest advances in HMIMO communications. In [8], the authors reviewed various emerging HMIMO architectures, discussed their core functionalities, and examined current communication applications as well as future networking

TABLE 1. Comparisons between related articles.

Ref.	Major contributions	Main limitations
[8]	• Provide an overview of HMIMO communications, focusing on architectures and functionalities. • Discuss the currently applications as well as future networking challenges.	• Primarily concentrate on theoretical aspects of HMIMO, without delving deeply into the unique characteristics and advantages specific to ELAA (Extra-Large Aperture Antenna) systems. • Do not thoroughly address the practical aspects of hardware deployment and architectural challenges associated with large-scale antenna arrays.
[9]	• Overview the physical aspects of HMIMO surfaces, including hardware structures, holographic design methodologies, tuning mechanisms, aperture shapes, and typical functionalities with such surfaces. • Theoretical foundations, latest progress about signal processing schemes, and comparison with mMIMO in HMIMO communications are provided. • Provide various research challenges and future directions.	
[10]–[12]	• Comprehensive tutorial providing an overview of the latest advances in HMIMO communications, including channel modeling and channel estimation, performance analysis, and beamforming techniques. • Highlight the open challenges and opportunities in HMIMO communications, as well as the interplay with other emerging technologies.	
[13]	• Discuss the difference between near-field and far-field communications in four perspectives: channel modeling, performance evaluation, beamforming techniques, and potential applications.	• Primarily concentrates on near-field communications and spherical waveform-related signal processing, with limited exploration of other critical aspects like spatial non-stationarity. • Lacks detailed discussion on the architectural and deployment considerations essential for near-field communication systems. • Does not cover more advanced near-field signal processing techniques, such as wavefront engineering, especially relevant at higher frequency bands.
[14]	• Explore the fundamental physical characteristics of near-field communications, detailing the spherical wave properties, near-field channel models, and the potential advantages of near-field beam focusing. • Highlight several promising applications that could greatly benefit from these near-field communication techniques.	
[15]	• Examine the key features of the near-field region in THz frequency bands. • Provide an in-depth analysis of how near-field effects impact both communication and sensing in the THz band. • Emphasize the major opportunities and challenges associated with THz near-field communications and sensing.	
[16]	• Contribute a comprehensive review that discusses the fundamental principles of near-field communications • Provides a comprehensive analysis of deterministic and stochastic near-field channel models, alongside a detailed evaluation of performance. • Existing signal processing methods for near-field communication, including channel estimation, beamforming design, and efficient beam training strategies are discussed.	
[17]	• Discusses near-field channel modeling with spherical waves and spatial non-stationarity. • Analyzes performance based on near-field models. • Reviews signal processing issues: beam codebook design, beam training, channel estimation, delay alignment modulation.	• Lacks a thorough review of fundamental aspects, including near-field boundaries and region definitions. • Lacks coverage of new wavefront engineering techniques and practical low-complexity algorithms.
[18]	• Summarizes system implementation and antenna characteristics for four ELAA hardware designs. • Provides tutorials on near-field channel modeling. • Reviews low-complexity signal processing and deep learning-based methods.	

challenges. They emphasized the potential of HMIMO systems to revolutionize wireless communications through their ability to dynamically shape electromagnetic fields, thereby providing greater flexibility and efficiency in signal transmission. In addition, [9] focused specifically on the physical aspects of HMIMO, delving into their theoretical foundations and exploring the enabling technologies for HMIMO systems. This comprehensive review sheds light on

the underlying principles of HMIMO operation and provides insight into the design considerations for implementing such systems in practical scenarios. In addition, [10], [11], [12] provided an overview of HMIMO communications, focusing on various aspects such as channel modeling and estimation, performance analysis, beamforming techniques, and opportunities and challenges associated with HMIMO deployment. These studies delve into the intricacies of HMIMO systems, discussing topics ranging from efficient beamforming algorithms to the impact of channel conditions on system performance. While these studies focus primarily on HMIMO as an alternative deployment to achieve large numbers of antennas, our article focuses primarily on the fundamentals and challenges associated with large aperture arrays. Although we will mention the concept of HMIMO and (approximately) continuous aperture (CAP) arrays, our primary goal is to explore the unique characteristics and potential applications of ELAA in next-generation wireless communication systems.

Near-field communication has been a subject of interest in recent research [13], [14], [15]. The authors in [13] explores the fundamental differences between spherical wave-based near-field communications and traditional plane-wave-based far-field communications. This exploration encompasses several dimensions, including channel modeling, performance evaluation, beamforming techniques, and potential applications. Reference [14] explored the fundamental physical characteristics of near-field communications, detailing the spherical wave properties, near-field channel models, and the potential advantages of near-field beam focusing. They also highlighted several promising applications that could greatly benefit from these near-field communication techniques. In addition to exploring the primary attributes of near-field communication within the THz frequency range, [15] delves into the enhanced sensing capabilities offered by near-field conditions. The paper provides insights into how near-field sensing can leverage high-frequency THz bands to achieve improved accuracy and resolution, highlighting the advancements in both communication and sensing technologies in this challenging spectrum. Together, these works provide valuable insights into the evolving landscape of near-field communication technology and its diverse applications in modern communication systems. In addition, [16] contributes a comprehensive review that discusses the fundamental principles of near-field communication, with particular emphasis on channel modeling, performance metrics, signal processing methods, and integration strategies with other emerging technologies. Specifically, The review distinguishes the fundamental principles of near-field communications from those of far-field communications, examining both physical and communication aspects to reveal their unique characteristics. It provides a comprehensive analysis of deterministic and stochastic near-field channel models, alongside a detailed evaluation of performance. The survey also covers existing signal processing methods for near-field communication, including channel estimation, beamforming design, and

efficient beam training strategies. These works provide a thorough examination of near-field communication, covering everything from the fundamental physical properties of spherical waves to channel modeling and signal processing techniques like beamfocusing. However, they primarily concentrate on near-field communications and the associated signal processing challenges, particularly concerning spherical waveforms. Other critical aspects of near-field channels, such as spatial non-stationarity, are not explored or discussed in detail. Additionally, there is a noticeable lack of focus on the architectural considerations and deployment strategies necessary for effective near-field communication systems. Moreover, these works do not delve into more advanced near-field signal processing techniques, such as wavefront engineering, which become increasingly important as communication moves into higher frequency bands.

Several comprehensive tutorials on near-field ELAA have been published, notably in [17], [18]. In [17], the authors explore new design challenges, focusing on aspects such as near-field channel modeling, performance analysis, channel estimation, and practical implementation. The tutorial begins by establishing a fundamental near-field model that incorporates the unique characteristics of spherical waves and spatial non-stationarity. Building on this model, the performance analysis is presented, followed by a detailed examination of various signal processing issues, including near-field beam codebook design, beam training, channel estimation, and delay alignment modulation transmission. Meanwhile, [18] provides a comprehensive summary of system implementation features and antenna characteristics across four different ELAA hardware designs. This tutorial also offers extensive guidance on near-field channel modeling and reviews low-complexity and deep learning-empowered signal processing schemes, highlighting their potential to facilitate practical implementation. However, compared to our work, these studies fall short in providing a thorough overview of the fundamental aspects of this technology, such as a detailed examination of near-field boundaries and region definitions. Moreover, they do not sufficiently address some of the latest challenges, practical implementation issues, and recent advancements. For instance, while beamfocusing techniques are discussed, there is a lack of coverage on emerging wavefront engineering approaches in near-field communication, especially at high-frequency bands. Additionally, the exploration of advanced hardware solutions and the development of low-complexity algorithms for practical deployment are not adequately addressed.

E. OUR CONTRIBUTIONS

To this end, a comprehensive review on ELAA is presented in this article[1]. The major contributions of our paper can be summarized as follows:

---

[1]We mainly focus on array systems with large aperture instead of densely packed (approximately continuous) antenna array, such as holographic MIMO [8], [9], [10], [11], [12], [19], [20].
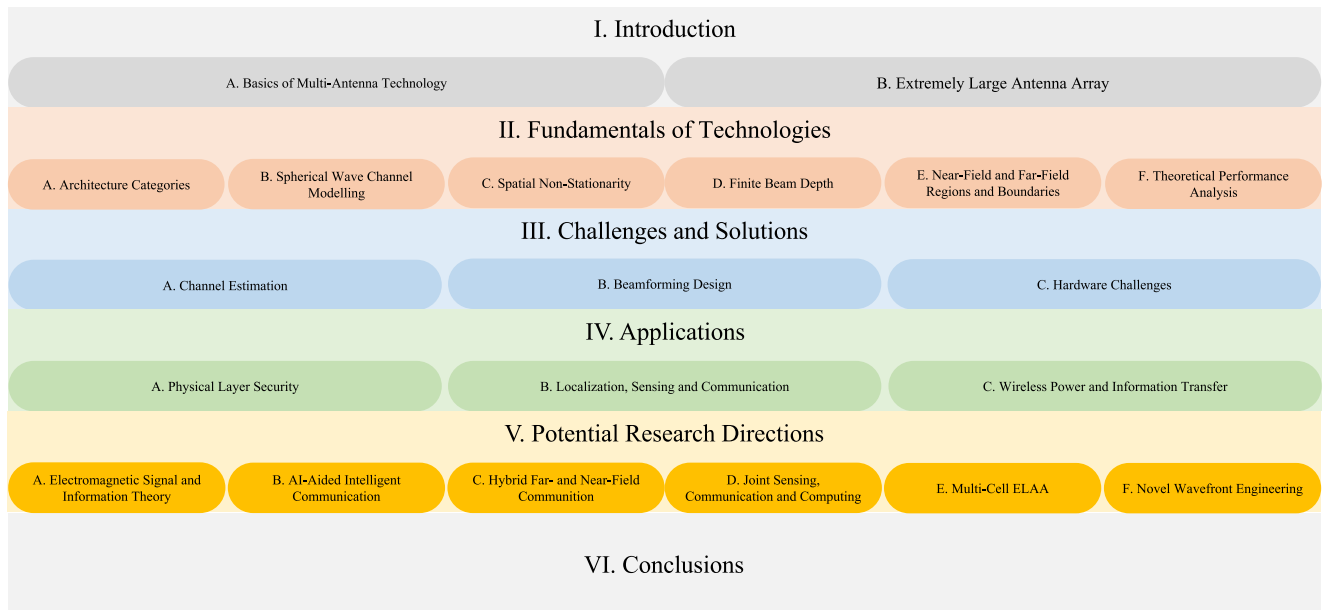
I. Introduction		
A. Basics of Multi-Antenna Technology		B. Extremely Large Antenna Array

II. Fundamentals of Technologies

A. Architecture Categories	B. Spherical Wave Channel Modelling	C. Spatial Non-Stationarity	D. Finite Beam Depth	E. Near-Field and Far-Field Regions and Boundaries	F. Theoretical Performance Analysis

III. Challenges and Solutions

A. Channel Estimation	B. Beamforming Design	C. Hardware Challenges

IV. Applications

A. Physical Layer Security	B. Localization, Sensing and Communication	C. Wireless Power and Information Transfer

V. Potential Research Directions

A. Electromagnetic Signal and Information Theory	B. AI-Aided Intelligent Communication	C. Hybrid Far- and Near-Field Communion	D. Joint Sensing, Communication and Computing	E. Multi-Cell ELAA	F. Novel Wavefront Engineering

VI. Conclusions

FIGURE 2. The organization structure of the paper.

- We begin with an introduction to the basics of ELAA technology. In particular, we review different ELAA architectures based on differentiation criteria. Then, as the array aperture increases, two fundamental properties of near-field communications are discussed, namely spherical wave channel modelling and spatial non-stationarity. We then discuss the phenomenon of finite beam depth in the near field, a critical aspect that distinguishes it from traditional far-field communication setups. This is followed by a comprehensive discussion of the general regions and boundaries between the near-field and far-field based on various criteria. Finally, we provide a comprehensive performance analysis framework for the near-field channel model.
- We outline the challenges associated with ELAA technology and propose potential solutions found in the literature. In particular, we illustrate the challenges associated with channel estimation and discuss various techniques proposed in the literature for estimating spherical wave and spatially non-stationary channels. In addition, we examine beam focusing designs adapted to the finite beam depth phenomenon and also novel wavefront engineering at high-frequency bands in the near field. Finally, we review signal processing schemes for ELAA from the perspective of hardware challenges, including hybrid beamforming, low-complexity transceiver design, and the potential use of radio stripes.
- Finally, we explore the intricate interplay between ELAA and advanced technologies, envisioning their collaborative potential to revolutionize various domains. By exploring the fusion of ELAA with advances in physical layer security, integration of localization, sensing, and communication, we highlight the synergistic

possibilities with ELAA technology. By identifying key research opportunities within the ELAA landscape, we uncover rich potential in areas such as electromagnetic signal and information theory, AI-based intelligent communication, hybrid far-field and near-field communication, integration of sensing, communication, and computing, multi-cell ELAA, and wavefront engineering. By highlighting these research avenues, we aim to inspire and guide future efforts to realize the full potential of ELAA technology.

F. ORGANIZATION

The remainder of this paper is structured as follows. Section II presents the fundamentals of ELAA technologies. In Section III, challenges related to ELAA and potential solutions in the literature, involving channel estimation, beam focusing design and hardware design are introduced. The applications of ELAA integrated with other emerging technologies are discussed in Section IV. Finally, a series of potential research directions on ELAA are discussed in Section V and we conclude the this article in Section VI. Fig. 2 illustrates the organization of this article. Important abbreviations are summarized in Table 2.

II. FUNDAMENTALS OF ELAA TECHNOLOGIES

In this section, we discuss the fundamental aspects of ELAA technology. First, we provide an overview of ELAA architectures and categorize them in comparison to conventional mMIMO systems. We then examine how increasing the number of antennas and the array aperture fundamentally changes the electromagnetic (EM) characteristics of the system. This transformation leads to the emergence of distinct near-field properties unique to large aperture arrays, including
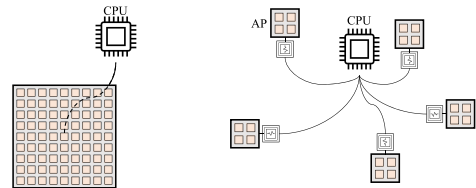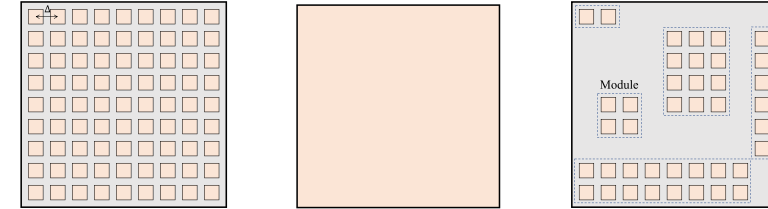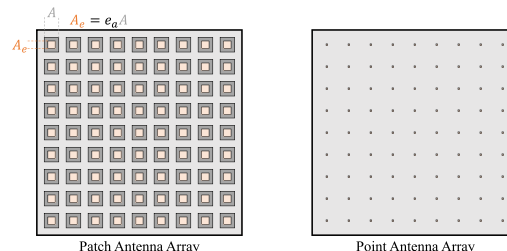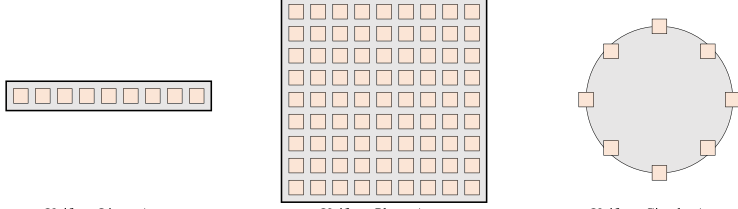
TABLE 2. List of Acronyms.

Explanation	Acronym	Explanation	Acronym
Access Point	AP	Location Division Multiple Access	LDMA
Adaptive Grouping Sparse Bayesian learning	AGSBL	Magnetic Field	H-field
Analog-to-Digital Converters	ADC	Massive Machine Type Communications	mMTC
Angle of Arrival	AoA	Massive Multiple-Input Multiple-Output	mMIMO
Angle of Departure	AoD	Matched Filter	MF
Artificial Intelligence	AI	Maximum Ratio Combining	MRC
Base Station	BS	Maximum Ratio Transmission	MRT
Beam Depth	BD	Mean Square Error	MSE
Central Processing Unit	CPU	Millimeter Wave	mmWave
Channel State Information	CSI	Mismatch Model	MM
Cloud Radio Access Network	C-RAN	Mobile Station	MS
Compressive sensing	CS	Model-Mismatch Error	MME
Continuous Aperture	CAP	Multi-Objective Optimization Problems	MOOP
Convolutional Neural Network	CNN	Multiple-Input Multiple-Output	MIMO
Coordinated Multipoint	CoMP	Non-Line-of-Sight	NLoS
Correlation-Based Stochastic Model	CBSM	Non-Uniform Spherical Wave	NUSW
Cramér-Rao bound	CRB	Orbital Angular Momentum	OAM
Curvature of Arrival	CoA	Orthogonal Matching Pursuit	OMP
Deep Learning	DL	Physical Layer Security	PLS
Degrees-of-Freedom	DoF	Radio Frequency	RF
Depth-of-Focus	DF	Radio-Frequency Identification	RFID
Discrete Fourier transform	DFT	Receive	Rx
Distributed MIMO	D-MIMO	Reconfigurable Intelligent Surface	RIS
Effective Degrees of Freedom	EDoF	Single-Input Single-Output	SISO
Effective Multiplexing Distance	EMD	Signal-to-Interference-Plus-Noise Ratio	SINR
Electric Field	E-field	Signal-to-Noise Ratio	SNR
Electromagnetic	EM	Simultaneous Wireless Information and Power Transmission	SWIPT
Electromagnetic Propagation Modelling	EPM	Sixth Generation	6G
Electromagnetic Signal and Information Theory	ESIT	Spatially-Discrete	SPD
Energy Harvesting	EH	Spatial division multiple access	SDMA
Enhanced Mobile Broadband	eMBB	Spherical Wave Model	SWM
Extended Reality	XR	Spectral Efficiency	SE
Extra-Large Massive MIMO	XL-MIMO	Super-Resolution	SR
Extremely Large Aperture Array	ELAA	Terahertz	THz
Extremely Large-Scale Uniform Linear Array	XL-ULA	Three-Dimensional	3D
Fifth Generation	5G	Transmit	Tx
Generative Adversarial Network	GAN	True Model	TM
Generative Artificial Intelligence	GAI	Ultra Reliable and Low Latency Communication	URLLC
Geometry-Based Stochastic Models	GBSM	Uniform Circular Array	UCA
Group Time Block Code	GTBC	Uniform Linear Array	ULA
Holographic MIMO	HMIMO	Uniform Planar Array	UPA
Information Decoding	ID	Uniform Plane Waves	UPW
Integration of Sensing and Communication	ISAC	Uniform Rectangular Planar Array	URPA
International Mobile Telecommunications 2030	IMT-2030	Uniform Square Planar Array	USPA
Internet of Things	IoT	Uniform Spherical Wave	USW
International Mobile Telecommunications-Advanced	IMT-Advanced	User Equipment	UE
Joint Activity and Channel Estimation	JACE	Visibility Region	VR
Joint Communication, Sensing, and Computation	JCSC	Wide-Sense Stationary	WSS
Key Performance Indicator	KPI	Wireless Energy Transfer	WET
Large Intelligent Surface	LIS	Wireless Power Transfer	WPT
Learning Iterative Shrinkage and Threshold Algorithm	LISTA	Zero-Forcing	ZF
Line-of-Sight	LoS	Ziv-Zakai Bound	ZZB
Lower Bound	LB		

spherical wave propagation, spatial non-stationarity, and finite beam depth. These properties are not accounted for in conventional mMIMO systems operating in the far field. After examining these differences in EM characteristics, we outline boundaries that characterize the transition between the near-field and far-field regions based on various criteria. This delineation is essential for understanding the operational limitations and performance trade-offs of ELAA systems.

TABLE 3. ELAA architecture categories.

Category	Architecture
Element Distribution	Co-located Antenna Array Distributed Antenna Array
Antenna Spacing	Spatial Discrete Aperture Antenna Array Spatial Continuous Aperture Antenna Array Modular Antenna Array
Element Size	$A_e = e_a A$ Patch Antenna Array Point Antenna Array
Geometry	Uniform Linear Array Uniform Planar Array Uniform Circular Array

Finally, we provide a comprehensive theoretical performance analysis focused on near-field communications. By studying the intricacies of near-field EM propagation, we aim to shed light on the potential benefits and challenges associated with deploying ELAA systems in practical scenarios.

A. ARCHITECTURE CATEGORIES

The architecture of ELAA is critical to the capabilities and performance of future wireless communications systems. ELAA represents a paradigm shift in antenna design, characterized by the use of large arrays of hundreds or even thousands of antenna elements. Unlike conventional antenna arrays, ELAA exploits the principles of near-field communication, where the distance between the transmitter and receiver is comparable to the wavelength of the transmitted signal. The large aperture enables ELAA to capture rich spatial information, facilitate beamforming and

support massive MIMO configurations, thereby increasing system capacity and spectral efficiency. In addition, ELAA's architectural design incorporates various components such as radio frequency (RF) chains, signal processing units, and beamforming algorithms, all of which work synergistically to optimize communications performance. The architectural intricacies of ELAA are discussed under four aspects: antenna array distribution, antenna spacing, antenna element size modelling, and array geometry. The characteristics of these hardware elements are summarized in the Table 3.

1) ANTENNA ARRAY DISTRIBUTION: CO-LOCATED AND DISTRIBUTED ANTENNA ARRAY

A fundamental consideration in the architecture of ELAA systems is the arrangement and distribution of antenna elements that directly impacts the system's performance, scalability, and applicability in various deployment scenarios.

This can be broadly categorized into co-located and distributed ELAA architectures.

In a co-located ELAA architecture is the standard array architecture where all antenna elements are centralised within a limited physical space with adjacent elements typically separated by half wavelength [21], [22], [23], [24], [25] as illustrated in Table 3. This arrangement typically involves a single antenna array unit where all the antennas are closely packed together (not necessarily in wavelength order). The centralisation of antenna elements simplifies management and control, and facilitates beamforming and signal processing algorithms. However, co-located architectures can face challenges related to mutual coupling and power distribution between closely spaced antennas. Co-located arrays are capable of achieving high spatial resolution due to the close spacing of antenna elements, which enhances the array's ability to perform fine-grained beamforming and DoA estimation. Co-located arrays are well-suited for applications where high spatial resolution and strong beamforming capabilities are required, such as in mmWave and THz communications, radar systems, and high-capacity MIMO systems.

In contrast, the distributed ELAA architecture disperses antenna elements over a larger physical area [21], [22], [23], [24], [25]. In this deployment strategy, antennas are placed in different locations, creating a distributed array. Distributed architectures offer advantages in terms of spatial coverage, diversity gain, and resilience to channel fading and interference. However, managing and coordinating distributed antennas presents challenges in terms of synchronization, signal processing complexity and resource allocation.

Distributed arrays offer the advantage of wide spatial coverage and increased diversity gain. By placing antennas over a large geographical region, the system can better handle shadowing and fading effects, providing more robust and reliable communication links, especially in environments with significant obstacles or when serving a large number of users spread across a wide area. Distributed array, such as coordinated multipoint (CoMP) [26], [27], cloud radio access network (C-RAN) [28], network MIMO [29], and cell-free massive MIMO [21], [23], [24], [25], are ideal for scenarios where extensive coverage and diversity are required, such as in cellular networks, large-scale wireless sensor networks, and distributed radar systems. They are also increasingly being explored for use in next-generation wireless systems, including 6G, where URLLC is essential.

The choice between co-located and distributed antenna arrays depends on several factors, including the specific application, environmental conditions, and system requirements. Co-located arrays excel in scenarios requiring high spatial resolution and precise beamforming, making them suitable for high-frequency, short-range communications. However, they face challenges related to mutual coupling and fabrication complexity. On the other hand, distributed arrays provide broader coverage and better resilience to

environmental variations, but they require sophisticated synchronization and coordination mechanisms to operate effectively. These arrays are particularly advantageous in large-scale deployments and environments where coverage and diversity are prioritized. Therefore, this article will mainly focus on collocated ELAA architectures.

2) ANTENNA SPACING: DISCRETE, CONTINUOUS, AND MODULAR ANTENNA ARRAY

Antenna spacing is a crucial element in the design of ELAA systems, as it has a significant impact on the array's performance in terms of beamforming, spatial resolution, and the handling of near-field effects. The choice of antenna spacing is vital for ensuring that the array effectively adapts to the propagation environment and meets the stringent requirements of high-frequency communication systems. ELAA systems can be categorized into discrete antenna arrays and continuous-aperture surfaces based on their implementation approach.

The current state-of-the-art in MIMO and massive MIMO systems predominantly utilizes discrete antenna arrays [30]. One approach to antenna spacing in ELAA systems is to maintain a distance between antenna elements equal to half the wavelength of the operating frequency [31], [32], [33]. This spacing ensures minimal mutual coupling between adjacent antennas, thereby reducing interference and improving antenna isolation. Another method involves setting the antenna spacing based on the total length of the array and the number of antennas, allowing for adjustable spacing that can be smaller or larger than the conventional half-wavelength. When the spacing is smaller, antennas are uniformly distributed across the array length, potentially enhancing array performance in certain scenarios. Conversely, sparse array is able to increase the total array aperture without increasing the number of antennas [34], [35]. However, increasing the spacing beyond half-wavelength to enlarge the array aperture can lead to the emergence of grating lobes, which are additional major lobes that can interfere with the main lobe, degrading overall system performance [34], [36], [37].

In response to the practical deployment challenges associated with traditional array configurations, a novel modular architecture has been proposed. ELAA's modular architecture involves the arrangement of antenna elements into distinct modules or subarrays, each of which comprises a subset of antennas [34], [38], [39], [40]. These antenna elements are systematically mounted on a common platform in a modular fashion. Each module consists of a flexible number of array antennas, with the inter-element spacing typically matching the signal wavelength. Different modules are separated by a relatively large inter-module spacing to enable conformal deployment with practical structures. For example, in complex environments like urban canyons or inside large industrial facilities, modular ELAA systems can be configured to fit the physical constraints of the deployment area. Compared to co-located ELAA setups with an equivalent number of antenna elements, modular

ELAA not only offers flexible deployment options, but also higher spatial resolution due to its larger physical dimensions. However, the larger inter-module spacing can result in unwanted grating lobes. Unlike distributed ELAA architectures, modular ELAA typically uses common signal processing without the need for sophisticated inter-site coordination or data exchange. This feature can reduce the synchronisation requirements and hardware costs associated with backhaul or fronthaul links for distributed ELAA setups.

Utilizing advanced meta-materials, ELAA systems leverage densely packed antennas arranged within a confined space, effectively creating an aperture that appears continuous for communication purposes. The array surface serves a dual purpose: actively generating beamformed RF signals and controlling the reflection of RF signals originating from other locations. This functionality corresponds to two prominent concepts in antenna engineering: *holographic MIMO* (HMIMO) [9], [10], [19], [41], [42], [43] and *large intelligent surface* (LIS) [44], [45], [46], [47], [48]. Continuous aperture arrays provide flexibility in shaping beam patterns and coverage areas, as well as scalability for large-scale deployments. Unlike traditional discrete antenna arrays, continuous-aperture surfaces can transmit and receive signals across their entire surface, leading to a fundamental shift in signal processing from the conventional hybrid digital-analog domain to the EM domain. However, the subwavelength architecture introduces significant mutual coupling and spatial correlation effects among the antenna elements, which must be carefully considered in practical modeling and communication scenarios [9], [10].

3) ANTENNA ELEMENT SIZE MODELLING: PATCH AND POINT ANTENNA

Patch antennas are commonly used as elements in ELAA systems due to their compact size and ease of integration [45], [49], [50], [51]. These antennas consist of a metallic patch mounted on a dielectric substrate, with a feed mechanism to excite the patch and radiate electromagnetic waves. The size of the patch antenna is typically of the order of the operating wavelength, allowing efficient radiation and reception of signals. The planar nature of patch antennas also facilitates the formation of arrays with precise control over beamforming and radiation patterns. However, the physical size of the patch can lead to limitations in terms of array density, particularly at higher frequencies where the wavelength is shorter, requiring careful design to mitigate mutual coupling and unwanted resonances.

Point antennas, in contrast, are idealized models representing antenna elements as dimensionless points [52], [53], [54], [55]. This abstraction simplifies the analysis of large arrays by focusing on the electromagnetic properties of the array as a whole rather than on the individual characteristics of each element. In practice, a point antenna can be considered when the physical size of the antenna element is much smaller than the operating wavelength, often assumed to be a small dipole or isotropic radiator. As shown in Table 3, the *effective antenna aperture A_e* of a point antenna, often referred to as the aperture efficiency, is given by,

$$A_e = e_a A, \qquad (2)$$

where e_a is the aperture efficiency factor ($0 \leq e_a \leq 1$). For a point antenna with e_a approaching zero, the antenna acts more like a theoretical isotropic radiator with minimal physical dimensions, allowing it to simplify the modeling of large-scale arrays. In ELAA systems, modeling antenna elements as point sources can be advantageous for analyzing large-scale array behaviors, such as beamforming and radiation patterns, without getting bogged down by the specific design details of each element. However, this simplification may overlook practical effects such as mutual coupling and spatial correlation that are critical in dense arrays.

The choice between patch and point antennas in ELAA systems is a trade-off between physical realism and analytical simplicity. Patch antennas provide a more accurate representation of real-world elements, including factors such as radiation pattern, impedance bandwidth, and mutual coupling effects. Point antennas, on the other hand, offer a simplified model that can facilitate the analysis of large arrays, particularly when dealing with theoretical or preliminary designs.

4) ARRAY GEOMETRY: UNIFORM LINEAR, PLANAR, AND CIRCULAR ARRAY

In the field of antenna arrays, the arrangement and geometry of the antennas play a critical role in determining the performance characteristics of the array. Array geometry refers to the spatial configuration of antennas within an array, which can greatly affect the array's radiation pattern, beamforming capabilities, and overall functionality. We examine various array geometries, including uniform linear array (ULA), uniform planar array (UPA), and uniform circular array (UCA), and explore their unique properties and applications in wireless communication systems.

A ULA is a common antenna configuration used in ELAA systems, consisting of antenna elements arranged in a linear fashion along a single axis [31], [32], [49], [56]. The spacing between adjacent elements in a ULA is uniform, typically half a wavelength or a multiple thereof. ULAs are simple to design and implement, making them suitable for various applications such as beamforming, direction finding and spatial diversity. The ULA is particularly effective in linear beamforming, where the array can steer beams in a single plane (typically the azimuth plane). By adjusting the phase shifts applied to each antenna element, the ULA can focus energy in a specific direction, enhancing directivity and improving SNR in that direction. Additionally, the linear configuration of ULAs makes them straightforward to implement and analyze. The mathematical models governing ULAs are well-established, allowing for accurate predictions of beam patterns and performance metrics, such as beam width and gain. However, the primary limitation of ULAs
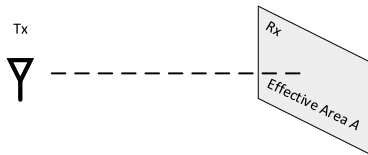
FIGURE 3. An example of transmit (Tx) and receive (Rx) antennas separated by *d*.

is their inability to steer beams in both azimuth and elevation simultaneously. This restricts their use in applications requiring 3D coverage or where beam steering in multiple planes is essential.

A UPA extends the concept of linear arrays into two dimensions, with antenna elements arranged in a regular grid pattern on a planar surface [54], [57], [58]. UPAs provide improved spatial coverage and flexibility over ULAs, allowing beam steering in both azimuth and elevation angles. The uniform spacing between elements in both dimensions provides precise control over the radiation pattern and beamforming capabilities of the array. Unlike ULAs, UPAs can steer beams in both the azimuth and elevation planes. This 2D beamforming capability allows the array to focus its energy more precisely, making it ideal for applications that require control over both horizontal and vertical coverage areas.

A UCA is characterized by antenna elements arranged along the circumference of a circle with uniform angular spacing between adjacent elements [59], [60], [61], [62], [63], [64]. UCAs offer unique advantages in omnidirectional coverage and beamforming capabilities. By exploiting the circular symmetry of the array geometry, UCAs can achieve 360-degree coverage and directional beamforming at any azimuth angle. This geometry is beneficial in various wireless communication systems, where the ability to dynamically direct signals in any horizontal direction is crucial. While UCAs provide excellent coverage in the azimuth plane, they have limitations in elevation beamforming unless combined with other array geometries (e.g., stacked UCAs or a combination of UCA with UPA). This limitation can be a constraint in applications requiring full 3D coverage.

B. SPHERICAL WAVE CHANNEL MODELLING
1) MOTIVATION

Traditionally, the study of channel gain has focused primarily on far-field communication scenarios where the distance between the transmitter and receiver is significantly greater than the wavelength of the signal. Consider a basic wireless communication scenario shown in Fig. 3, where electromagnetic waves carrying information are emitted from the transmitter in free space (i.e., without obstacles) and eventually reach a receiver antenna separated by a distance *d*. As a result, the received power P_r is a fraction of the total transmitted power P_t depending on the effective area A in the receiving antenna. In particular, assuming the transmit antenna is ideally isotropic while the receive antenna is lossless, the received power P_r is proportional to the power

density of the plane wave incident on the receive antenna at a distance *d* from the transmit antenna and the effective area A given by

$$P_r = \frac{A}{4\pi d^2} P_t \tag{3}$$

and the following factor refers to the channel gain.

$$\beta_d = \frac{A}{4\pi d^2} \tag{4}$$

In general, the channel gain in a wireless communication system is small. This typically occurs when the transmitted signal must travel a long distance, experiences significant path loss, or encounters significant obstacles and interference along its propagation path. As the carrier frequency increases, the channel gain decreases over the same range of distances due to a reduction in effective area. To mitigate significant path loss, one approach is to increase the effective area by deploying additional antennas of the same type. Assuming *N* antennas are deployed at the receiver, and each antenna has an orientation and polarization matched to the received signal, the total received power increases by *N* times given by

$$P_{r,N} = NP_r = N\beta_d P_t. \tag{5}$$

It can be seen that as the number of antennas increases, the received power follows an asymptotic growth trajectory, apparently approaching infinity. However, this trajectory violates the fundamental principle that receiving antennas cannot capture more power than was originally transmitted, making such a scenario physically implausible. The reason for this lies in the scenario shown in Fig. 3, with the deployment of additional antennas, the receive planar array cannot be considered as a point receiver because the propagation distances from the transmit antenna to the elements within the receive planar array vary. Unlike Massive MIMO, which benefits from channel hardening due to the averaging of small scale fading effects over many antennas with similar channel gains, we cannot expect the same level of channel hardening in ELAA when the distance between antennas varies. [22], [65], [66].

This is primarily because well-separated antennas in ELAAs tend to have significant differences in channel gain. Consequently, the assumption that each element antenna within a planar array experiences the same channel gain is no longer valid. As a result, the behavior of the channel path between each transmitter and receiver pair should be analyzed individually, e.g., mathematically, the complex-valued LoS channel component[2] between the transmit antenna located at $\boldsymbol{p}_t$ and the receive point $\boldsymbol{p}_r$ can be represented as

$$h(\boldsymbol{p}_t, \boldsymbol{p}_r) = |h(\boldsymbol{p}_r - \boldsymbol{p}_t)| e^{-j\frac{2\pi}{\lambda}\|\boldsymbol{p}_r - \boldsymbol{p}_t\|} \tag{6}$$

---

[2]While discussing channel modeling, it is pertinent to acknowledge the existence of another Green's function-based channel model used for CAP antennas. However, this article focuses primarily on spatially discrete (SPD) antennas, i.e., ELAA, and therefore does not discuss this alternative model. For brevity and relevance, further discussion of the CAP model is omitted.
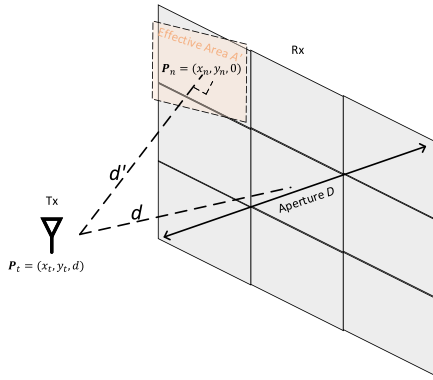
FIGURE 4. Illustration of fundamental properties accounting for ELAA, i.e., distance variation, effective area variation and polarization mismatch.

with both the channel gain $|h(\boldsymbol{p}_r - \boldsymbol{p}_t)|^2$ and the phase shift depending on the distance between each antenna pair. This requires the development of a more accurate model to describe the behavior of the channel gains in the near-field region.

2) CHANNEL GAIN MODELING

As the aperture of the antenna panel increases, the channel is more likely to be in the near-field region, where the conventional plane-wave assumption made to simplify channel modeling and performance analysis in the far-field region is no longer valid. Several criteria that delineate the boundary between the near-field and far-field regions will be discussed later. As a result, it becomes imperative to carefully consider the novel channel characteristics associated with spherical waves. In particular, when investigating the near-field behavior, careful consideration must be given to several essential characteristics of spherical waves that induce variations in channel gains within the array.

In the quest to establish the fundamental principles of near-field communication with ELAAs, a comprehensive study of the unique characteristics associated with radiative near-field communication is essential. In examining the near-field behavior, the following aspects cannot be overlooked, as they are critical to modeling the variations in signal amplitude across array elements. Fig. 4 illustrates the fundamental effects that must be considered when studying near-field behavior where an ideal isotropic transmitter is placed directly in front of ELAA, separated by a distance d. The scenario where ELAA acts as the receiver is considered to illustrate the model, but similar results can be obtained when the roles of transmitter and receiver are reversed. Firstly, the distances travelled by the signal are different. As shown in the figure, the wave has to travel an additional distance to reach the edge of the array compared to the central antenna element. It is therefore essential to account for the additional path loss due to the distance variations within the array elements. Secondly, the effective area of each receiving antenna depends on its geometric orientation and alignment relative to the direction of the transmitter.

If the receiving antenna is perfectly perpendicular to the direction of propagation, its effective area is A. However, for any other orientation, the effective area is less than A. Therefore, the variation in effective antenna area due to the different angles from which the antennas are viewed is a noteworthy feature in the context of the near field. In addition, the geometric position and rotation of the antenna also introduces the polarisation mismatch, a factor that must be considered when formulating the near-field channel gain model.

In the existing literature, numerous channel gain expression models have been proposed to study the behaviour of the near-field region, where these models take into account one or more of the additional characteristics when examining the variation of signal amplitude across array elements. In [67], the author considered distance variations in the channel gain model and derived a closed-form expression for the received SNR specific to extremely large uniform linear arrays (XL-ULA). Reference [68] introduced an analytical spherical-wave channel model for large linear arrays and provided theoretical insights into how spherical wavefronts enhance channel decorrelation. Taking into account the variation of distance and effective antenna area, [44] investigated the effective channel under LoS propagation environment and analysed a normalised capacity per unit area. In the existing literature, the channel gain model has also been derived from RIS when studying the near-field behaviour.

[69], [70], [71] have performed numerical studies and discussed the near-field behavior. However, it is crucial to emphasize that the results, while insightful, are approximations due to the absence of polarization considerations and the assumption of a constant projected aperture for all array elements in [69], [71]. In the near-field, this assumption does not hold because elements are observed from different angles, introducing an additional source of approximation error. In [72], the authors demystified the potential advantage of using IRS where the SNR increases as N^2 instead of linear N in mMIMO and derived the power scaling law of IRS by capturing the variation of distance and effective area. An accurate analytical expression for the link gain and the available spatial degrees of freedom (DoF) were derived starting from electromagnetic arguments avoiding prohibitive computation [45].

Following the work in [45], the channel gain expression derived by [73] incorporates three crucial properties-variations in distance, effective antenna area, and polarization mismatch-through a deterministic propagation model in a planar array. Specifically, they derived the upper bound of LoS channel gain, where three fundamental properties are stated explicitly in the expression, given by Eq. (7) shown at the bottom of next page, where $\boldsymbol{p}_t = (x_t, y_t, d)$, $\boldsymbol{p}_r = (x_r, y_r, 0)$ and $\boldsymbol{p}_n = (x_n, y_n, 0)$. $\boldsymbol{p}_n$ is the n-th receive antenna element centered at $(x_n, y_n, 0)$ and has area $a \times a$, as illustrated in Fig. 4. This expression is then used to illustrate the SNR behavior and establish the corresponding power scaling law [73], which states that only one-third of

TABLE 4. List of fundamental channel properties consideration and scenarios.

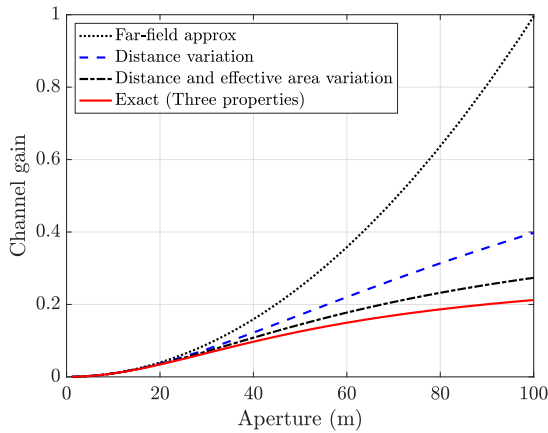| Ref.	Distance Variation	Effective Area Variation	Polarization Mismatch	2D	3D
[67]	✓	-	-	✓	-
[68]	✓	✓	-	-	✓
[69]	✓	-	-	-	✓
[71]	✓	-	-	-	✓
[70]	✓	✓	-	-	✓
[72]	✓	✓	-	-	✓
[73]	✓	✓	✓	-	✓
[74]	✓	✓	✓	-	✓
[49]	✓	✓	-	-	✓

FIGURE 5. The total channel gain for a varying aperture size in UPA, where essential propagation properties in near field are considered for comparison [74].

the total transmitted power can asymptotically be received as $N \to \infty$ at fixed antenna spacing. An intuitive reason for the finiteness of this limit, despite the infinite size of the array, is that as each new receiving antenna is placed farther away from the transmitter, the effective area (perpendicular to the direction of propagation) becomes progressively smaller, and polarization losses increase at the same time. As illustrated in Figure 5, the significance of accounting for these properties in near-field analysis, particularly in asymptotic limits, has been underscored in studies such as [73], [74]. Neglecting any of these factors–distance variation, effective area variation, or polarization mismatch–can result in an overestimation of the channel

gain. When the aperture size is small, the exact near-field propagation aligns closely with far-field approximations because the variations are minimal. However, as the array size increases, these variations become more pronounced, causing the channel gain to diverge significantly from the far-field model.

In addition, references [38], [49], [51] considered three-dimensional (3D) channel gain modeling, which requires consideration of azimuth and elevation for more comprehensive channel modeling and accurate performance analysis, and in [49] the author also introduced a channel model that bridges the representation of discrete antenna arrays and the emerging continuous holographic surface [8], [19]. This model achieves this by explicitly incorporating the physical size and projected aperture of each element, departing from the conventional treatment of these elements as dimensionless points. However, as noted above, the architecture of continuous surfaces is beyond the scope of this investigation. In addition, channel gain has been studied in some other array architectures. For example, [75] derived the closed-form array response of the lens antenna array when using spherical waves. Table 4 summarizes the contribution of related work in channel gain modelling.

C. SPATIAL NON-STATIONARITY

Understanding the dynamics and subtleties of channel models is paramount to system design and performance evaluation. There is a substantial body of literature devoted to conventional massive MIMO channel models, such as the i.i.d. Rayleigh fading model [76], [77], [78], which are simple and efficient for performance analysis. In addition, correlation-based stochastic models (CBSMs) [79], [80],

$$\zeta_{\boldsymbol{p}_t,\boldsymbol{p}_n,a} = \frac{1}{4\pi} \int_{x_n-a/2}^{x_n+a/s} \int_{y_n-a/2}^{y_n+a/2} \underbrace{\frac{d}{\sqrt{(x_r-x_t)^2 + (y_r-y_t)^2 + d^2}}}_{\text{Effective area variation}}$$

$$\times \underbrace{\frac{(x_r-x_t)^2 + d^2}{(x_r-x_t)^2 + (y_r-y_t)^2 + d^2}}_{\text{Polarization mismatch}} \underbrace{\frac{\partial x_r \partial y_r}{4\pi\left((x_r-x_t)^2 + (y_r-y_t)^2 + d^2\right)}}_{\text{Distance variation}}, \tag{7}$$

such as the Kronecker model [81], represent a class of channel models that account for correlation effects while offering the advantage of low complexity for assessing system performance. Another important category of channel models are the geometry-based stochastic models (GBSMs), which focus on the channel impulse responses determined solely by the geometric relationships between scatterers[3] and the receiver or transmitter. Several GBSMs have been standardised, and notable examples include the WINNER II model [82] and the International Mobile Telecommunications-advanced (IMT-Advanced) model [83]. These standardised models emphasise the characterisation of the geometrical relationships involved in the initial and final interactions of scatterers within the channel.

However, the traditional MIMO channel models mentioned above are not directly applicable to modeling massive MIMO channels. For example, measurements on large array channels in [84] show that the statistical properties of the received signal vary significantly over the large array, such as the average received power and the angles of the multipath components. In addition, the channel measurements in [85], [86] provide insight into the variation of mean delay, delay spread, and cluster power within the large array, implying that within an array, individual antenna elements may perceive different sets of clusters. Consequently, the wide-sense stationary (WSS) assumption that the statistical properties of the wireless channel remain largely constant over a significant spatial region no longer holds for ELAAs. With the significant increase in array aperture, a new characteristic of ELAA emerges: spatial non-stationarity [84], [85], [86], [87]. This phenomenon occurs because signals experience distinct multi-path propagation across different parts of the array. There are two aspects that make the channel spatially non-stationary. First, since the array aperture is large, it is more likely that some clusters are located in near-field regions where a spherical rather than a plane wavefront should be considered. Second, partially visible property in clusters could be observed when large arrays are adopted. In other words, different group of clusters are only visible to a part of large array instead of interacting with the whole array in conventional massive MIMO system. As a result, the WSS assumption of spatial dimension does not hold for ELAAs. Consequently, to fully characterize the spatial non-stationarity of large aperture arrays, two additional critical aspects must be considered: the visibility region (VR) and the birth-death process. These aspects represent the spatial and temporal properties, respectively,

and are essential for understanding the complex behavior of signals in ELAA systems.

1) VISIBILITY REGION

The VR refers to the spatial segment of the array where a particular signal or set of signals is observable or detectable. Due to the expansive nature of ELAAs, different portions of the array may experience varying signal strengths and multi-path propagation characteristics. The concept of the VR was first introduced in the COST 2100 model to represent spatially non-stationary MIMO channels [88]. This model characterizes the spatial variability in signal propagation by defining regions where specific multi-path components are observable. Building on this statistical model, an extension was proposed for the mMIMO channel model [89]. In this extended model, only the array elements within the VR can detect the cluster, while the array elements outside the VR cannot. According to [87], the concept of VR can be categorized into two distinct domains: the terminal domain and the array domain, illustrating scenarios where a cluster is only visible to a subset of user terminals and array elements, while all clusters are visible to both all terminals and the entire array under the stationary assumption, as shown in Fig. 6(b). In the terminal domain, VR characterizes situations where a cluster of scatterers is visible only to a particular subset of user terminals. This means that different terminals within the communication system may or may not have line-of-sight (LoS) to the same clusters. The VR varies depending on the location and orientation of each individual terminal, resulting in different visibility patterns. As illustrated in Fig. 6(a), UE 1 receives signals scattered by the associated cluster, specifically cluster 1, while moving into the VR. This transition is mathematically represented by a VR gain, which increases from 0 to 1 as the UE enters the VR. In the array domain, the VR concept is used to represent situations where the visibility of a cluster is limited to a portion of the array elements within the antenna array. Not all elements in the array have an unobstructed view of the entire set of clusters. Instead, the visibility of a cluster depends on the relative positions, orientations, and characteristics of the array elements themselves.

The occurrence of non-stationarity differentiates the channel model from traditional far-field models. To accurately capture the characteristics of non-stationary channels, extensive validations through channel measurements and modeling have demonstrated its effectiveness. A common approach to account for channel non-stationarity involves using an indicator variable, such as $\mathbb{1} \in {0, 1}$, to represent the visibility and invisibility regions of the BS, UE, and clusters. For instance, considering the VR, the multi-path channel vector can be modeled as [60], [90], [91]

$$\boldsymbol{h} = \sum_{l \in L} \alpha_l \boldsymbol{a}_l \odot \mathbb{1}_l, \tag{8}$$

where L and α_l denote the total number of path and complex coefficient of the l-th path, $\boldsymbol{a}_l$ represents the

---

[3]In the context of near-field channel modeling, scatterers are physical objects in the environment that cause multipath propagation by reflecting, diffracting, or scattering the transmitted signal. These scatterers are often grouped into 'clusters' based on their spatial proximity and similar propagation characteristics. A cluster, therefore, represents a collection of scatterers that contribute collectively to a set of multipath components arriving from a particular direction. This clustering approach simplifies the channel modeling process, particularly in GBSMs, where the multipath components are analyzed in terms of their respective clusters rather than individual scatterers.

(a) Conventional spatial stationary mMIMO.
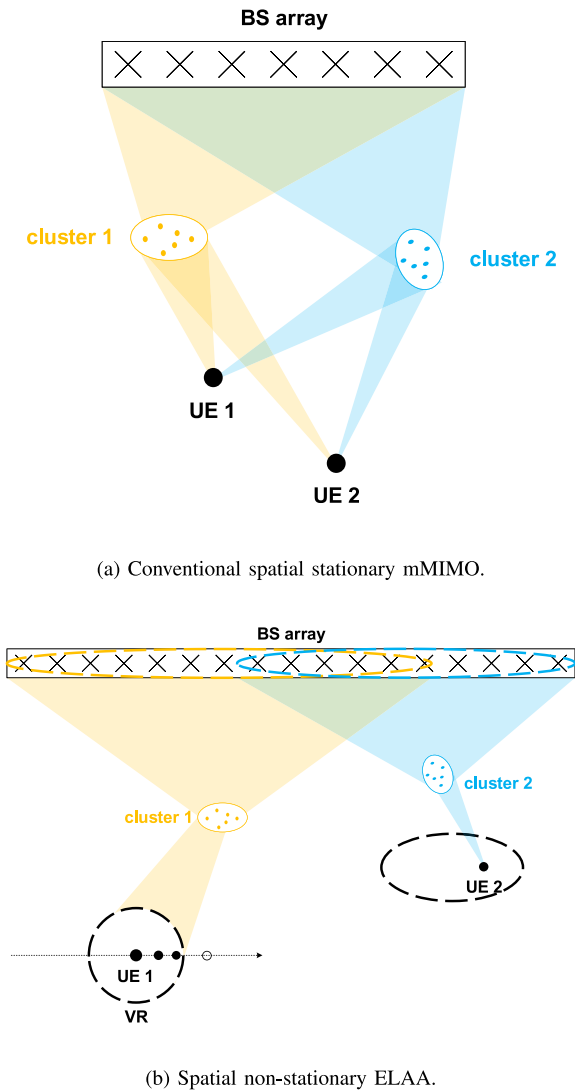

(b) Spatial non-stationary ELAA.

FIGURE 6. The diagram for the spatial stationary mMIMO and spatial non-stationary ELAA.

steering vector of the l-th path, and $\odot$ takes Hadamard product. Additionally, apart from the multipath channel model, the spatial correlation-based model is another widely used approach that considers second-order channel statistics. To develop a spatial correlation-based channel model that incorporates VR characteristics, a diagonal matrix $\boldsymbol{D}$ is introduced, where the non-zero entries denote the visibility of antennas from the BS or UE side. Specifically, the spatial correlation matrix of the VR channel can be modeled as [92]

$$\boldsymbol{R}_{\mathrm{VR}} = \boldsymbol{D}^{\frac{1}{2}} \boldsymbol{R} \boldsymbol{D}^{\frac{1}{2}}, \tag{9}$$

where $\boldsymbol{R}$ denotes the conventional far-field spatial correlation matrix.

2) BIRTH-DEATH PROCESS

Based on the concept of the visible region (VR), modeling non-stationarity comprehensively requires consideration of another crucial aspect: the birth-death process. This process accounts for the dynamic appearance (birth) and disappearance (death) of multipath components over time, effectively capturing the temporal variability of the channel. It represents the emergence and fading of propagation paths, clusters, or other channel features as they evolve in a non-stationary environment, following specific survival probabilities. The birth-death process is essential for understanding and modeling the temporal aspects of non-stationary channels. It characterizes how multipath components (MPCs) dynamically change over time, providing a statistical framework for their creation and annihilation. This approach allows for a more accurate representation of the channel's behavior, particularly in scenarios where the environment or user movement leads to significant variations in propagation conditions.

The authors of [88], [93], [94], [95], [96], [97], [98], [99], [100], [101], [102], [103] have done pioneering work in modeling the birth-death process. For instance, the authors in [93], [96], [98], [99], [100], [101], [102] observed and modeled the lifetimes of multi-path components with certain probability, such as exponential distribution, log-normal distribution, and Birnbaum-Sanders distribution, which have been used to describe the statistical behavior of multipath component lifetimes when tracked along a straight line segment at the UE side.

D. FINITE BEAM DEPTH

By adjusting the phase and amplitude of individual antenna elements within an array, beamforming can steer the transmitted or received signal in a desired direction, improving signal quality and reducing interference. In far-field conditions as shown in Fig. 7(a), the radiated electromagnetic waves become nearly parallel, allowing for simplified mathematical modeling and analysis, i.e., plane waves. Therefore, the incoming waves can be approximated as plane waves with uniform phase throughout the array. In other words, the signal received or transmitted at the antenna array can be approximated as a superposition of plane waves characterized by two essential parameters: a channel gain and an angle of arrival (AoA). On the other hand, thanks to the need to consider the spherical waveform at the antennas in the near field communication (i.e., the variation of the channel gain and the phase shift of each element present in the array) as shown in Fig. 7(b), an antenna array with an extremely large aperture has the ability to resolve not only the angle but also the propagation distance, which could potentially provide a high spatial resolution. This remarkable spatial resolution offered by ELAAs is expected to result in channels to different users becoming nearly orthogonal [22], [44], [84], a phenomenon known as favorable propagation [65], [66]. Consequently, this favors signal transmission specific to a particular point in space rather than toward a desired target direction, known as finite-depth beamforming [6]. In other words, in contrast to conventional beam-like transmission, signal transmission
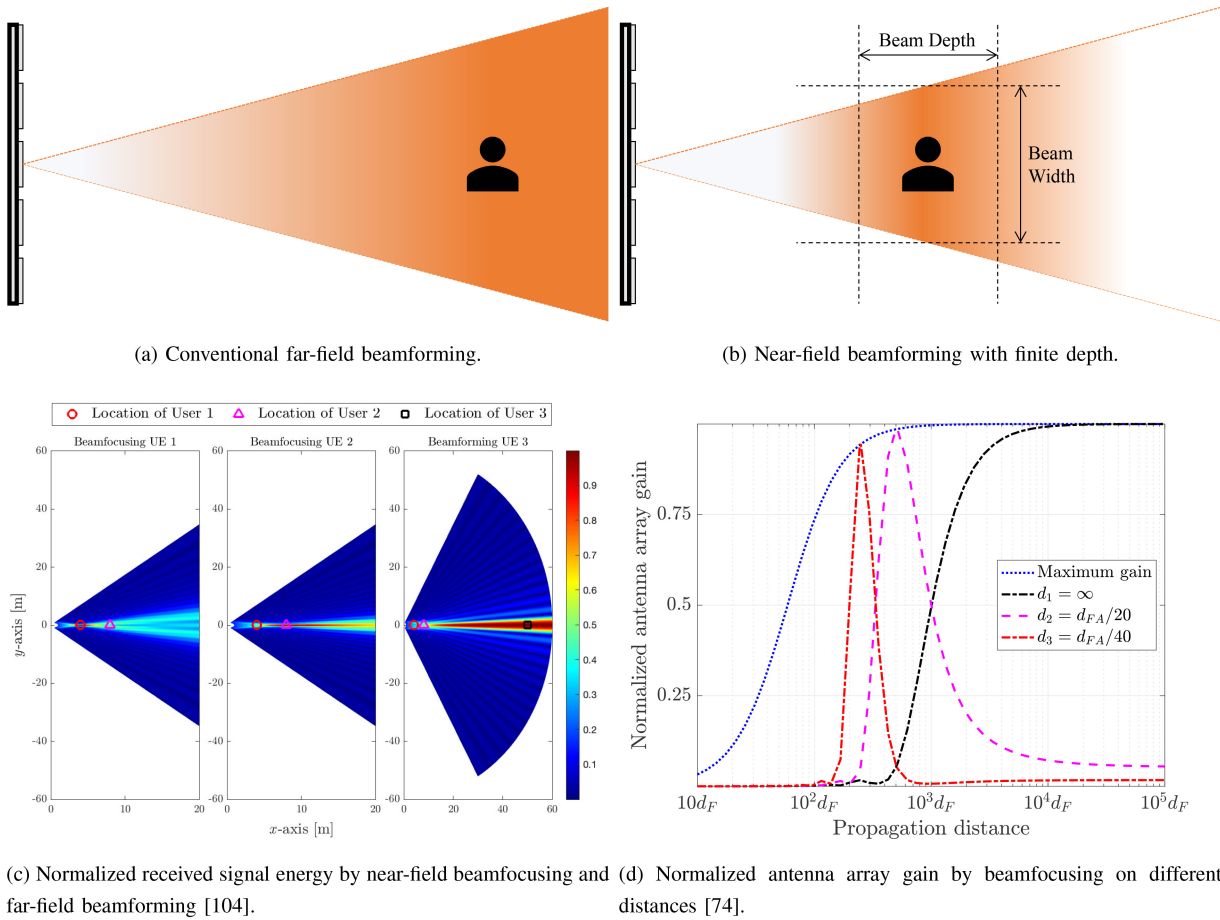
(a) Conventional far-field beamforming.

(b) Near-field beamforming with finite depth.

(c) Normalized received signal energy by near-field beamfocusing and far-field beamforming [104].

(d) Normalized antenna array gain by beamfocusing on different distances [74].

FIGURE 7. Finite beam depth in the near-field enables multiplexing in the same direction.

from the array can be better described as the presence of strong, coherent signal amplification occurring at specific, well-defined points in space. As illustrated by the beam pattern in Fig. 7(c) and Fig. 7(d), beamfocusing allows for the concentration of energy at specific spatial locations. Users 1 and 2, who are located in the near field, benefit from this focused beam, which results in higher signal strength and improved communication quality. The concept of finite beam depth is evident here, where the beam can be focused at different depths, allowing for selective targeting of users within a certain range. Due to the finite beam depth, multiple users, such as user 1 and user 2, can be served simultaneously along the same direction without causing significant interference to each other. This spatial multiplexing is enabled by the distinct focal points created at different depths, which are a result of the precise beamfocusing capabilities in the near field. In contrast, user 3, located in the far field, experiences a broader, less focused beam, which is less effective for multiplexing. The primary advantages of near-field beamfocusing and multiplexing are evident when comparing the near-field users, e.g., user 1 and user 2, to the far-field user, e.g., user 3. Near-field users benefit from higher signal gain due to the concentrated energy at their specific locations, which enhances the overall communication performance. Additionally, the ability to perform spatial multiplexing in the near field allows for more efficient use of the spectrum, as multiple users can be served simultaneously with minimal interference. This results in increased system capacity and spectral efficiency, making near-field communication an attractive approach for future wireless networks, particularly in dense environments where user proximity and capacity demands are high.

Focusing the beam not only in the angular domain but also in the distance domain improves the performance in terms of spectral efficiency achieved by compact arrays. References [44], [45], [73], [74] investigated the channel gain in the LoS channel condition where matched filtering is applied to each array element at the receiver side to compensate for the phase shift and to accumulate the received power of each individual element. After deriving the closed-form array response of the lens antenna array by considering the spherical wave, the investigation of the near-field beam radiation pattern in the distance domain is of growing interest recently [74], [105], [106], [107] because it is essential to understand not only the beam width, which is a fundamental parameter used to characterise the angular width of the main lobe in far-field communication, but also the beam depth (BD) in the distance domain. [74], [105], [107] derived the

BD, which is characterised as the gain of the antenna array that is 3 dB lower than the maximum value using matched filtering. The result generalised the characteristics of the 3 dB BD in the near field and proved that the BD in the far field is a special case where the depth of focus is infinite. Reference [106] further investigated and analysed the characteristics of BD using a tunable width-to-height array instead of a square array.

E. NEAR-FIELD AND FAR-FILED REGIONS AND BOUNDARIES

Based on EM and antenna theory, it is observed that the regions surrounding a transmitter[4] exhibit different EM properties and behaviors as dictated by their respective distances, i.e., the near field and the far field. The near field is the region immediately surrounding the antenna and is characterized by pronounced and dynamic electromagnetic interactions. This near-field region can be further divided into two sub-regions: the reactive near-field and the radiative near-field, each characterized by unique electromagnetic properties and behavior [108], [109], [110], [111], [112]. In contrast, the far field extends beyond the near field, where electromagnetic waves propagate as plane waves with well-defined characteristics. Since far-field regions are well described in the existing literature, This section discusses various distances associated with the near-field as described in the existing literature and outlines various criteria for delineating the boundaries between the near-field and the far-field.

1) GENERAL FIELD REGIONS

Traditionally, three regions are defined for antennas: the reactive near-field, the radiative near-field, and the far-field.

- *Reactive Near-Field:* The reactive near-field region, adjacent to the antenna, is characterized by predominantly reactive electromagnetic fields. In this region, the electric field (E-field) and the magnetic field (H-field) are 90 degrees out of phase, resulting in a predominantly reactive nature. These fields store and release energy rather than propagating as radiating waves. This region is dominated by evanescent waves and is associated with inductive coupling [13], [37], [53], commonly used in applications such as radio frequency identification (RFID) tags, albeit with limited range.
- *Radiative near field:* The radiative near-field, also known as the Fresnel region, lies beyond the reactive near-field and extends up to several wavelengths from the antenna. Within this region, propagating waves exhibit spherical wavefronts, where the electromagnetic energy propagates in a spherical pattern around the antenna. The radiative near field is characterized by the transition of the EM fields from predominantly reactive

to radiative. However, because this transition is not complete, the shape of the radiation pattern continues to vary with distance.

- *Far field:* The far field, also known as the Fraunhofer region, is the region farthest from the antenna. In the far field, EM fields behave predominantly as plane waves, where the E and H fields are orthogonal to each other, and the energy propagates outward in a well-defined direction. The far field is characterized by the inverse square law, where the intensity of the electromagnetic field decreases inversely with the square of the distance from the antenna.

For electromagnetic fields to radiate or propagate effectively, the E and H fields must be orthogonal (perpendicular) to each other and in phase. However, in the reactive near-field region, which is characterized by its typically short range and the rapid exponential decay of evanescent waves with distance, these waves cannot be considered as conventional electromagnetic waves suitable for propagation. Consequently, our focus is solely on the radiated electromagnetic waves characterized by spherical wavefronts, although they can be approximated as planar waves in the far field. For simplicity, we will use the term *near-field* to denote the radiative near-field region.

This section discusses the different distances associated with the near-field in the literature and presents and quantifies the different boundaries with their respective criteria for distinguishing the near-field from the far-field. Traditionally, apart from the reactive near-field with a short range close to the antenna, which is beyond the scope of this article, the field regions are divided into three regions [108], [109], [110], i.e., near region, the Fresnel region, and Fraunhofer/far-field region. More specifically, in the far-field region, where the distance between the transmitter and receiver is much greater than the wavelength, both amplitude and phase variations within the array become negligible. This is the most commonly used model, which assumes that the dimensions of the array are significantly smaller than the link distance. This condition allows an effective approximation of the incoming waves at the receiver array as uniform plane waves (UPW) [113], [114]. In this context, the amplitude depends mainly on the propagation distance, while the phase variations are mainly influenced by the angle of incidence of the incoming wave. When the dimensions of the array are moderately expanded, or when the coupling distance is moderately reduced, the plane wave assumption no longer holds. This situation occurs in the Fresnel region, where the amplitude variations across the array aperture remain negligible, but a noticeable phase variation appears. In such cases, it becomes imperative to use the uniform spherical wave (USW) model to accurately account for the phase variations across the array elements [115], [116]. In the final scenario, when the receive antenna is positioned even closer to the ELAAs within near-field region, varying propagation distances affect different

---

[4]These regions are delineated from the perspective of the transmitter, but can also be understood from the perspective of the receiver due to the principle of reciprocity.

array elements. Consequently, the non-uniform spherical wave (NUSW) model [68], [117] must be employed. This model takes into account the significant variations in both amplitude and phase across array elements that arise in this specific context.

Similarly, references [32], [49], [74], [73], [105] also proposed and characterized the near-far-field boundary based on their channel models and scenarios. In particular, the work of [49] introduced a new distance criterion that takes into account both amplitude and phase shift differences between array elements and extended the classical Fraunhofer distance based on his channel model that considers the variation of the projected aperture. References [73], [74], [105] proposed two boundaries between near and far field based on the derivation of beam depth and maximum gain. Finally, [32] defined the near-field ranges in the mixed LoS/NLoS MIMO configuration. It is worth noting that these regions are delineated and characterized by different definitions. In general, however, the criteria considered often include amplitude and/or phase variations that are noticeable in the near-field. Furthermore, based on these criteria, the boundaries between near-field and far-field are also considered in various applications in the literature, e.g., LoS/NLoS, SIMO/MISO, MIMO, and RIS. The total near-field and far-field distances for antenna arrays in the literature are summarized in Table 5.

2) BOUNDARY DETERMINATION VIA PHASE VARIATION METRIC

a) Rayleigh Distance: Consider an isotropic transmit antenna and an ELAA receiver with aperture D as shown in Fig. 4. As the transmit antenna approaches the ELAA, moving from the far-field to the Fresnel region, the first noticeable variations are in the phase mismatch across the array rather than in the strength of the signals. Therefore, to account for the worst-case scenario of the transmitted wave approaching the receiver perpendicularly, one must consider the maximum phase differences resulting from the propagation of spherical waves across the span from the center to the edge of the array. Since the plane wave can be well approximated by its first-order Taylor expansion in the far field, the concept of the *Rayleigh distance* (also known as the *Fraunhofer distance*) [37], [108], [109], [110] is motivated by ensuring that the approximation of the phase shift across array antenna elements can be accurately described by a linear relationship. In the literature [110], $\pi/8$ is treated as the maximum phase shift that can be considered negligible (i.e., $\cos(\pi/8) = 0.92$). When the communication distance exceeds the Rayleigh distance, the UE is considered to be in the far-field region, also known as the Fraunhofer region, where the planar wave assumption applies. Conversely, if the communication distance is less than the Rayleigh distance, the UE is considered to be in the near-field region, which requires the consideration of spherical waves.

This condition serves as a critical guideline for understanding the transition from near-field to far-field behaviour,

especially in scenarios where accurate wavefront analysis and phase considerations are essential. As shown in the Table 5, the Rayleigh (Fraunhofer) distance $d_F = \frac{2D^2}{\lambda}$ in SIMO or MISO scenarios is directly proportional to the square of the array aperture D and inversely proportional to the wavelength λ. For example, consider the SIMO case where the receiver is equipped with ELAA as shown in Fig. 4. The carrier frequency is $f = 3$ GHz, the wavelength $\lambda = 0.1$ m. In the case of an antenna with an aperture of the same order as the wavelength $D = \lambda$, the Fraunhofer distance d_F is only 0.2 metres. However, by using many antennas in an array system (i.e., ELAA), the Fraunhofer array distance increases to $d_{FA} = 2$ km for ELAA with an aperture of 10 m. This observation implies that the Fraunhofer distance is relatively short for conventional MISO and SIMO systems. Consequently, such systems typically operate in the far-field communication scenario where the distance between the transmitter and receiver is, in most practical cases, well beyond this Fraunhofer distance. When dealing with ELAAs, however, the near-field scenario must be considered. This is because the Fraunhofer distance for ELAAs can be quite large, making near-field effects more pronounced and requiring special analysis and consideration for these unique scenarios.

It is important to note that the derivation of the classical Rayleigh distance, which defines the boundary between the near-field and far-field based on phase differences, is derived under the worst-case assumption of a normal incident wave. In this scenario, the transmitter is positioned directly in front of the ELAAs, ensuring that the transmitted wave is perpendicular to the receiver. Following the definition of the classical Rayleigh distance, [49] extended the result to *directional Rayleigh distance* (i.e., $\arg\min_d \Delta\varphi(d, \theta, \phi) \leq \frac{\pi}{8}$) to account for the effect of signals from any direction on the phase variations across the array elements. This extension takes into account the signal direction, represented by angles(θ, ϕ), and considers the phase variations across array elements in three-dimensional scenarios. Although a general closed-form solution is difficult to find, it demonstrates consistency with the classical Fraunhofer distance to establish the accuracy of the proposed channel model.

In the scenario discussed above, either the transmitter or receiver is equipped with a single antenna. It is noteworthy that the results for MISO or SIMO setups are essentially identical. This equivalence arises because these cases are defined from the perspective of the transmitter, but can be interpreted equivalently from the perspective of the receiver. This principle is known in electromagnetic theory as reciprocity [110]. Reciprocity ensures that the channel characteristics and EM behaviour remain consistent regardless of whether we consider the transmitter or receiver end. However, in scenarios where both the transmitter and receiver are equipped with antennas (i.e., MIMO systems), each transmitter and receiver antenna pair will experience different LoS paths in the near field. This means that the receiver with a large aperture cannot be perceived as a point receiver from the perspective of

TABLE 5. Existing near-field and far-field boundaries.

Criterion	Boundary	Distance Expression	Config.	Distance Definition	Ref.
Phase Variation	Rayleigh / Fraunhofer Distance	$\frac{2D^2}{\lambda}$	MISO/SIMO, arbitrary array aperture.	Maximum phase discrepancy less than $\pi/8$ based on first-order Taylor expansion.	[110]
		$\frac{2(D_t+D_r)^2}{\lambda}$	MIMO, arbitrary array aperture.		[32], [104]
	Directional-dependent Rayleigh Distance	$\arg\min_d \Delta\varphi(d,\theta,\phi)$	MISO/SIMO, arbitrary array aperture.	Maximum phase discrepancy for a user with link distance d and direction (θ,ϕ) less than $\pi/8$ based on first-order Taylor expansion.	[49]
	Fresnel Distance	$0.62\sqrt{\frac{D^3}{\lambda}}$	MISO/SIMO, arbitrary array aperture.	Maximum phase discrepancy for a user with link distance d and direction (θ,ϕ) less than $\pi/8$ based on second-order Taylor expansion.	[110], [118]
		$0.5\sqrt{\frac{D^3}{\lambda}}$			[36], [110], [119]
Gain Variation	Björnson Distance	$2D$	MISO/SIMO, UPA	The normalized antenna array gain is close to 1.	[74], [105]
	Critical Distance	$9D$	MISO/SIMO, ULA	The power ratio between the weakest and strongest array elements remains above a specified threshold. Specifically, critical distance was derived based on a threshold of 80% while uniform power distance considered threshold Γ_{th} with additional consideration of the variation of the projected aperture across the antenna array.	[67]
	Uniform Power Distance	$\sqrt{\frac{\Gamma_{th}^{2/3}}{1-\Gamma_{th}^{2/3}}}\frac{D}{2}$	MISO/SIMO, UPA		[49]
	Equi-Power Line	$2.86D$	MISO/SIMO, ULA	The ratio of the received power obtained with the SWM to that obtained with the PWM approaches 1, i.e., 0.99.	[120]
	Equi-Power Surface	$3.96D$	MISO/SIMO, UCPA		
	Finite Beam Depth Distance	$\frac{d_{FA}}{10}$	MISO/SIMO, UPA	Finite 3 dB beam depth upper bound.	[74], [105]
	Effective Rayleigh Distance	$0.367\cos^2(\theta)\frac{2D^2}{\lambda}$	MISO/SIMO, ULA	The normalized beamforming gain under the far-field assumption is no less than 95%.	[31]
Information Theoretic Perspective	Capacity Based Threshold Distance	$4D_{tx}D_{rx}\cos\theta_T\cos\theta_R$	MIMO, ULA	Capacity underestimation error between SWM and PWM reaches 50% between SWM and PWM.	[121]
	Eigenvalue Based Threshold Distance	$\frac{\Gamma_{th}d_t d_R \cos\theta_T\cos\theta_R}{\lambda}$	MIMO, ULA	The ratio of the largest eigenvalues, as given by SWM and PWM, reaches a predefined threshold.	[122]
	Effective Multiplexing Distance	$\frac{D_T D_R}{\lambda S^*_{asy,m}(\gamma)}$	MIMO, ULA	The channel can efficiently accommodate m independent spatial streams simultaneously at a specific SNR.	[123]
	Effective Degrees of freedom Based Distance	$\frac{2D_{tx}D_{rx}}{\lambda}$	MIMO, CAP	Communication mode / EDoF is greater than 1 in LoS.	[124]
Non-Communication Perspective	Mismatch Model Boundary	$10\log_{10}\left(\frac{|CRB_{TM}-LB|}{CRB_{TM}}\right)$	MISO/SIMO, ULA	Normalized CRB model mismatch between near-field true model and far field lower bound is the 3 dB.	[125]
	Phase Ambiguity Distance	$\frac{D_r^2}{2\lambda}$	MISO/SIMO, UPA	The difference between the unknown integer periods at any two receiving elements is 0 or 1. (The phase ambiguity can be eliminated by difference method).	[126]
	Spacing Constraint Distance	$\max\{\frac{l_s^2}{\lambda}, 3.6l_s\}$		The difference between the unknown integer periods is 0 or 1 when two receiving elements are located at $\frac{l_s}{2}$ and $\frac{3l_s}{2}$.	

the transmitter, and vice versa. In this case, the channel model must be built by considering the channel gain and phase shift for each transmitter-receiver pair individually.

References [32], [104] introduced the concept of MIMO Rayleigh distance to provide the near-field region for the MIMO scenario. Specifically, the MIMO Rayleigh distance is
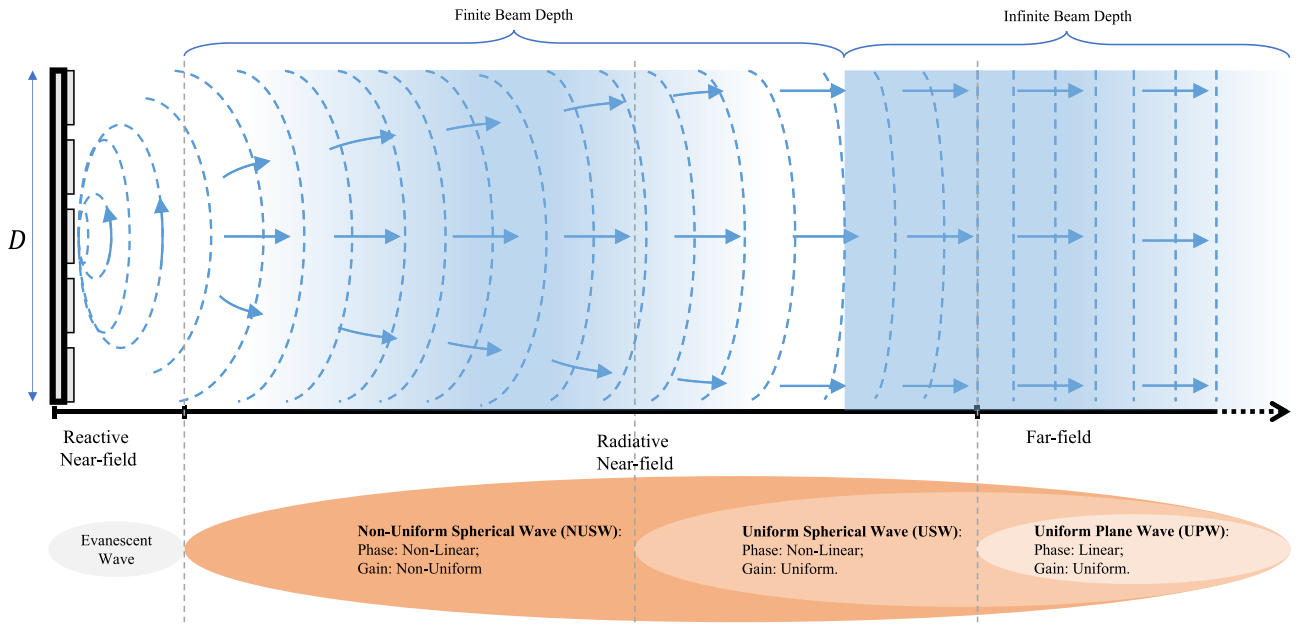
FIGURE 8. Field regions and boundaries with respect to an ELAA.

derived based on the fact that the maximum phase discrepancy, approximated by the first-order Taylor expansion, between the MIMO array elements is greater than $\pi/8$.

In the context of MIMO scenarios where ELAAs are used on both the transmitter and receiver sides of the communication link, it is essential to include both the transmitter array aperture (D_t) and the receiver array aperture (D_r) in the Rayleigh distance calculation, i.e., $\frac{2(D_t+D_r)^2}{\lambda}$. According to the MIMO scenario in Table 5, this implies that the near-field range is directly proportional to the square of the sum of the transmitter and receiver array aperture and inversely proportional to the wavelength. In addition, the Rayleigh distance has been extended to RIS-based communication systems [104]. Therefore, when calculating the phase discrepancy, it is essential to consider both the distance between the BS and the RIS and the distance between the RIS and the UE. By determining the maximum phase discrepancy, typically set at $\pi/8$, the near-field range in RIS systems is determined by the harmonic mean of the BS-RIS distance ($d_{\text{BS-RIS}}$) and the RIS-UE distance ($d_{\text{RIS-UE}}$).

b) Fresnel Distance: When the communication distance is less than the Rayleigh distance, the maximum channel phase error induced by the far-field approximation exceeds $\pi/8$. This implies that the phase discrepancy resulting from the first-order Taylor expansion becomes non-negligible. Therefore, the use of a second order Taylor expansion allows a more accurate approximation of the phase for boundary derivation purposes. Adhering to the same criterion of the maximum allowable phase error of $\pi/8$ radians, the Fresnel region approximated by Taylor series up to the second-order terms has been determined for any planar aperture with uniform phase distribution [110]. Therefore, the dominant

phase error will not exceed $\pi/8$ when the communication distance exceeds the Fresnel distance. While the derived Fresnel distance is based on either MISO or SIMO systems, in scenarios where both the BS and UE are equipped with ELAAs, the Fresnel distance can also be determined by replacing the aperture D with the sum of the BS array aperture and the UE array aperture [37].

Note that although the Fresnel distance is typically derived assuming a $\pi/8$ phase error, there are variations in the literature due to different reported conditions. Consequently, slightly different Fresnel distances are obtained by considering different phase differences. For example, in [36] the Fresnel distance is calculated based on the maximum phase difference of $\pi/8$ for line sources, using Fresnel approximations as described in [118], i.e., $0.5\sqrt{\frac{D^3}{\lambda}}$. On the other hand, Polk [110], [118], [119] derived the Fresnel distance based on scalar diffraction theory specifically for a rectangular aperture, i.e., $0.62\sqrt{\frac{D^3}{\lambda}}$. According to the Table 5, although all derivations of the Fresnel distance are based on the assumption of the maximum phase error, variations in the derivation arise from the use of different methods of phase approximation.

After determining the Rayleigh distance and the Fresnel distance, the general EM field regions - including the reactive near-field, the radiative near-field, and the far-field - are clearly delineated, as shown in Fig. 8. In particular, the far-field region, beyond the Rayleigh distance, is characterized by EM fields that predominantly behave as plane waves. The radiative near-field region is defined by the boundary between the Rayleigh and Fresnel distances, where propagating waves exhibit spherical wavefronts. Conversely, the reactive near-field region, located within the Fresnel

distance, is characterized by dominant evanescent waves with limited range.

3) BOUNDARY DETERMINATION VIA GAIN VARIATION METRIC

According to the Table 5, the distances used to distinguish the near-field from the far-field are dependent on the size of the array aperture and the wavelength, particularly when phase discrepancies are taken into account. As a result, near-field communication is more likely to be achieved either by increasing the aperture of the array by using additional antennas, or by increasing the frequency of the signal to reduce the wavelength. These strategies help to push the near-field boundary further away from the antenna, allowing more effective far-field communication.

However, the boundaries from a phase error perspective have a weak correlation with key channel performance metrics such as channel gain, which is a critical factor in practical wireless communication systems. While the channel gain increases linearly with the number of antennas in the far-field region, it saturates for large arrays due to variations in the gain of each array element in the near-field region. On the other hand, it should be remembered that one of the benefits of integrating multiple antennas is to achieve greater beamforming gain, which could lead to higher SNR with a linear increase in the number of antennas. In addition, the spherical wavefront in the near field has an additional depth domain for multiplexing. Therefore, the loss of beamforming gain, especially in the depth domain, serves as another significant indicator to distinguish the boundary between near and far field. Consequently, a closer look at the boundary in terms of gain error is more practical for determining the boundary.

a) Björnson Distance: In [74], [105], *Björnson distance* is introduced to determine the boundary between near-field and far-field from a gain variation perspective. The scenario where a square planar array receiver with patched antenna elements and a point transmitter equipped with single antenna is considered. From EM perspective, following the concept of *antenna gain*, which reflects the efficiency of an antenna compared to an isotropic antenna, the authors define *normalized antenna array gain*. This metric is defined as the ratio between the total received power of all antenna elements in an array and the received power of the largest antenna in the far-field, with the same number of antenna elements. This measure ranges between 0 and 1, indicating the extent of power variations across the array. Once the maximum value, i.e., 1, is attained, the propagation distance is sufficiently large, and each antenna element experiences the same power as in the far-field scenario with a plane incident wave. Björnson distance is defined as twice the array aperture, i.e., $2D$, aiming for a normalized antenna array gain close to unity. In the context of a square planar array, it is crucial to note that Björnson distance scales with the square root of the number of antennas, unlike the linear growth observed in Rayleigh distance. Additionally, unlike the Rayleigh distance, Björnson distance is wavelength-independent. This is attributed to its derivation from geometric principles rather than relying on specific electromagnetic wave properties.

b) Critical Distance & Uniform Power Distance: The conventional method of delineating the near- and far-field regions relies on phase error metrics, such as the Rayleigh distance. However, advancements in signal processing techniques, such as maximum ratio transmission (MRT) or maximum ratio combining (MRC), allow for precise alignment of signal phases across antenna elements. Consequently, the influence of phase errors is mitigated. To address this, the authors in [67] introduced a novel distance criterion known as the *critical distance*, which incorporates considerations of amplitude or power differences. The distance defined as the power ratio between weakest and strongest array elements is no smaller than a certain threshold. In [67], the author established a threshold of 80%, resulting in the critical distance being solely contingent on the physical dimensions of the antenna array, i.e., $9D$. This implies that amplitude differences become relatively minor and can be disregarded for communication distances exceeding the critical distance. Conversely, when the distance is less than the critical distance, significant amplitude variations occur across the antenna array. In the study [67], these two regions are denoted as the upper near-field region and the lower near-field region.

Extending the boundary criterion outlined in [49], where the power ratio between the weakest and strongest array elements surpasses a specified threshold Γ_{th}, the authors further define the critical distance as the uniform-power distance, i.e., $\sqrt{\frac{\Gamma_{th}^{2/3}}{1-\Gamma_{th}^{2/3}}}\frac{D}{2}$. This extension incorporates additional factors, such as the uniform planar array structure and the variability of the projected aperture across the antenna array. Importantly, the authors take into account scenarios in three dimensions and provide the boundary when the receiver is situated perpendicularly at the center of the array shown in Table 5.

c) Equi-Power Line & Equi-Power Surface: In a point-to-point LoS single-input multiple-output (SIMO) path scenario, maximum channel gain is achieved with maximum ratio combining (MRC), regardless of the phase of the received signal. To delineate the boundary between the near-field and far-field regions, [120] examines the ratio of channel gain between the plane wave (PWM) and spherical wave (SWM) models. As the distance approaches infinity, the received power under SWM approaches that of PWM, resulting in a ratio that converges to unity. In addition, electromagnetic (EM) propagation varies across the array structure, so the limit must be determined based on different array configurations.

In [120], the boundaries for ULA and Uniform Circular Planar Array (UCPA) structures are established using a predefined threshold of 0.99, termed the equi-power line and equi-power surface, respectively. Closed-form analytical

expressions for this ratio are derived and presented in Table 5 for the scenario where the source is perpendicular to the centre of the array (i.e., $2.89D$ and $3.96D$). However, for sources at other angles, numerical methods are used to determine the equi-power line and equi-power surface. In addition, the authors in [120] explore other array configurations, such as uniform square planar array (USPA) and uniform rectangular planar array (URPA) structures, although closed-form expressions are not provided for these cases.

4) Finite Beam Depth Distance: The use of MRC allows maximum channel gain to be achieved. In the far field, the matched filter (MF) relies solely on the AoA/AoD of the array response vector due to the use of the plane wave approximation. Conversely, in the near field, where spherical curvature comes into play, the MF is influenced by both angle and distance. As discussed in Section II-D, beams have a limited depth of focus (DF), resulting in the need to focus the beam not only in the angular domain, but also in the distance domain. In studies such as [74], [105], the UPA structure is considered. Using the definition of the normalised antenna array gain in the derivation of the Björnson distance, the authors also derive the *3 dB Depth-of-Focus* when using the MF focusing at z. The 3 dB depth of focus is given by $[\frac{d_{FA}z}{d_{FA}+10z}, \frac{d_{FA}z}{d_{FA}-10z}]$, where d_{FA} is the Rayleigh array distance. The upper limit of the 3 dB depth of focus extends to infinity when the beam is focused beyond $d_{FA}/10$. This means that if the focus is on a receiver closer than d_{FA}, the beam will have a limited depth of focus. Conversely, for focal points further away, the 3 dB BD extends indefinitely, consistent with conventional far-field beamforming principles. Furthermore, as the focal point extends to infinity, the lower limit approaches d_{FA}, acting as a natural boundary between near-field and far-field beamforming.

5) Effective Rayleigh Distance: Recognising that the classical Rayleigh distance tends to overestimate the true near-field range, [31] proposes an alternative boundary known as the *effective Rayleigh distance*, which is determined based on the loss of beamforming gain. This approach considers scenarios involving a uniform linear array with a single-antenna UE, extending the analysis beyond the conventional assumption that the UE is perpendicular to the array. In contrast to previous works that only considered simple scenarios, this approach considers UE positions at different angles relative to the array [74], [105]. The boundary between the near-field and far-field regions is determined by considering the achievable beamforming gain, which reflects the coherence between the near-field channel and its far-field approximation. As the UE approaches the BS, resulting in a noticeable near-field effect and a decrease in beamforming gain, the boundary is defined by the point at which this loss in gain exceeds a predefined threshold. In [31], the effective Rayleigh distance is derived based on the criterion that the normalised coherence between the near-field and far-field channels is greater than 95%, which is $0.367\cos^2(\theta)\frac{2D^2}{\lambda}$.

Unlike the conventional Rayleigh distance, the effective Rayleigh distance incorporates additional variables such as beamforming gain loss and angle of arrival to address the limitations of the classical approach.

4) BOUNDARY DETERMINATION VIA INFORMATION-THEORETIC METRIC

In wireless communication systems, accurate delineation of the near-field/far-field boundary is essential for optimising system performance. Traditional methods based on phase error have limitations in capturing important performance metrics such as channel gain, capacity and multiplexing capability. In this section, we explore novel approaches to boundary determination based on information-theoretic metrics. By using concepts such as degrees of freedom, channel capacity and multiplexing gain, these methods provide a more comprehensive understanding of the transition between near-field and far-field operation, thereby enabling more effective system design and optimisation.

a) Capacity Based Threshold Distance: The authors in [121] propose a method to determine a threshold distance below which the capacity of the spherical wave model exceeds that of the planar wave model by more than 1.5 times for a given array size. This threshold marks the point at which the capacity underestimation error reaches 50% when using the plane-wave model, and this error increases significantly for distances shorter than the threshold. The study considers a ULA scenario with rotation angles θ_R and θ_T at the transmitter and receiver. The generalised threshold distance, given by $4D_{tx}D_{rx}\cos\theta_T\cos\theta_R$, also corresponds to the 0.225 dB beamwidth distance of the array.

b) Eigenvalue Based Threshold Distance: Expanding on an estimation of the dominant eigenvalue of LoS MIMO channels using the ULA structure, [122] investigates the impact of precise spherical wave propagation modelling versus approximate plane wave propagation modelling on the MIMO channel matrix characteristics. As the transmission distance increases, the singular value characteristics of the MIMO channel matrix according to the spherical wave model gradually converge to those dictated by the simpler plane wave model. The authors define a threshold distance at which the ratio of the largest eigenvalues derived from SWM and PWM exceeds a predefined threshold Γ_{th}, i.e., $\frac{\Gamma_{th}d_t d_R\cos\theta_T\cos\theta_R}{\lambda}$. This threshold distance correlates with the antenna distances d_T and d_R at the transmitter and receiver sides, an auxiliary variable τ_g and rotation angles at both ends. While this method demonstrates relative accuracy with fewer antennas, it faces challenges with larger antenna arrays due to the impracticality of accurately determining the largest eigenvalue. Furthermore, the reliance of this approach on the largest eigenvalue alone limits its accuracy in defining the threshold distance.

c) Effective Multiplexing Distance: In [123], the concept of effective multiplexing distance (EMD) is introduced as a measure of channel capacity in a variety of setups. EMD is defined as the distance between the transmitter and

receiver where the channel can support a given number of simultaneous signal streams at a given SNR. It provides insight into the system configuration required to support the multiplexing gain. Specifically, $D_{\max}^m(\gamma)$ represents the maximum distance at which the channel can effectively accommodate m independent spatial streams simultaneously at a given SNR γ. Table 5 shows the calculated distance for $m = 2$, denoted as $D_{\max}^2(\gamma)$ (i.e., $\frac{D_T D_R}{\lambda \tilde{S}_{\text{asy},m}^*(\gamma)}$), while analytical expressions for $m > 2$ pose challenges for derivation. In addition, $\tilde{S}_{\text{asy},m}^*(\gamma)$ serves as an auxiliary parameter that defines the threshold at which the MIMO system can support m independent spatial streams under the specified SNR γ.

Based on $D_{\max}^m(\gamma)$, the distance regions can be segmented into three intervals. For distances less than the Rayleigh distance, full multiplexing gain can be achieved, allowing maximum transmission rates. This criterion is easily met by adjusting the antenna orientations or directly reducing the antenna spacing. In the communication range between the Rayleigh distance and the effective multiplexing distance, the channel has at least m eigenvalues of comparable magnitude, facilitating multiplexing support. Here, the use of multiple antennas provides both multiplexing and power gains. However, for distances beyond the effective multiplexing distance, the transmit and receive ULAs are significantly separated, resulting in only one dominant eigenvalue in the channel, regardless of the number of antennas at either end. In such scenarios, multiple antennas provide only a power gain.

d) Effective Degrees of Freedom Based Distance: For a MIMO system, channel capacity is a common criterion for assessing system performance, representing the ability of a communication system to transmit information. This capacity is closely related to the effective degrees of freedom (EDoF) of the channel, which is the equivalent number of single-input, single-output subchannels. Because of its direct relationship to spectral efficiency, the EDoF-based limit provides a more accurate characterisation of key channel performance than the traditional Rayleigh distance. Further analysis of performance based on EDoF is discussed in Section II-F.

The authors in [124] investigate a MIMO system using a ULA structure with a continuous aperture. The derived EDoF depends on factors such as the aperture size of the transceiver, the signal frequency and the communication distance. When the distance exceeds the EDoF-based distance, the communication mode for the continuous aperture MIMO system is singular. Therefore, this EDoF-based distance criterion can be thought of as the demarcation line separating the near field from the far field, i.e., $\frac{2D_{\text{tx}} D_{\text{rx}}}{\lambda}$.

5) BOUNDARY DETERMINATION VIA NON-COMMUNICATION METRIC

With the development of cellular technology, more functionalities are integrated into the mobile communication system.

a) Model Mismatch Boundary from Localization Perspective: In 6G mobile communication systems, the integration of higher frequency bands (ranging from mmWave to THz), wider bandwidth, and massive antenna arrays enables high-accuracy and high-resolution sensing. This ISAC in a single system has the potential to revolutionize wireless communication. However, the widely used simplified, stationary, narrowband far-field channel model, although beneficial for radio localization due to its compact formulation, is inadequate. With the increased array size in ELAA systems and the expanded bandwidth at the upper mmWave bands, the impact of channel spatial non-stationarity, spherical wave model (SWM), and beam squint effect cannot be ignored.

In a study by the authors in [125], the model-mismatch error (MME) is defined as the log-normalized difference between the lower bound (LB) and the Cramér-Rao bound (CRB) of the true model. Therefore, the authors introduce a model mismatch boundary as the -3 dB contour of the MME between the true model (TM) and the mismatch model (MM), that is $10 \log_{10}(\frac{|\text{CRB}_{\text{TM}} - \text{LB}|}{\text{CRB}_{\text{TM}}}) = 3\text{dB}$. It is crucial to note that this boundary is derived from a general estimation problem and is applicable to any localization parameters, such as angle, delay, and position.

b) Phase Ambiguity Distance & Spacing Constraint Distance: When it comes to acquisition and positioning, the UE is usually considered as a point target in the traditional wireless channel model. This oversimplified model prevents the array from estimating the attitude of the UE, which is typically described by the spatial orientation. As a result, in order to capture the attitude parameter of the UE, a comprehensive electromagnetic propagation modelling (EPM) based on electromagnetic theory has been developed to accurately model the near-field channel.

However, the joint attitude and position estimation problem established by the EPM model is non-linear and difficult to solve due to the complex exponential coupling. The decoupling method causes a phase ambiguity problem. Specifically, the actual phase can form a mapping relationship with the position of the UE, i.e., $\frac{2\pi}{\lambda} d = \Theta_{\text{actual}} \in [0, \infty)$, while the obtained known phase contradicts this relationship, i.e., $\frac{2\pi}{\lambda} d \neq \Theta_{\text{actual}} \in [0.2\pi)$. Consequently, the authors in [126] proposed *phase ambiguity distance* as a quarter of the Fraunhofer distance (also known as the Rayleigh distance), i.e., $\frac{D_r^2}{2\lambda}$, with the length of the long side of the observed long strip $D_r \geq 4.8\lambda$. The phase ambiguity can be eliminated by the *difference method* if the location of the UE is further than the phase ambiguity distance.

Conversely, if UE is less than the distance, the phase ambiguity cannot be eliminated by arbitrarily selecting to receive elements. Therefore, the distance between the two receiving elements must be reduced. In particular, the authors in [126] defined the *spacing constraint distance* as $\max\{\frac{l_s^2}{\lambda}, 3.6 l_s\}$ when two elements are centred at $l_s/2$ and $3l_s/2$, where l_s is the length of the short side of the observed long strip. Then the unknown integer of the multiple phase

rotation can be obtained and the phase ambiguity can be removed.

F. THEORETICAL PERFORMANCE ANALYSIS

ELAA represents a transformational advance in wireless communication systems, offering unprecedented capabilities to meet the escalating demands for high-speed and reliable connectivity. In this section we begin a comprehensive analysis of the performance characteristics inherent in ELAA systems. The increasing demand for high-speed wireless communications requires a move to higher frequencies, such as millimetre wave and terahertz, where larger bandwidths are readily available [6]. In addition to the antenna array [127], the emergence of innovative technologies such as intelligent surfaces composed of metamaterials has been proposed, allowing the manipulation of EM filed as quasi-continuous sources [44], [128], [129], [130], [131], [132], [133].

There are two important concepts in information theory, i.e., the effective degree of freedom (EDoF) and degree of freedom (DOF). The EDOF of an MIMO system quantifies its equivalent number of independent SISO systems [134], [135], [136], [137]. The DOF denotes the number of significant singular values (eigenvalues) of the channel (correlation) matrix. Therefore, the DoF conveniently summarizes the performance of the MIMO system using a single numerical value whereas the EDOF is directly associated with the spectral efficiency slope [138], and consequently, with the overall channel performance. The relationship between them is that the DOF of an MIMO system has been demonstrated as the upper bound of its EDOF using EM methods [139]. Therefore, the assessment of the maximum EDOF can be conducted by leveraging literature on the number of DoF based on the spatial band limitation properties of the field. Besides, [45] proposed a practical concept of *communication modes* while analysing the performance of LISs, especially in the near-field region. Communication modes correspond to orthogonal channels established between pairs of antennas, enabling a significant enhancement in channel capacity through the parallel multiplexing of data [140].

Based on information theory analysis [141], the channel capacity increases linearly with the number of spatial DoFs, which depends on both the scattering environment and the antenna array geometries. Numerous previous studies have investigated MIMO performance under different propagation conditions and array geometries [41], [43], [44], [137], [142]. In work [43], a Fourier orthonormal expansion was developed to calculate the DoF limit in the far-field region. The number of communication modes or degrees of freedom for scalar waves can be written in closed form, depending on the dimension and shape of the antennas, the link distance and the operating frequency [143]. In addition, [144] introduced a CAP MIMO framework that achieves near-optimal performance with low complexity. This is achieved by generating orthogonal beams in the angular domain using aperture antennas that provide high flexibility in shaping the EM wavefront.

Unfortunately, with the trend towards higher frequencies, multipath propagation tends to become sparse, while LoS propagation becomes dominant, limiting the ability to improve DoF. As a result, these models based on the far-field EM propagation assumption (e.g., Friis' transmission formula) may prove inadequate [20], [73], [72], [105], especially with the significant increase in antenna aperture and higher operating frequencies. This shift towards near-field communication has emerged as a more practical scenario. In recent decades, numerous studies have demonstrated the potential to achieve multiple channels by placing antenna arrays in close proximity to each other or by using very large arrays (in discrete source, e.g., $\lambda/2$ antenna spacing to make mutual coupling negligible), especially in the near-field region, even in LOS, thus without relying on multipath propagation. [121], [122], [145]. However, discrete sources cannot fully exploit the ultimate limits of the wireless channel and the possibilities offered by metamaterials due to the discrete sampling of the EM channel and waves [146]. In addition, alternative practical approaches proposed in recent years, focusing on the generation of orbital angular momentum (OAM) beams [147], [148], [149], [150], [151], [152], have shown that the maximum number of communication modes is limited [140]. Therefore, near-field modelling, spatial DoF and its capacity limit are essential. Several efforts have been made to bridge this gap, drawing on Green's function and electromagnetic theory for either free space or multipath environments [46], [52], [121], [135], [138], [153], [154], [155], [156], [157]. For example, [46] proposed a practical method based on the multiple beam focusing capability of a large aperture array in the near-field region to generate multiple quasi-orthogonal beams (i.e., communication modes), and derived a closed-form approximation for the number of communication modes in the near-field. However, the channel model in this work is based on the scalar Green's function and thus cannot capture the full polarisations of the EM fields.

As a result, [52] the DoF and EDoF limits of a space-constrained MIMO system are derived based on the EM channel matrix derived from the full-polarisation dyadic Green's function. Reference [53] determined the extra DoF and capacity limit within a generalised stochastic spatially stationary monochromatic channel, taking into account evanescent waves in reactive near-field communication. Reference [124] derived closed-form expressions of the EDoF quantifying the number of equivalent SISO channels for both discrete and continuous aperture antennas. In particular, for continuous aperture antennas, the EDoF depends on the aperture size of the transceiver, the link distance and the operating frequency. On the other hand, for discrete antennas, the antenna spacing plays a significant role, while the aperture size of each antenna element does not affect the value of the EDoF. Reference [124] also showed that the performance of the discrete MIMO system approaches that of the continuous aperture MIMO system with appropriate adjustments in antenna spacing and element

size. Finally, the study described in [39] investigates the performance of a novel array architecture known as modular ELAA. In this architecture, a large number of array elements are organised in a modular fashion. The authors derived a closed-form expression for the maximum SNR achievable with MRC beamforming. They showed that the maximum SNR is affected by several factors, including array geometry (such as array aperture and module spacing) and user location. In addition, their asymptotic analysis showed that as the array size increases by adding more modules, the SNR tends to converge to a constant value determined by the module separation and the projected distance of the user to the modular ELAA.

III. CHALLENGES AND SOLUTIONS
A. CHANNEL ESTIMATION

Channel modeling and channel estimation are essential components in wireless communication systems, playing a pivotal role in achieving reliable and efficient data transmission. Channel modeling provides a theoretical foundation for understanding how electromagnetic waves propagate in the wireless environment, enabling engineers and researchers to simulate and analyze system performance accurately. It helps in assessing the impact of various factors such as distance, interference, and environmental conditions on signal quality. On the other hand, channel estimation is a practical process that involves estimating the current state of the wireless channel based on received signals. This real-time information is critical for adapting the communication system to changing conditions, optimizing resource allocation, and mitigating interference. The relationship between channel modeling and channel estimation is symbiotic. Accurate channel models serve as a reference for designing estimation algorithms, while channel estimation provides valuable feedback to refine and validate the models. To effectively estimate the channel for ELAA systems, it is imperative to account for the unique characteristics of the near-field environment. These include spherical wave properties, spatial non-stationarity, EM polarization characteristics, and mutual coupling effects. Incorporating these aspects is crucial for accurate channel estimation in ELAA systems. However, achieving this accuracy often involves a tradeoff with computational complexity, especially considering the dynamic nature of near-field interactions and the high-dimensional parameter space involved. Striking the right balance between accuracy and computational complexity is therefore a key consideration in designing efficient channel estimation algorithms for ELAA systems.

1) ESTIMATION FOR SPHERICAL WAVEFRONT

a) Channel Sparsity based Method: Sparse representation has attracted considerable research interest in wireless communications, particularly in scenarios where a large number of antennas are deployed. The main reasons for this are as follows. First, sparse representation exploits the idea that in many wireless environments, the channel response is not uniformly active across all antennas. Sparse channels better reflect real-world scenarios where only a limited number of propagation paths carry significant power, while the rest have negligible contributions. Using a sparse representation reduces the complexity of channel estimation by focusing on characterising the significant channel components rather than estimating an overwhelming number of parameters associated with each antenna element. This not only conserves computational resources, but also minimises the overhead required for training and feedback in complex MIMO systems. In 5G MIMO systems, a far-field beamformer codebook has been introduced to exploit the sparsity of the channel in the angular domain. This codebook is designed so that each codeword corresponds to a planar wave associated with a specific angle of incidence. By exploiting the concept of far-field communication, where the signal propagates as plane waves and the angular information is particularly important, this codebook optimally adapts the beamforming patterns to the characteristics of the wireless channel. This approach enhances the system's ability to direct and focus transmitted signals to the intended receiver, improving signal quality, reliability and overall spectral efficiency.

Compressive sensing (CS)-based channel estimation techniques have emerged as a revolutionary approach in wireless communications. CS techniques exploit signal sparsity to efficiently recover the channel state from fewer measurements than traditional methods, leading to significant advantages in reducing pilot overhead and improving spectral efficiency [158], [159], [160], [161], [162], [163], [164]. For example, the orthogonal matching pursuit (OMP) algorithm and its extensions have been employed to recover the angular domain channel. In this method, the channel is transformed into its angular domain representation using the standard spatial Fourier transform. This approach exemplifies the application of compressive sensing techniques in channel estimation, where the angular domain information is recovered effectively through such algorithms [159]. OMP and related algorithms then facilitate the reconstruction of this transformed channel, effectively capturing the critical angular information while exploiting its inherent sparsity.

In addition, it should be noted that methods for estimating angular domain parameters, such as Angle of Departure (AoD) and Angle of Arrival (AoA), are often based on the assumption that these parameters are discrete and fall on a predefined grid of angular values. This is referred to as an "on-grid" method. However, there are also techniques for estimating these parameters in a continuous manner, known as "off-grid" methods [165], [166], [167], [168]. These off-grid methods address the limitations of on-grid algorithms by offering improved and the ability to estimate angles more accurately. However, conventional channel estimation methods, which rely on the sparsity of angular parameters such as AoDs and AoAs, have limitations when applied to ELAAs. This is primarily due to the fact that the assumption of channel sparsity in the angular domain is invalid in the near field, where the receiver is positioned close to
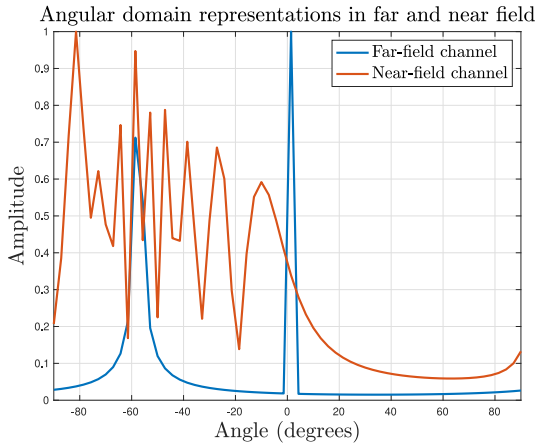
FIGURE 9. Comparison of angular-domain representations between far-field and near-field channels. The near-field channel exhibits an energy spread effect, leading to a broader angular distribution compared to the concentrated far-field response. An example with $L = 2$ propagation paths is shown to illustrate the difference in angular dispersion.

the transmitter array. As a result, traditional approaches that assume angular sparsity fail to accurately capture the channel characteristics in this regime. To address this challenge, it is crucial to investigate channel estimation techniques that exploit the spherical wavefront and corresponding sparsity characteristics inherent to the near-field environment.

- *Polar domain sparsity:* In near-field communications, the wavefront is more accurately modelled under the spherical wavefront assumption [68]. This model is influenced not only by the AoD/AoA but also by the distance between the BS and potential scattering objects in the environment. Reference [56] brought to light the energy spread effect that occurs when classical angular domain channel estimation methods are applied. As shown in Fig. 9, these methods result in significant energy dispersion over multiple angles when attempting to represent the near-field channel in the angular domain. Consequently, when estimating channels in the near-field, it is critical to account for both angular sparsity and distance-related variations. To address this, [56] proposed a polar-domain representation specifically tailored to capture the sparsity of near-field channels. This approach involves designing a new transform matrix by minimizing the coherence between codewords based on the Fresnel approximation. In this representation, angular components are sampled uniformly, while distance components are sampled non-uniformly to better align with the characteristics of the near-field environment. By transforming the channel from the spatial domain to the polar domain, this method effectively leverages the inherent sparsity of the near-field channel. This transformation facilitates the application of compressive sensing techniques, enabling low-overhead and efficient channel estimation in scenarios involving ELAA.

- *Block sparsity exploitation:* Although the proposed polar-domain representation method effectively adapts to the near-field propagation environment by ensuring the sparsity of the near-field channel in the polar domain [56], it introduces significant challenges. The mapping process tends to increase the number of total channel taps substantially, leading to a corresponding rise in computational complexity. Additionally, the large number of non-zero channel taps, which can exceed the upper limit of sparsity, renders conventional channel estimation methods unreliable. In the near-field, due to energy dispersion and scatterer aggregation effects, the channel exhibits a block structure in the angular domain. By exploiting this block sparsity, it is possible to achieve exceptional channel estimation accuracy [169], [170]. Specifically, three key perspectives are considered to enhance the sparsity threshold necessary for accurate channel estimation: previous-time slot information, joint correction across different sub-carriers, and the aggregation of multi-path energy [169]. Furthermore, considering the dual-band deployment common in practical communication systems, a dual-band near-field communication model is proposed. This model leverages the likelihood that high-frequency systems will be deployed alongside lower-frequency systems, providing a more comprehensive approach to channel estimation [170]. Theoretical analyses are conducted to ensure minimal estimation error, and a suite of algorithms is developed to capitalize on this finely-tuned side information.

- *Angular-distance decomposition:* When employing grid-based methods to achieve a sparse representation of polar-domain channels, one major challenge is the inability to maintain strict orthogonality between different grids, leading to energy leakage and reduced accuracy. Furthermore, the process of gridding angular and distance parameters results in a complex three-dimensional grid space, making the search for geometric path parameters inefficient and computationally burdensome, especially in systems with a large antenna count. Consequently, there is a pressing need for a refined gridding technique that balances efficiency, complexity, and robustness to enhance channel estimation performance. Several approaches have been developed to address these challenges [171], [172], [173]. Specifically, parametric deconstruction techniques were proposed in [171], [172] for a more general uniform planar array (UPA) scenario, which includes both two-dimensional azimuth-elevation angles and distance parameters. In this approach, the coupled geometric parameters–comprising pairs of elevation-azimuth angles and distance–are independently decomposed by mapping the original channel matrix to three separate covariance matrices, each corresponding to a single geometric parameter. This decomposition transforms the problem

TABLE 6. Complex valued channel response representations.

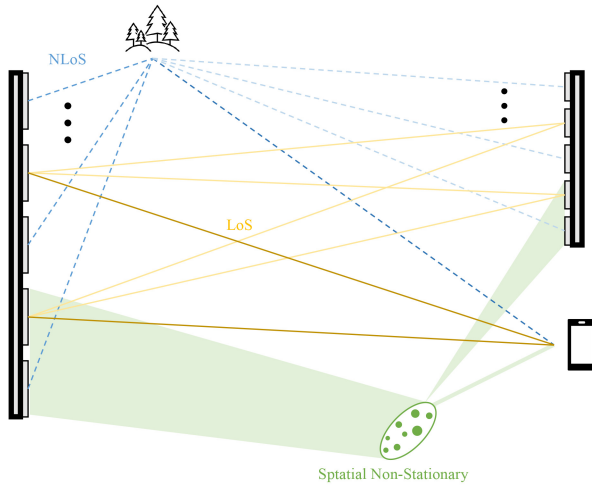| Category	scenario	Expression	Sparse Representation
Far-field	MISO NLoS	$\mathbf{h_{ff}} = \sqrt{\frac{N}{L}} \sum_{l=1}^{L} \alpha_l \mathbf{a}(\theta_l)$	$\mathbf{h_{nf}} = \mathbf{F}\mathbf{h^P}$
	MIMO NLoS	$\mathbf{H_{ff}} = \sqrt{\frac{N}{L}} \sum_{l=1}^{L} \alpha_l \mathbf{a}(\theta_l^r) \mathbf{a^H}(\theta_l^t)$	$\mathbf{H_{ff}} = \mathbf{F_r} \mathbf{H^P} \mathbf{F_t^H}$
Near-field	MISO NLoS	$\mathbf{h_{nf}} = \sqrt{\frac{N}{L}} \sum_{l=1}^{L} \alpha_l \mathbf{b}(\theta_l, \mathbf{r}_l)$	$\mathbf{h_{nf}} = \mathbf{D}\mathbf{h^P}$
	MIMO NLoS	$\mathbf{H_{nf}} = \sqrt{\frac{N}{L}} \sum_{l=1}^{L} \alpha_l \mathbf{b}(\theta_l^r, \mathbf{r}_l^r) \mathbf{b^H}(\theta_l^t, \mathbf{r}_l^t)$	$\mathbf{H_{nf}} = \mathbf{D_r} \mathbf{H^P} \mathbf{D_t^H}$
	MIMO LoS	$\mathbf{H_{nf}} = \frac{1}{r_{n_2,n_1}} e^{-j\frac{2\pi}{\lambda} r_{n_2,n_1}}$	-

FIGURE 10. ELAA multipath and spatial non-stationary channel model.

into three independent one-dimensional (1D) parameter recovery tasks that can be efficiently solved using compressive sensing techniques. This method significantly reduces complexity, shifting from a multiplicative to an additive complexity order. Meanwhile, the authors in [173] introduced a wavefront transformation-based approach to approximate or convert a near-field channel into a far-field channel. By applying a discrete Fourier transform (DFT) matrix, the channel is projected onto the angle domain, preserving its sparsity. Unlike far-field channels, near-field channels include an additional distance matrix, representing the phase deviation across different antenna elements. To mitigate the effects of this phase deviation, a full-rank matrix orthogonal to the space of the far-field steering vector matrix is constructed, leveraging the structural similarities between near-field and far-field channels.

- *Hybrid near-far field and Mixed LoS/NLoS path:* As the array aperture expands, both near-field and far-field effects coexist, creating a hybrid near-far field scenario. This duality complicates traditional channel modeling, which typically assumes either a pure near-field or far-field environment, leading to inaccuracies in channel estimation and signal processing. Moreover, in practical deployments, communication paths often consist of a mixture of LoS and Non-Line-of-Sight (NLoS) components as shown in Fig. 10. The simul-

taneous presence of these paths introduces additional complexity, as LoS paths are typically deterministic while NLoS paths are subject to significant scattering and reflection, further challenging traditional models. Thus, to accurately characterize and leverage the potential of modern communication systems, it is essential to develop models that account for both the hybrid near-far field effects and the mixed LoS/NLoS propagation paths. [174], [175] investigated accurate channel estimation for hybrid-field MISO channels. Specifically, [174] proposed an efficient hybrid-field channel estimation scheme by accurately modelling the ELAAs channel, which contains both far-field and near-field components. Reference [175] further proposed a practical strategy to realise efficient channel estimation by considering hybrid-field MIMO channels, which do not require the ratio of the number of far-field and near-field paths as prior knowledge. For near-field MIMO channels, where both transmitters and receivers are equipped with multiple antennas, the LoS and NLoS path components of the near-field MIMO channel models are different. The existing near-field XL-MIMO channel models that accurately describe the NLoS path component of near-field MIMO could be described as the product of the near-field response array vector [176], which is similar to the far-field NLoS path channel model. However, due to the large aperture of ELAAs, each transmit and receive antenna pair experiences a different propagation path and should therefore be modelled individually [32]. A two-stage channel estimation algorithm has been proposed to estimate the mixed LoS and NLoS paths. Table 6 summarises the channel model with different categories, where $\boldsymbol{a}(\theta)$ and $\boldsymbol{b}(\theta, r)$ denote the far- and near-field steering vectors, and L represents the total number of path. To address the challenges posed by hybrid channel estimation in environments where both near-field and far-field effects coexist, particularly in the presence of power diffusion that can severely degrade performance, a novel approach has been proposed in [177]. This method introduces a joint angular-polar domain channel representation, which incorporates both near-field and far-field steering vectors into the compressed sensing dictionary. In detail, the near-field region is partitioned two-dimensionally, accounting for both direction and distance using near-field steering vectors, while the

far-field region is partitioned one-dimensionally in direction using far-field steering vectors. This dual-domain partitioning allows the model to more accurately capture the hybrid characteristics of the channel. By calculating the extent of power diffusion, the proposed method identifies and eliminates the power diffusion effect from the channel estimation process. This ensures that the estimation of the remaining path components is unaffected by power diffusion, thereby making the standard Orthogonal Matching Pursuit (OMP) algorithm reliable in this context. An important advantage of this approach is that it does not require prior knowledge of the number of near-field and far-field paths, making it highly adaptable to various scenarios in ELAA-based systems. A unified ELAA channel model, presented by [178], offers a concise closed-form expression with minimal approximation error. This model effectively integrates the differences between LoS and NLoS paths, spherical and planar wavefront propagation, and scenarios involving single-antenna and multiple-antenna users within a single framework. Additionally, a low-complexity compressive sensing-based scheme, specifically the OMP algorithm, was developed utilizing this unified framework.

b) Learning based Method: Learning-based channel estimation in ELAA near-field scenarios is a burgeoning research area that leverages machine learning techniques to accurately estimate channel characteristics in the vicinity of ELAAs. As traditional channel estimation methods may face challenges in near-field environments due to the complex electromagnetic interactions, learning-based approaches provide a promising alternative by exploiting data-driven and model-driven algorithms to adaptively capture channel dynamics. These methods aim to enhance the efficiency and accuracy of channel estimation processes, ultimately facilitating the optimization of communication performance in ELAA-enabled networks.

Reference [179] investigated a hybrid spherical- and planar-wave channel model and proposed a two-phase channel estimation approach based on subarray partitioning. Initially, a convolutional neural network (CNN) was meticulously designed to effectively estimate crucial channel parameters such as azimuth and elevation angles of departure and arrival, amplitude of path gain, and communication distances between reference subarrays. Subsequently, leveraging the geometric relationships between reference subarrays, the remaining channel parameters were accurately estimated in the second phase of the channel estimation process. The findings highlighted the rapid convergence and high-resolution parameter estimation capabilities of the designed neural network, resulting in significantly reduced complexity while achieving precise channel estimation.

To address the hybrid characteristics of far-field and near-field channels, an effective deep learning-based channel estimator was introduced in [180], [181], which has adaptive

complexity and a linear convergence guarantee. Inspired by fixed-point theory, each iteration of orthogonal approximate message passing was transformed into a contractive mapping by replacing the nonlinear estimator with a carefully trained CNN. A notable algorithmic advance was the use of fixed-point iteration to compute the channel estimate, while accommodating neural networks of arbitrary depth and adapting to the unique conditions of hybrid field channels. The proposed method has several advantages, including low complexity and robustness to the complex channel conditions typically encountered in practical THz environments. Furthermore, the framework can be seamlessly extended to wideband systems, effectively addressing challenges such as the beam squint effect.

To exploit the sparsity inherent in polar domain channels, learning-based approaches have been introduced, as demonstrated in [182], [183], [184]. More specifically, the authors in [182] introduced a distance-parameterized angular-domain sparse model for representing the near-field channel. They developed a channel estimation algorithm based on joint dictionary learning and sparse recovery, where the user's distance is treated as an unknown parameter within the dictionary. By addressing the coupling between angle and distance, this approach effectively overcomes challenges associated with the polar-domain method, such as storage burden and high column coherence. Unlike the polar-domain representation, the size of the constructed dictionary in this method is solely determined by the angular resolution. Reference [183] proposes a novel deep unrolling algorithm that enhances the sparsity-inducing capabilities of the iterative shrinkage and thresholding algorithm (LISTA) for sparse channel estimation. This approach mitigates the computational burden associated with conventional spatial gridding dictionaries by integrating the sparse representation process into each layer of LISTA as a neural network layer. Consequently, the proposed method optimises a sparse dictionary during the training phase of LISTA by exploiting the intrinsic properties of near-field channels. In [184], a channel estimation approach that exploits the sparsity inherent in polar-domain channels in XL-MIMO systems is presented. The method employs a polar domain multiple residual dense network, which is specifically designed to exploit channel sparsity. In addition, an Atrous spatial pyramid pooling based residual dense network is proposed to address multi-scale features. This incorporates Atrous spatial pyramid pooling as a parallel branch alongside the residual dense network. Finally, a polar domain multi-scale residual dense network is introduced to further improve the estimation accuracy.

2) ESTIMATION TECHNIQUES FOR SPATIAL NON-STATIONARITY

The adoption of ELAA introduces unique characteristics to the near-field channel environment, distinguished notably by the presence of spherical wavefronts and spatial non-stationarity. While conventional techniques such as CS

remain applicable in ELAA systems, leveraging polar-domain representation at higher frequencies (e.g., [56]), challenges arise due to the spatially non-stationary nature of the channel. Unlike traditional scenarios where sparse representations effectively capture channel characteristics, spatial non-stationarity induces inconsistencies in the sparsity patterns across different channel parts as shown in Fig. 10. Consequently, novel approaches are required to address the intricacies of channel estimation in the presence of spatial non-stationarity, ensuring both accuracy and computational efficiency in ELAA systems.

a) Compressive Sensing based Method: Despite the spatially non-stationary nature of the channel in ELAA systems, which poses a challenge for the design of sparse channel estimation schemes based on CS due to the large size of the antenna array, it is worth noting that the spatially stationary channel condition remains applicable within each sub-array. In these sub-arrays, the sparsity of the channel can still be exploited for effective channel recovery. Therefore, to address the challenges posed by the spatially non-stationary multipath channel in ELAA systems, algorithms such as those proposed in [90], [185] advocate sub-array-wise channel estimation. By exploiting the sparsity inherent in these non-stationary channels, these algorithms divide the array into sub-arrays and capture the sparse characteristics of the delay domain. They then apply CS-based methods for channel estimation, typically using a two-stage approach. First, the channel is coarsely estimated on a higher-layer grid, followed by the application of threshold-based denoising methods to refine the support. Numerical evaluations, particularly in terms of mean square error (MSE), illustrate the effectiveness of these proposed algorithms.

While the overall channel exhibits spatial non-stationarity over the entire antenna array, it's noteworthy that the channel associated with each sub-array can still be considered spatially stationary. Exploiting this property, various CS-based channel estimation algorithms can be applied to recover the corresponding subchannels with minimal pilot overhead. However, due to the hybrid precoding structure, extracting the received signals corresponding to each sub-array poses a significant challenge as the received signals are a mixture of all BS antennas. Inspired by the Alamouti scheme, a novel scheme based on Group Time Block Code (GTBC) has been proposed to facilitate signal extraction [186], [187]. During coding, the antennas within each group exhibit consistent behaviour, allowing the extraction of signals corresponding to each group. At the decoding stage, the original received signal is combined based on the designed GTBC, allowing the extraction of signals corresponding to each sub-array for further processing. Based on the proposed GTBC-based signal extraction scheme and the channel estimation algorithms in [56], novel near-field channel estimation schemes have been proposed. These include an on-grid GTBC-based polar-domain Simultaneous Orthogonal Matching Pursuit algorithm and an off-grid GTBC-based polar-domain Simultaneous Iterative Gridless Weighted algorithm, both tailored to efficiently estimate spatially non-stationary channels. These schemes promise improved accuracy and computational efficiency in capturing the complex channel characteristics of Extra Large MIMO systems subject to spatial non-stationarity.

b) Joint Activity and Channel Estimation: In wireless networks, accurate estimation of both user activity (e.g., the presence or absence of users in a wireless network) and channel characteristics is essential to optimise system performance and resource allocation. The joint activity and channel estimation (JACE) problem in ELAA systems, especially those subject to spatial non-stationarity, is a significant challenge in wireless communications. XL-MIMO systems exhibit spatial non-stationarity characterised by VRs, which lead to a subarray-wise sparse structure of the channel matrix. In grant-free access mode, where only a fraction of potential users are active at any given time slot, the channel matrix further exhibits a doubly sparse and user-specific structure, where each user activity and each sub-array activity are jointly modelled by a nested Bernoulli-Gaussian distribution. To address this complex inference problem, novel Bayesian bilinear inference algorithms have been proposed [188], [189], which are able to simultaneously capture the different structured sparsities inherent in the channel matrix. These algorithms use expectation maximisation-based auto-parameterisation to jointly estimate channel coefficients, user activity patterns and sub-array activity patterns, effectively mitigating the effects of spatial non-stationarity. In addition, a Matérn cluster point process based approach is introduced to realistically model clustered activity patterns within VRs. Through extensive numerical simulations, the effectiveness of the proposed bilinear JACE algorithm is demonstrated, outperforming state-of-the-art methods and approaching the performance of a ghost-based scheme over a wide range of SNRs and activity scenarios.

c) Learning based Method: Despite their advantages, the aforementioned schemes rely on abstracted channel models with specific characteristics, such as channel sparsity, and their application to practical systems remains challenging, especially when considering hardware imperfections. In addition to model-based channel estimation schemes, model-free approaches to channel estimation, coupled with recent advances in deep learning (DL) technologies, have been explored for use in practical wireless communication systems. For example, the authors in [190] used the super-resolution (SR) image recovery scheme to model nonlinear interpolation relationships in conventional channel estimation problems without relying on prior statistical channel knowledge during online interpolation, which achieves better interpolation results in stationary and non-stationary channel fading environments. The numerical channel coefficients are generated and trained offline according to statistical channel models. The proposed unified SR-based channel estimation scheme demonstrates superior performance compared to

several baselines, providing valuable insights for future deep learning-based wireless communication systems.

Sparse Bayesian learning provides a principled framework for estimating complex and high-dimensional models, especially in scenarios with limited or incomplete data, by promoting sparsity in the underlying parameters or features. The paper [191] proposes an adaptive grouping sparse Bayesian learning (AGSBL) scheme for uplink channel estimation. By judiciously designing a hierarchical prior model controlled by tunable hyperparameters, the proposed scheme efficiently exploits the partial joint sparsity shared by groups of channel vectors. This adaptive approach significantly improves the channel estimation performance, which is confirmed by simulation results demonstrating the superiority of AGSBL over related schemes.

B. BEAMFORMING DESIGN

Beamforming is a signal processing technique used in antenna arrays to transmit or receive directional signals. By combining elements in an antenna array so that signals at certain angles experience constructive interference while others experience destructive interference, beamforming improves the performance and efficiency of wireless communication systems.

1) BEAM FOCUSING DESIGN

With known channel state information (CSI), traditional MIMO beamforming design techniques such as MRC, zero-forcing (ZF) and minimum mean square error (MMSE) can be used for near-field beamforming to achieve spatial multiplexing. As explained above, the presence of a spherical wave in the near field enables the phenomenon of finite beam depth. This phenomenon allows the concentration of radiated energy at a specific focal point (beam focusing), as opposed to the more directional transmission characteristic of far-field beamforming. Recently, [45] derived accurate analytical expressions for the link gain and available spatial DoF using an electromagnetic-based approach and the available spatial DoF was obtained. Remarkably, the available DoF was shown to be greater than one even under LoS conditions when using LIS. This is in contrast to conventional MIMO systems where spatial multiplexing gains are typically only achievable in high scattering environments, i.e., NLoS. Reference [192] introduced the basic principles and applications of near-field shaping around the focal point.

The concept of finite spatial-depth beamforming, which exploits the spherical wave in near-field communications, was introduced in [6], [104] and provided a profound perspective on the potential of ELAAs. Reference [75] also revealed a window effect for the energy focusing property of an extremely large lens antenna array, which has great potential for position sensing and multi-user communication. Similarly, the concept of location division multiple access (LDMA) was proposed in [193] to improve spectrum efficiency by introducing additional resolution in the near-field distance domain compared to spatial division multiple

access (SDMA), where angular orthogonality occurs only in the far-field. In addition, [194], [195] further investigated the beam characteristics in the wide bandwidth and proposed potential techniques to solve a wide bandwidth phenomenon known as beam squint. Reference [33] proposed an efficient wideband beam training scheme with low training overhead to create beams focused at multiple locations at different frequencies using time-delay beamforming [196].

2) CODEBOOK DESIGN

Codebook design is a fundamental aspect of beamforming, particularly in the context of MIMO and mmWave technologies. A codebook consists of a set of predefined beamforming vectors or matrices that are used to direct the transmitted signal to the receiver in the most efficient manner. The primary objective of codebook design is to optimise the selection of these beamforming vectors to maximise system performance in terms of coverage, capacity and signal quality. Near-field codebook design is essential for wireless communication systems operating in the near-field region, which is of particular relevance to ELAA. Unlike far-field communications, where wavefronts can be approximated as planar, near-field communications deal with spherical wavefronts due to the proximity of the transmitter and receiver. Designing a codebook for near-field beamforming involves several unique challenges and considerations: spherical wave propagation, spatial non-stationarity, beam focusing and complexity.

In [197], the authors investigated the quantization performance of codewords in near-field ULA and UPA systems. They found that the quantization performance of ULA codewords exhibits symmetry and stationarity, which can be represented by an elliptic formula. In contrast, the correlation formula for UPA codewords is non-stationary and asymmetric, which can be approximated by an ellipsoid formula. Based on these adjusted correlation formulas, the authors proposed near-field codebook schemes designed to maximise the minimum correlation. These schemes aim to improve performance by ensuring that the codewords are optimally spaced. In addition, they introduced a dislocation codebook to further reduce the quantization overhead for both ULA and UPA systems. Analytical results demonstrated the benefits of oversampling in the angular domain, which is crucial for designing near-field codebooks with high minimum quantization correlation. This study highlights the importance of tailored codebook design in near-field communication systems, emphasising how geometric properties and spatial configurations can significantly affect quantization performance.

3) BEAM TRAINING DESIGN

Beam training is a critical process in modern wireless communication systems, particularly at mmWave and THz frequencies where directional communication is essential due to high path loss. The primary objective of beam training is to establish the best possible directional paths between the

transmitter and receiver by aligning their beam patterns. This process involves a series of steps to identify the optimum beam pair from a predefined codebook of beam patterns. Beam training typically involves initial access, where the transmitter and receiver scan through possible beam directions to establish a link, followed by beam refinement to fine-tune the alignment for optimum performance. Effective beam training improves link reliability, increases data rates and ensures robust communications, especially in dynamic environments where users and obstacles can cause frequent changes in the communication channel.

Compared to conventional far-field beam training, which simply searches for the optimal beam direction, near-field beam training is more complex. This complexity arises because, due to the spherical wavefront propagation model, it requires beam search in both angular and distance domains. Near-field beam training using a polar-domain codebook and on-grid range estimation, as proposed in [56], faces challenges such as long training overhead, high codebook storage requirements, and degraded estimation accuracy. Efficient beam training schemes are needed to overcome these problems. In [198], the authors observed that the actual spatial direction of the user is approximately in the centre of a newly defined dominant angle region. Based on this, they proposed a two-phase fast beam training method to significantly reduce the near-field beam training overhead compared to exhaustive search methods. In the first phase, the user's candidate angles are determined using a far-field codebook and angle-domain beam sweeping. In the second phase, a customised polar domain codebook is used to find the best effective distance of the user given the shortlisted candidate angles. This approach avoids the need for a full angle-domain search, effectively reducing the training overhead. Another approach to reduce training overhead is off-grid estimation. In [199], two efficient beam training schemes with off-grid range estimation using a conventional Discrete Fourier Transform (DFT) codebook have been proposed. The first scheme estimates the user angle based on a defined angular support and resolves the user range using an approximated angular support width. The second scheme improves the range estimation accuracy by estimating the user range and minimising a power ratio MSE. These approaches aim to improve beam training efficiency while maintaining high estimation accuracy. The authors in [33] demonstrated that the near-field beam splitting effect can also facilitate fast near-field beam training in wideband ELAA systems. Exploiting this phenomenon, they proposed a fast wideband beam training scheme that generates beams focused at multiple locations at multiple frequencies using time-delay beamforming. This approach increases the efficiency and speed of the beam training process, making it particularly suitable for wideband ELAA applications.

Hierarchical beam training schemes are considered to be an effective way to reduce overhead in near-field scenarios [200], [201], [202]. The authors in [200] proposed a two-stage hierarchical beam training method, inspired by the observation that the near-field energy spread effect can be mitigated by properly activating a central sub-array of the ELAA beam training system. In the first stage, different from determining the central position within a dominant-angle region in [198], they estimate the coarse user direction using the sub-array technique to implement conventional far-field hierarchical beam training. In the second stage, they progressively refine the user direction and effective range using a dedicated polar domain hierarchical codebook and a novel beam training method. Similarly, [201] proposes a near-field two-dimensional hierarchical beam training scheme using multi-resolution codebooks. In these multi-resolution codebooks, codewords are searched layer by layer, gradually reducing the angle and distance ranges. This method effectively narrows the search space, thereby reducing the training overhead. In addition, addressing beam training in near-field spatially non-stationary channels is critical. Inspired by joint time-frequency analysis for non-stationary signals, the authors in [202] project the near-field beam steering vector into a two-dimensional spatial angular plane to capture its spatial non-stationary characteristics. They propose a novel spatial chirp-based hierarchical beam training scheme for near-field ELAA. This scheme not only reduces the training effort compared to exhaustive search, but also flexibly adapts to the specific distance-related dominant region for each near-field beam. Overall, these hierarchical beam training schemes improve the efficiency of near-field beam training by reducing the search space and accommodating the unique characteristics of near-field channels.

Recent results have demonstrated that deep learning methods, when applied to near-field beam training, can significantly reduce pilot effort. Taking advantage of the powerful ability of neural networks to learn non-linear relationships, [203] proposed a deep learning-based beam training scheme for the near-field domain in ELAA systems. This approach involves designing two neural networks based on the received signals of the far-field wide beam: one network estimates the angle, while the other estimates the distance of the optimal near-field beam. In addition, an improved scheme for performing additional beam testing has been introduced, which significantly improves the performance of beam training.

4) NOVEL WAVEFRONT ENGINEERING AT HIGH-FREQUENCY BANDS

The shift to high-frequency communication systems, including millimeter-wave mmWave [204] and THz bands [205], [206], [207], opens up new possibilities as well as significant challenges for wireless networks. The shorter wavelengths associated with these frequencies enable ultra-fast data transmission and support for a vast number of connected devices, making them essential for the evolution of next-generation wireless technologies. However, as frequencies push further into the THz range, propagation losses become a critical issue. A widely adopted approach to counteract these losses is the use of high-gain antennas

that generate highly focused beams [208]. This, however, increases the vulnerability of THz links to blockages, as obstacles like people and objects can easily disrupt the LoS connection [209]. While NLoS communication can occasionally be achieved via reflections or scattering from environmental structures, or with the help of RIS, these alternative paths often lack the necessary signal strength to maintain high data rates.

Given the near- and far-field boundaries outlined in Table 5, the use of large-aperture antenna arrays at high-frequency bands significantly increases the likelihood of users operating within the near-field region. This is a departure from traditional wireless systems, which primarily function in the far-field range. As a result, the unique propagation characteristics of the near-field region must be considered when designing and optimizing high-frequency communication systems. Alternative approach to mitigating blockage-related disruptions involves the use of novel wavefronts through wavefront engineering [210], [211]. According to the Huygens-Fresnel principle, the beam's characteristics are entirely determined by the phase and amplitude distribution of the electric field at the radiating aperture [211]. Thus, generating a desired beam requires engineering the corresponding wavefront through a specific phase profile. This can be achieved not only with antenna arrays but also with custom-designed lenses or by leveraging reflectarrays and metasurfaces.

Beamfocusing and beamforming are essential techniques in wireless communication, each suited for different operational environments in the near and far fields. In beamfocusing, the transmitting array is designed with a lens-like quadratic phase profile, which concentrates the signal at a specific focal point in the near field. This creates a converging wavefront, leading to peak beam intensity at the focal point, with the beam spot size determined by the Abbe limit. This method is highly effective for targeting energy to a precise location but requires exact CSI and continuous mobility tracking to maintain focus. On the other hand, beamforming is the far-field equivalent, where the focal point is effectively at infinity. Here, the quadratic phase profile becomes uniform, resulting in a planar wavefront that forms a beam, which gradually diverges as it propagates due to the finite aperture size. This creates a highly directional beam that can reduce interference and maximize signal strength over long distances. While beamforming is effective for long-range communication, it is only suitable in the far field and is less capable of withstanding obstructions. Both techniques are crucial for optimizing high-frequency communication, yet each comes with specific limitations, especially regarding resistance to blockages.

a) Bessel Beams: Bessel beams are a class of waveforms characterized by their unique ability to maintain a non-diffracting, self-reconstructing profile as they propagate through space. Unlike traditional Gaussian beams, which tend to spread out and lose focus over distance, Bessel beams exhibit an inherent resistance to diffraction. This

remarkable property stems from their underlying structure, where the beam's intensity is described by a Bessel function of the first kind [212], [213], [214]. The resulting wavefront of a Bessel beam features a central core surrounded by concentric rings of light or electromagnetic energy, forming a pattern that remains stable over an extended range. The generation of Bessel beams typically involves the superposition of multiple plane waves converging at specific angles, which creates a central peak with a series of surrounding concentric rings. This configuration allows the beam to maintain its focus and intensity even in the presence of obstacles, as the central peak can self-reconstruct if partially obstructed. This self-healing property is particularly advantageous in environments where blockages or scatterers might otherwise disrupt the signal path [215], [216], [217]. In high-frequency communication systems, such as those operating at mmWave and THz frequencies, Bessel beams offer significant benefits [210], [211], [213]. These systems are often plagued by issues like severe path loss, diffraction, and susceptibility to blockages, which can severely degrade signal quality. Bessel beams, with their non-diffracting nature and resilience to obstacles, provide a robust alternative for maintaining reliable communication links in such challenging environments. Additionally, their ability to maintain a consistent intensity profile over long distances makes them ideal for applications requiring precise beam control and stability, such as in LoS communications and wireless power transfer. Overall, the use of Bessel beams in wireless communication represents a promising approach to overcoming some of the fundamental challenges associated with high-frequency signal propagation, offering enhanced reliability, stability, and performance in a variety of advanced applications.

b) Self-Accelerating Beams: Self-accelerating beams [218], [219], often exemplified by Airy beams, are a fascinating class of optical and electromagnetic waveforms that exhibit the unique ability to bend or curve along a predefined trajectory without the need for an external force or medium to guide them. Unlike traditional beams, which generally propagate in straight lines or spread out due to diffraction, self-accelerating beams can follow curved paths, making them highly valuable in a variety of advanced optical and wireless communication applications.

The most iconic example of a self-accelerating beam is the Airy beam, named after the British astronomer Sir George Biddell Airy, who first described the Airy function in the context of wave theory. An Airy beam's intensity profile is shaped by the Airy function, which gives rise to a main lobe and a series of diminishing side lobes. One of the most striking properties of an Airy beam is its ability to maintain its shape and energy distribution while accelerating transversely in free space, meaning it can curve naturally as it propagates [210], [218], [219]. This self-bending behavior occurs because of the beam's unique phase structure. The phase front of an Airy beam is designed in such a way that the different parts of the wavefront

interfere constructively and destructively to produce a curved trajectory. This trajectory is typically parabolic, and the beam can exhibit self-healing properties, similar to Bessel beams, where it can reconstruct itself after encountering obstacles. Self-accelerating beams can be generated using various methods, including phase masks, spatial light modulators, and metasurfaces, which imprint the necessary phase and amplitude profiles onto an input beam to create the desired accelerating trajectory. These beams are not limited to optics and can be extended to electromagnetic waves in the RF and THz domains, making them relevant for a wide range of applications.

In wireless communication, self-accelerating beams like Airy beams offer significant advantages in environments where the direct LoS may be obstructed or where complex propagation paths are required [220], [221]. For example, in urban settings where buildings and other structures frequently block signals, the ability of self-accelerating beams to bend around obstacles can help maintain a stable communication link without the need for additional relay stations or complex routing. Furthermore, their self-healing property ensures that even if part of the beam is blocked or scattered, the remaining portion of the beam can continue to propagate along its intended path, reducing signal loss and improving overall communication reliability. This makes self-accelerating beams particularly suitable for high-frequency applications, where traditional beams might struggle with diffraction, scattering, and path loss.
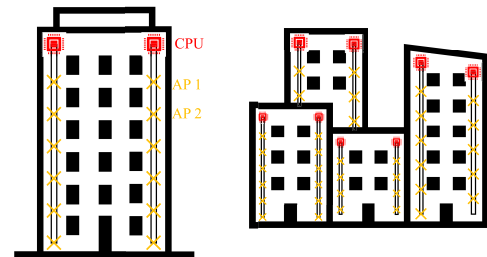
C. HARDWARE CHALLENGES

The combination of hardware cost and complexity presents a significant challenge in connecting all the antenna elements in large antenna arrays with dedicated RF chains and high resolution analogue-to-digital converters (ADCs). This challenge is particularly pronounced in scenarios involving ELAAs or massive MIMO systems. Firstly, acquiring and installing large numbers of RF chains and high-resolution ADCs can be expensive. ELAAs can have thousands or even tens of thousands of antenna elements, each requiring dedicated hardware components, which can quickly escalate costs. Secondly, operating a large number of RF chains and high resolution ADCs requires a significant amount of power. This is particularly relevant in wireless communication systems where energy efficiency is a critical consideration. Thirdly, managing and synchronising a large number of RF chains and ADCs can be very complex. Precise calibration and synchronisation is required to ensure that the array operates effectively. Finally, the integration of a large number of antennas operating coherently presents practical implementation challenges, particularly in terms of the significant front-haul capacity and signalling requirements, which can be costly. To overcome these challenges, hybrid beamforming, low complexity transceiver design and radio stripes are discussed.
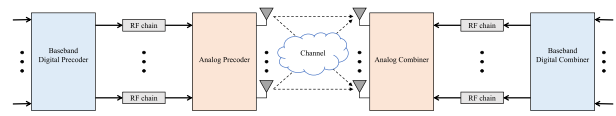
(a) Hybrid beamforming.
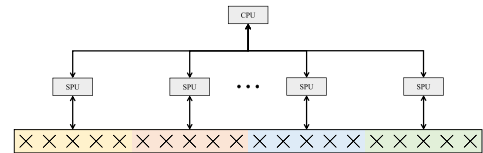
(b) Decentralized low complexity transceiver design.

(c) Radio stripes.

FIGURE 11. Examples of Solutions for ELAA hardware challenges.

1) HYBRID BEAMFORMING

Hybrid beamforming has emerged as a critical technique in ELAAs for several compelling reasons. ELAAs, characterised by a large number of antenna elements, present unique challenges in terms of power consumption, hardware complexity and signal processing. Therefore, hybrid beamforming architectures, where a few RF chains are connected to a large number of antennas, strike a balance between the performance benefits of fully digital beamforming and the practical limitations associated with ELAAs. In addition, hybrid beamforming is more easily scalable to a large number of antennas. Adding more antennas to the array does not necessarily require a proportional increase in RF hardware components. This simplifies system expansion. The implementation of hybrid analogue-digital architectures in communication systems offers a versatile approach to take advantage of both analogue and digital processing. There are several ways to implement such architectures, depending on the specific requirements and constraints of the system. For example, the most flexible architecture is the fully connected architecture, where all RF chains are connected to all antennas, while the partially connected hybrid beamforming

type uses a separate antenna array for the RF beamformer of a single RF chain, i.e., sub-array hybrid beamforming. Recently, dynamic hybrid architectures [222] have been proposed which allow for adaptability and flexibility while maintaining a simpler and more efficient implementation that can adapt the beamforming strategy based on the instantaneous channel conditions. This adaptability ensures that the communication system makes optimal use of its resources, such as beamforming direction and power allocation.

2) DECENTRALIZED LOW COMPLEXITY TRANSCEIVER DESIGN

The presence of an exceptionally high number of antennas in the base station raises a challenging issue, mainly centred on the increased complexity of the architecture. Even with simple linear transceivers, the base station could perform complex operations, such as large dimensional matrix inversion, which makes the complexity of the operations a formidable task. Therefore, the design of an efficient transceiver with low complexity is challenging. In practical applications, compared to a centralised deployment, distributed signal processing deployment is necessary by reducing the computational cost of central processing to local processing unit. In addition, non-stationary characteristics facilitate distributed processing methods.

Since ports are only visible to a subset of subarrays due to the presence of VRs, a bipartite graph can be used to represent the connections between ports and subarrays. When terminals are connected to a limited number of sub-arrays, the resulting graph exhibits sparsity, making it a valuable tool for simplifying the design of low-complexity transceivers. For example, [223] considered user assignments for both sum-rate and user-rate maximisation problems with distributed LIS deployment. The optimal user assignments could be achieved by linear assignment problems defined on a bipartite graph. Compared to the linear fusion of subarray techniques, where subsets of subarrays are involved at each hierarchical level, nonlinear processing may also be beneficial to improve performance. Inspired by successive interference cancellation and coded random access, [91] proposed low-complexity data detection algorithms to reduce the computational complexity of the centralised scheme. In particular, the presence of spatial non-stationarities leads to different multi-terminal interference patterns across the array. Consequently, a single terminal will encounter different interference conditions at each of the sub-arrays. To effectively address this challenge, it is advantageous to identify a specific terminal from the sub-array where it experiences favourable interference. Once identified, the contributions from that terminal can be selectively removed from the other subarrays. This process significantly improves the signal-to-interference ratio for all other terminals, thereby optimising the overall quality and efficiency of the communications system.

3) RADIO STRIPES

The overall objective of ELAAs is to integrate a large number of coherently operating antennas to ensure that each user benefits from mutually orthogonal channels. This configuration aims to achieve a throughput per user similar to that achievable in an additive white Gaussian noise channel, where there is no propagation loss. As mentioned above, the spatial resolution of an array is not just a function of the number of antennas it contains. Instead, it is mainly determined by the aperture of the array. Consequently, the distribution of antennas over a larger aperture has significant advantages, particularly in maximising the benefits of ELAA, such as facilitating effective near-field communication.

While hybrid beamforming architectures and low-complexity transceiver designs help manage the immense computational complexity of ELAA processing, providing interconnections between all the components in a system with many cooperating antennas remains costly. Rather than pushing antenna design to the size of a small matchbox, an alternative approach is to create antennas that are small and flexible enough to be integrated into adhesive tape. This innovative solution, known as radio stripes [25], [224] (radio wave deployments in a linear topology), has the potential to provide truly ubiquitous connectivity in certain areas.[5] It consists of a stripe connected to a CPU with a large number of antennas working together in phase coherence. These access points (APs) are stacked and connected sequentially on the same cable, using a daisy-chain architecture. This arrangement enables synchronisation, data transfer and power supply over a single link, eliminating the need for separate front-haul links between each AP and its CPU.

Sequential networks have several advantages. They facilitate easy deployment and cabling in a variety of real-world environments, such as train stations, museums and factories. In these networks, many APs are connected by a single fronthaul cable that serves multiple purposes, including data transport, power, and synchronisation. This consolidated connection makes it easier to effectively handle node failures through routing mechanisms, thereby increasing fault tolerance. In contrast, other topologies may have at least one AP or the CPU with more than one transmit or receive link, which could introduce additional complexity in implementation and timing synchronisation [25], [225]. In addition, the design of fault-tolerant routing mechanisms for such topologies can be challenging, depending on their structure. In addition, the sequential implementation of mMIMO has the potential to deliver the benefits of mMIMO with much lower fronthaul requirements compared to centralised approaches.

The authors in [21], [24] propose a novel sequential processing algorithm with normalised linear minimum mean square error combining at each AP. This approach is tailored for the uplink of a cooperative mMIMO system using the

---

[5]While radio stripes are often associated with cell-free mMIMO systems, they can also find some application in ELAA systems.

radio stripe network architecture and featuring a sequential fronthaul between APs. By implementing this algorithm, interference can be effectively mitigated at a low cost, and fronthaul requirements can be met. Furthermore, the algorithm was shown to be optimal in terms of both maximum spectral efficiency (SE) and minimum spectral efficiency (MSE). The study in [226] investigates an uplink power allocation technique aimed at improving network SE, which is modelled as an optimisation-constrained problem explicitly considering the max-min fairness scenario. To circumvent the limitations of both centralised and distributed schemes, where centralised approaches often encounter high fronthaul load and distributed schemes may suffer from performance degradation, [23] introduces a novel Cooperative Regularised Zero-Forcing algorithm. This innovative technique approximates MMSE using channel estimation in both uncorrelated and correlated channels, ensuring both high performance and low fronthaul loading. In addition, the C-RZF algorithm involves joint signal processing by both the AP and the CPU, further enhancing its effectiveness. Radio striations are also promising for wireless energy transfer (WET). Researchers in [227] have developed optimal and suboptimal precoders designed to minimise the transmit power of radio stripes. These precoders use information about the power transfer efficiency of the energy harvesting (EH) circuits at the UEs to optimise the overall energy transfer process.

In a Distributed MIMO (D-MIMO) network, the fronthaul links connecting the APs to the central processing unit (CPU) can adopt a radio stripe configuration in series. Researchers in [228] proposed a decentralised approach to processing and combining signals in the uplink for a D-MIMO network using a subset method. Their results indicate that this subset method has a highly scalable balance between complexity and performance. In addition, they proposed the use of Kalman filters with a square-root implementation for estimating received uplink signals in [229]. Through computational analysis, they have compared the complexity and cost implications of various combining methods and demonstrated that the Kalman filter implementation can achieve similar spectral efficiency and signal-to-interference-plus-noise ratio (SINR) as the MMSE method, while offering greater flexibility in signal aggregation.

IV. APPLICATIONS
A. PHYSICAL LAYER SECURITY
The inherent nature of the broadcast wireless channel underscores the critical importance of information security. While the development of various encryption algorithms in the upper protocol stack achieves secure transmission of private data, the computational complexity remains a challenge. Physical Layer Security (PLS) has emerged as an effective solution for ensuring the security of wireless communications by exploiting the inherent propagation characteristics of wireless channels, such as interference. By enhancing the mutual information between the transmitter and the desired UE, PLS effectively protects private messages from eavesdropping by unauthorised third parties.

Unlike the directional focusing of beamforming in far-field communications, the finite beam depth property enabled by the spherical wave channel model in near-field communications, supported by ELAA, allows the energy of the transmitted signal to be concentrated at the location of legitimate users rather than just in their direction (i.e., beam focusing). This effectively reduces information leakage at the location of eavesdroppers and improves the capacity of the system's secure channel.

The study in [230] examines the effects of SWM on PLS in ELAA systems with multiple eavesdroppers and one legitimate user. Both colluding and non-colluding strategies are analysed for different eavesdroppers. The results show that the propagation features associated with the SW model enable higher secrecy rates and reduce the areas where eavesdroppers can compromise secure communication. In addition, they also investigate the achievable secrecy spectral efficiency in a multi-user ELAA system and propose a joint scheduling and precoding scheme that improves the secure performance of the system in [231].

Large-scale antenna arrays with full-digital beamforming structures typically lead to exponential hardware costs. Hence, the exploration of cost-effective beam-focusing schemes for secrecy ELAA networks has become a current research priority. A secure beam-focusing technique based on a hybrid beamforming architecture was proposed to effectively reduce the RF link overhead [232]. Utilizing the spherical wave channel state information of both legitimate users and eavesdroppers, a two-stage algorithm was introduced to maximize the near-field secrecy capacity. Additionally, authors in [233] proposed a near-field directional modulation system toward secure transmissions at both angular and distance scale by considering the a full analog secure precoding scheme to reduce hardware cost.

B. LOCALIZATION, SENSING AND COMMUNICATION
1) POSITIONING
In traditional far-field communication, the AoA of signals is primarily determined by the phase difference based on plane wave model assumption. Consequently, multiple positioning anchors are typically deployed in a distributed manner to estimate the three-dimensional coordinates of the target. Alternatively, the position of target could be determined by distance estimation, where the signal travel time between the transmitter and receiver is measured with clock synchronization. Additionally, a large bandwidth is usually required to enhance the accuracy of both the angle and distance measurements. In contrast, the amplitude and phase of the signal can be used to precisely determine the arrival angle and distance information based on the spherical wave model. This enables us to directly derive the position of the target using a single ELAA, thereby enhancing positioning accuracy. Specifically, the location of UE can be directly estimated based on the curvature of arrival
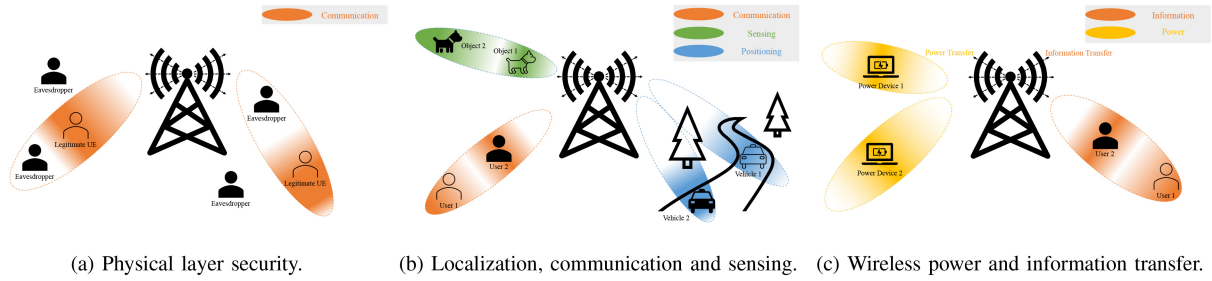
(a) Physical layer security.   (b) Localization, communication and sensing.   (c) Wireless power and information transfer.

FIGURE 12. Examples of integration with other technologies.

(CoA) of the spherical wavefront, enabling a single array to determine both distance and direction simultaneously.

The authors in [234] derived the CRB based on EPM, which is a more accurate model compared to SWM without any approximation. The results reveal that using multiple receiving antennas can significantly enhance the estimation accuracy of dimensions parallel to the receiving surface. In addition, with the EPM, the attitude parameter of UE is able to be sensed. In [126], a low-complexity algorithm for joint position and attitude estimation was proposed. The Ziv-Zakai Bound (ZZB) was derived for all SNR regimes to investigate the impact of random noise on joint estimation performance, and the expected CRB was further provided with a closed-form expression in high SNR regimes. Through the ZZB, the authors demonstrated that the attitude estimation can reach the 0.1-level and achieve millimeter-level accuracy in position estimation.

2) COMMUNICATION AND SENSING

In the context of IMT-2030 [235], which serves as the foundation for standardization forums to develop the 6G mobile, ISAC has emerged as a novel application with enhanced high-precision sensing capabilities within the scope of 6G. ISAC has garnered significant attention from both academia and industry, providing a comprehensive support for a broad array of applications [236], [237], such as XR. Unlike traditional wireless positioning and channel estimation methods where pilot signals are transmitted by active devices, the essence of ISAC relies on the echo signal reflected by passive target to create harmonious synergies between communication and sensing by sharing the same spectrum and hardware resources.

In wireless sensing, the key metrics of interest are the angle, distance and velocity of the sensing target. In traditional far-field sensing, the performance of these metrics depends on specific factors: for example, the size of the antenna array for angle estimation, the bandwidth of the sensed signals for distance estimation, and the sensing time for velocity estimation. However, when the sensing target is in the near field, the propagation of signals in a SWM introduces revolutionary changes to the acquisition of these metrics. In particular, in a far-field sensing system, achieving accurate target positioning typically requires a large bandwidth. In particular, angle and distance sensing often

requires either significant bandwidth or the collaborative support of multiple sensing nodes. In the near-field, however, the use of spherical wave modelling allows the use of large aperture antenna arrays, facilitating the acquisition of both angle and distance information of the target being sensed, dramatically reducing the cost and complexity of the system. In terms of velocity estimation, in the far field only radial velocity can be captured, as only angles can be distinguished under PWM. However, in the near-field, additional transverse velocity information of the target can be captured simultaneously. This comprehensive motion state information enables accurate prediction of the target position at the next time interval.

Reference [238] derives the near-field SNR scaling laws. In contrast to the conventional UPW model, where the SNR scales linearly with the number of transceiver antennas, the SNR in the near field increases with diminishing returns. They also derived CRBs for both angle and distance estimation with the USW model [239]. The results show that the bounds for angle and distance estimation in the near field are finite. This differs from the conventional far-field UPW model, where the CRB for angle decreases indefinitely as the number of antennas increases, and the CRB for distance is infinite as it has no distance estimation capability.

Thanks to powerful sensing capabilities, harmonious synergies between C&S have been achieved by sharing the same spectrum and hardware. On the one hand, the additional distance domain enables the BS to focus beams at different distances based on SWM, while far-field beamforming directs beam energy along a specific direction. This effectively improves the degree of freedom of the channel and further increases system capacity by reducing interference between UEs. On the other hand, in wireless sensing applications, a large aperture array provides an extended estimation range for the target range, together with improved spatial resolution in both angular and range domains. This feature reduces the need for distributed arrays and the need for synchronisation between them.

The CRB for near-field joint distance and angle sensing is established [240]. The ISAC signal is jointly optimized to maximize near-field sensing performance, while ensuring the minimum communication rate in the near-field, for both fully digital antennas and hybrid digital and analog antennas. Numerical results demonstrate the performance improvement

achieved by incorporating the additional distance dimension in near-field ISAC compared to far-field ISAC.

C. WIRELESS POWER AND INFORMATION TRANSFER

With the rapid advancement of mobile communication technologies, there has been a proliferation of IoT smart devices integrated into various scenarios of our lives. In the upcoming 6G era, wireless power transfer (WPT) emerges as a promising solution for charging these mobile low-power devices. By eliminating the need for complex wiring and ensuring efficient and sustainable operations, WPT has distinct advantages in terms of security and flexibility, making it an indispensable technology for future society.

The use of large antenna arrays increases the importance of near-field spherical wave, which enables beam-focusing techniques to concentrate RF signal energy around the receiver, facilitating efficient energy transfer. In addition, the characteristics of the near-field spherical wave provide high-precision position information and significantly improve the efficiency of energy transfer. At the same time, beam focusing has the potential to effectively reduce electromagnetic pollution and limit human exposure to radiated energy. Since electromagnetic waves can carry both information and energy, the integration of WPT with mobile communications can lead to simultaneous wireless information and power transmission (SWIPT), which maximises the use of electromagnetic waves. In near-field communications, the use of extremely large antenna arrays enables higher spatial resolution in the near-field range by exploiting the radio channel characteristics modelled by spherical waves. As a result, base stations can accommodate higher densities of SWIPT terminals.

While much current research focuses on either near-field or far-field communication, there is a growing trend to explore hybrid communication models that integrate both near-field and far-field users within the system [241], [242]. This hybrid model may be particularly relevant in mixed near-field and far-field SWIPT scenarios, where energy harvesting (EH) and information decoding (ID) receivers are located in the near-field and far-field regions of the ELAA, respectively. The optimisation objective is to maximise the weighted sum power harvested at all EH receivers with constraints on the maximum sum rate and BS transmit power. The optimisation process involves the joint design of BS beam scheduling and power allocation, shedding light on the trade-offs inherent in SWIPT.

V. POTENTIAL RESEARCH DIRECTIONS

In this section, several potential research challenges and directions related to ELAA are explored.

A. ELECTROMAGNETIC SIGNAL AND INFORMATION THEORY

The integration of Maxwell's equations with communication theory, and the exploration of the relationship between electromagnetic theory and communication theory, has generated much discussion and debate in the scientific community [112]. Electromagnetic Signal and Information Theory (ESIT) is the framework that encompasses physics-based information theory and signal processing for communication, with the goal of achieving physically consistent signal processing in communication systems.

Communication and information are inherently physical phenomena. Electromagnetic waves, governed by Maxwell's equations, are the medium through which information is transmitted wirelessly. The physical properties of these waves, including their frequency, wavelength and propagation characteristics, fundamentally affect how information is encoded, transmitted and received. Understanding the physics of electromagnetic waves enables the development of more efficient and robust communication systems. By integrating the principles of electromagnetism with information theory, researchers can optimise signal processing techniques to better match the physical realities of wave propagation.

1) EVANESCENT WAVE MODELLING

As discussed in Section II-E, evanescent waves become prominent in the reactive near field as the array aperture increases. In the presence of evanescent waves in the near field, the spatial bandwidth in the wave number domain becomes infinite, rendering the Petersen-Middleton theorem [243] invalid. Therefore, accurate modelling and understanding of the role of evanescent waves and the near-field can enable us to optimally generate and shape electromagnetic waves, thereby improving the performance of near-field communication systems.

2) MUTUAL COUPLING

Furthermore, while sub-wavelength antenna inter-spacing facilitates the capture of evanescent waves, it is essential to employ appropriate models for metasurfaces, ensuring electromagnetic consistency and accounting for the mutual coupling among scattering elements. Moreover, the development of signal processing algorithms that consider electromagnetic mutual coupling during the design phase is crucial. Reference [244] proposed an electromagnetically consistent model for wireless communications, which incorporates mutual coupling and is applicable to free space and multipath channels using multiport network theory. Consequently, gaining a thorough understanding of the role of electromagnetic mutual coupling can enable us to assess and quantify the distinctions and similarities between continuous-type and discrete-type antenna-array models.

B. AI-AIDED INTELLIGENT COMMUNICATION
1) ELAA FOR AI

a) Semantic Communication: Semantic communication represents a paradigm shift in wireless networks, transcending the traditional transmission of data to enable deeper understanding and contextual awareness within communication systems [245], [246]. By endowing networks with the ability to comprehend the meaning and context of transmitted

information, semantic communication lays the foundation for more intelligent, adaptive, and user-centric communication experiences. On the Other hand, ELAA provides unprecedented opportunities for enhancing wireless communication systems through their massive scale and spatial diversity. By combining the principles of semantic communication with the capabilities of ELAA, we can unlock new frontiers in communication efficiency, reliability, and adaptability.

Semantic communication in ELAA systems enables networks to perceive and interpret the contextual nuances of communication scenarios. By leveraging contextual cues such as environmental conditions, user preferences, and network dynamics, ELAA networks can dynamically adjust transmission parameters, beamforming strategies, and resource allocations to optimize performance and meet user requirements in real-time. Reference [247] introduced a semantic transmission framework designed to facilitate the seamless transmission of sensing information from the physical world to Metaverse. Unlike conventional methods that involve data recovery, this approach focuses on achieving the sensing objective directly. Additionally, a game theory-based incentive mechanism was incorporated to encourage users to upload data more frequently. As a result, the framework significantly reduces the volume of sensing data that needs to be transmitted.

b) Federated Learning: Federated learning is an emerging machine learning paradigm that enables training models across decentralized edge devices without exchanging raw data [248], [249]. This approach has the advantages of privacy preservation, reduced communication overhead, and improved scalability. In the context of ELAA, federated learning is a novel avenue for harnessing the distributed intelligence of edge devices within the antenna array to collectively learn and refine communication strategies while upholding user privacy and minimizing the reliance on centralized data processing. Given the unique characteristics of near-field channels between users and base stations in ELAA systems, it becomes imperative to redefine the convergence model for federated learning systems based on near-field channels. This entails establishing an energy and delay model specific to federated learning systems operating in near-field communication environments. By jointly optimizing communication and learning parameters tailored to near-field communication, we can achieve optimal resource allocation and enhance the efficiency of federated learning in ELAA setups.

2) AI FOR ELAA

a) AI-Aided Transmission: Either spherical wavefronts in near-field communication with a novel degree of freedom enabling spatial multiplexing or visibility region causing non-stationary channels is more complex than traditional massive MIMO systems. This leads to high non-linearity in the model and computational cost in performing algorithm, such as channel estimation and beamforming. Consequently, the integration of artificial intelligence (AI) with ELAAs can enhance performance, especially in highly dynamic and complex wireless environments. For example, in near-field channel estimation, the size of near-field codebooks is usually much larger than far-field codebooks. This leads to high complexity channel estimation and near-field codebook design also accounts for non-linear phase shift. To address those challenges in codebook based near-field channel estimation, [183] proposed a learning based algorithm, which sparsifys the dictionary for compressive sensing. As AI continues to advance, its role in ELAAs is expected to evolve and redefine the capabilities of these systems in future wireless communication networks.

b) Generative AI enabled Transmission: Although traditional AI models have demonstrated effectiveness, their performance has inherent limitations. The recent evolution of generative artificial intelligence (GAI) has led to groundbreaking applications such as ChatGPT citeray2023chatgpt. Consequently, researchers are now exploring GAI to enhance physical layer communications. For example, vision-aided blockage prediction and beamforming were investigated in [250]. Inspired by GAI's significant performance in image classification, a deep learning algorithm was developed to learn from visual and wireless data, enabling proactive blockage prediction and user hand-off using cameras deployed at the base stations. This algorithm allows the wireless network to proactively make hand-off decisions, reducing unnecessary latency. Additionally, the authors in [251] proposed using a generative adversarial network (GAN) to reconstruct low-dimensional channel feedback from the receiver, facilitating hybrid beamforming at the transmitter and resulting in lower communication overhead. However, the applications of GAI in emerging technologies such as ELAA are still underexplored. Thus, there is growing interest in advancing GAI applications within physical layer communications to harness their full potential.

C. HYBRID FAR- AND NEAR-FIELD COMMUNICATION

In real-world communications, the systems often encompass both far-field and near-field signal elements. On the one hand, some users and scatters are distant from the BS, while others reside in the near-field vicinity of the BS in multi-user setups with multi-path channels, creating a hybrid far- and near-field communication scenario. On the other hand, in ultra-wideband or frequency-hopping systems covering a broad frequency spectrum, the near-field range can vary significantly across the bandwidth. This variability means that signal components at lower frequencies may operate within far-field regions, while those at higher frequencies, with larger Rayleigh distances, propagate in the near-field areas. As a result, hybrid-field communications emerge as both practical and pivotal considerations for future 6G networks.

Reference [252] derived a closed-form expression for the inter-user interference experienced by near-field users due to far-field beams. Their analysis revealed the presence of significant interference, particularly when near-field and

far-field users align relatively closely with respect to the BS. This finding underscores the importance of exploring transmission techniques managing both far-field and near-field signal components. Such exploration is crucial for gaining a comprehensive understanding of their implications and potential in propelling advancements in wireless communication technologies.

D. JOINT SENSING, COMMUNICATION AND COMPUTING

Expanding research efforts in the joint sensing, communication, and computing domain holds tremendous potential for unlocking new capabilities and addressing emerging challenges in wireless networks. ELAA's extensive spatial degrees of freedom and high resolution in spatial domain offer unprecedented opportunities for joint sensing, communication, and computing (JCSC). The primary goal of JCSC in ELAA is to optimize these functions synergistically, ensuring efficient spectrum utilization, enhancing performance, and meeting diverse application requirements. Based on an analysis of the functional design of communication, sensing, and emerging intelligent computation systems, [253] proposed the JCSC framework for the 6G intelligent machine-type communication network. This framework aims to achieve low latency and high reliability of communication, highly accurate sensing, and rapid environmental adaptation. In addition, multi-objective optimization problems (MOOP) has become increasingly prevalent for multi-objective tasks. Reference [254] proposed two typical joint beamforming design algorithms based on MOOP with the weighted overall performance maximization and total transmit power minimization.

E. MULTI-CELL ELAA

Multi-cell communication is a fundamental framework of modern wireless networks, enabling efficient utilization of resources and improved system performance through coordinated operation across multiple BSs and UEs. Most existing work on near-field communication only focuses on single-cell systems. In conventional multi-cell scenarios, each BS serves its designated cell independently, often relying on centralized coordination and information exchange for interference management and resource allocation. However, the emergence of mMIMO systems, coupled with the deployment of ELAA, introduces new dimensions to multi-cell communication paradigms. Firstly, although the large-scale antenna arrays equipped with beamforming capabilities enable enhanced spatial processing and interference mitigation, thereby having opportunities to redefine multi-cell communication strategies, it is difficult to directly apply the CoMP transmission to multi-cell ELAA communications [26], due to higher computation complexity and larger amount of information exchange among coordinated BSs as compared to existing MIMO and massive MIMO systems. Hence, there is a pressing need to explore low-complexity interference mitigation techniques tailored for multi-cell ELAA communications. Moreover, the challenge

of pilot contamination persists as a critical issue in such scenarios [255], [256], particularly when dealing with a limited number of orthogonal pilots. Therefore, it is clearly imperative to investigate efficient methods for multi-cell ELAA channel estimation under the constraints posed by pilot contamination.

F. NOVEL WAVEFRONT ENGINEERING

As wireless communication systems progress into higher frequency bands, particularly within the THz range, the deployment of novel wavefronts like Bessel beams and Airy beams presents promising advantages over conventional far-field beamforming and near-field beamfocusing techniques [207]. These advanced wavefronts, such as the non-diffractive Bessel beams and self-accelerating beams that can navigate curved paths, significantly extend the capabilities of high-frequency communication systems. Recent research has underscored the potential of these wavefronts in overcoming the limitations of conventional techniques. For instance, the authors in [221] demonstrated a high bit-rate data link that successfully curved around an obstacle, utilizing the entire aperture of the transmitter, even portions without a direct LoS to the receiver. This represents a significant advancement, as it allows for more robust communication in environments where obstacles would otherwise block or degrade the signal. Moreover, the application of these wavefronts in the near field opens new avenues for enhanced sensing capabilities. In [210], the foundational principles of Bessel beams were applied to sensing with RIS at THz frequencies, revealing substantial improvements in performance metrics such as SNR, resolution, and bandwidth.

VI. CONCLUSION

This paper has provided a comprehensive exploration of ELAA technologies, beginning with an elucidation of their fundamental concepts. We have carefully examined various ELAA architectures, highlighting their diverse characteristics and applications. We also discussed the nuanced properties of near-field communications, revealing phenomena such as spherical wave propagation and channel spatial non-stationarity that distinguish ELAA from traditional far-field communications paradigms. The critical aspect of finite near-field beam depth has been meticulously dissected, highlighting its implications and challenges. In addition, the boundaries between the near and far fields were delineated, providing a comprehensive understanding of their delineation based on various criteria. A detailed performance analysis framework for near-field channel models was presented, providing insights into the capabilities and limitations of ELAA technology. Beyond the theoretical underpinnings, we highlighted the practical challenges associated with ELAA technology and proposed potential solutions drawn from the literature. From channel estimation to beamforming design and hardware considerations, we navigated through the complexities of ELAA implementation, suggesting ways

to overcome obstacles and optimise performance. We also explored the symbiotic relationship between ELAA and emerging technologies, envisioning their collaborative potential to reshape diverse domains. From physical layer security to localisation, sensing and communication, we envisioned synergistic opportunities that could redefine conventional paradigms. To identify key research opportunities, we discussed future research themes such as electromagnetic signal and information theory, AI-driven intelligent communication, and hybrid far-field and near-field communication. In addition, the integration of sensing, communication and computing, and within multi-cell ELAA architectures, promises to improve the connectivity and scalability of future wireless networks.

REFERENCES

[1] J. G. Andrews et al., "What will 5G be?" *IEEE J. Sel. Areas Commun.*, vol. 32, no. 6, pp. 1065–1082, Jun. 2014.

[2] K. David and H. Berndt, "6G vision and requirements: Is there any need for beyond 5G?" *IEEE Veh. Technol. Mag.*, vol. 13, no. 3, pp. 72–80, Sep. 2018.

[3] R. Li, "Network 2030: Market drivers and prospects," in *Proc. 1st Int. Telecommun. Union Workshop Netw.*, pp. 1–21, 2018.

[4] M. Cooper, *The Myth of Spectrum Scarcity*, DYNA LLC, Del Mar, CA, USA, Mar. 2010.

[5] H. T. Friis, "A note on a simple transmission formula," *Proc. IRE*, vol. 34, no. 5, pp. 254–256, May 1946.

[6] E. Björnson, L. Sanguinetti, H. Wymeersch, J. Hoydis, and T. L. Marzetta, "Massive MIMO is a reality—What is next?: Five promising research directions for antenna arrays," *Digit. Signal Process.*, vol. 94, pp. 3–20, Nov. 2019.

[7] B. T. Csathó, B. P. Horváth, and P. Horváth, "Modeling the near-field of extremely large aperture arrays in massive MIMO systems," *Infocommun. J.*, vol. 12, no. 3, pp. 39–46, 2020.

[8] C. Huang et al., "Holographic MIMO surfaces for 6G wireless networks: Opportunities, challenges, and trends," *IEEE Wireless Commun.*, vol. 27, no. 5, pp. 118–125, Oct. 2020.

[9] T. Gong et al., "Holographic MIMO communications: Theoretical foundations, enabling technologies, and future directions," *IEEE Commun. Surveys Tuts.*, vol. 26, no. 1, pp. 196–257, 1st Quart., 2024.

[10] J. An, C. Yuen, C. Huang, M. Debbah, H. V. Poor, and L. Hanzo, "A tutorial on holographic MIMO communications—Part I: Channel modeling and channel estimation," *IEEE Commun. Lett.*, vol. 27, no. 7, pp. 1664–1668, Jul. 2023.

[11] J. An, C. Yuen, C. Huang, M. Debbah, H. V. Poor, and L. Hanzo, "A tutorial on holographic MIMO communications—Part II: Performance analysis and holographic beamforming," *IEEE Commun. Lett.*, vol. 27, no. 7, pp. 1669–1673, Jul. 2023.

[12] J. An, C. Yuen, C. Huang, M. Debbah, H. V. Poor, and L. Hanzo, "A tutorial on holographic MIMO communications—Part III: Open opportunities and challenges," *IEEE Commun. Lett.*, vol. 27, no. 7, pp. 1674–1678, Jul. 2023.

[13] Y. Liu, J. Xu, Z. Wang, X. Mu, and L. Hanzo, "Near-field communications: What will be different?" 2023, *arXiv:2303.04003*.

[14] H. Zhang, N. Shlezinger, F. Guidi, D. Dardari, and Y. C. Eldar, "6G wireless communications: From far-field beam steering to near-field beam focusing," *IEEE Commun. Mag.*, vol. 61, no. 4, pp. 72–77, Apr. 2023.

[15] Z. Wang, X. Mu, and Y. Liu, "Terahertz near-field communications and sensing," 2023, *arXiv:2306.09723*.

[16] Y. Liu, C. Ouyang, Z. Wang, J. Xu, X. Mu, and A. L. Swindlehurst, "Near-field communications: A comprehensive survey," 2024, *arXiv:2401.05900*.

[17] H. Lu et al., "A tutorial on near-field XL-MIMO communications towards 6G," *IEEE Commun. Surveys Tuts.*, early access, Apr. 12, 2024, doi: 10.1109/COMST.2024.3387749.

[18] Z. Wang et al., "A tutorial on extremely large-scale MIMO for 6G: Fundamentals, signal processing, and applications," *IEEE Commun. Surveys Tuts.*, vol. 26, no. 3, pp. 1560–1605, 3rd Quart., 2024.

[19] A. Pizzo, T. L. Marzetta, and L. Sanguinetti, "Spatially-stationary model for holographic MIMO small-scale fading," *IEEE J. Sel. Areas Commun.*, vol. 38, no. 9, pp. 1964–1979, Sep. 2020.

[20] D. Dardari and N. Decarli, "Holographic communication using intelligent surfaces," *IEEE Commun. Mag.*, vol. 59, no. 6, pp. 35–41, Jun. 2021.

[21] Z. H. Shaik, E. Björnson, and E. G. Larsson, "Cell-free massive MIMO with radio stripes and sequential uplink processing," in *Proc. IEEE Int. Conf. Commun. Workshops (ICC Workshops)*, 2020, pp. 1–6.

[22] Z. Chen and E. Björnson, "Channel hardening and Favorable propagation in cell-free massive MIMO with stochastic geometry," *IEEE Trans. Commun.*, vol. 66, no. 11, pp. 5205–5219, Nov. 2018.

[23] Y. Ma, Z. Yuan, G. Yu, and Y. Chen, "Cooperative scheme for cell-free massive MIMO with radio stripes," in *Proc. IEEE Int. Conf. Commun. Workshops (ICC Workshops)*, 2021, pp. 1–6.

[24] Z. H. Shaik, E. Björnson, and E. G. Larsson, "MMSE-optimal sequential processing for cell-free massive MIMO with radio stripes," *IEEE Trans. Commun.*, vol. 69, no. 11, pp. 7775–7789, Nov. 2021.

[25] G. Interdonato, E. Björnson, H. Q. Ngo, P. Frenger, and E. G. Larsson, "Ubiquitous cell-free massive MIMO communications," *EURASIP J. Wireless Commun. Netw.*, vol. 2019, no. 1, pp. 1–13, 2019.

[26] D. Gesbert, S. Hanly, H. Huang, S. S. Shitz, O. Simeone, and W. Yu, "Multi-cell MIMO cooperative networks: A new look at interference," *IEEE J. Sel. Areas Commun.*, vol. 28, no. 9, pp. 1380–1408, Dec. 2010.

[27] R. Irmer et al., "Coordinated multipoint: Concepts, performance, and field trial results," *IEEE Commun. Mag.*, vol. 49, no. 2, pp. 102–111, Feb. 2011.

[28] M. Peng, Y. Sun, X. Li, Z. Mao, and C. Wang, "Recent advances in cloud radio access networks: System architectures, key techniques, and open issues," *IEEE Commun. Surveys Tuts.*, vol. 18, no. 3, pp. 2282–2308, 3rd Quart., 2016.

[29] K. Hosseini, W. Yu, and R. S. Adve, "Large-scale MIMO versus network MIMO for multicell interference mitigation," *IEEE J. Sel. Topics Signal Process.*, vol. 8, no. 5, pp. 930–941, Oct. 2014.

[30] R. W. Heath, N. Gonzalez-Prelcic, S. Rangan, W. Roh, and A. M. Sayeed, "An overview of signal processing techniques for millimeter wave MIMO systems," *IEEE J. Sel. Topics Signal Process.*, vol. 10, no. 3, pp. 436–453, Apr. 2016.

[31] M. Cui and L. Dai, "Near-field wideband beamforming for extremely large antenna arrays," 2024, *arXiv:2109.10054*.

[32] Y. Lu and L. Dai, "Near-field channel estimation in mixed LoS/NLoS environments for extremely large-scale MIMO systems," *IEEE Trans. Commun.*, vol. 71, no. 6, pp. 3694–3707, Jun. 2023.

[33] M. Cui, L. Dai, Z. Wang, S. Zhou, and N. Ge, "Near-field rainbow: Wideband beam training for XL-MIMO," *IEEE Trans. Wireless Commun.*, vol. 22, no. 6, pp. 3899–3912, Jun. 2023.

[34] H. Wang and Y. Zeng, "Can sparse arrays outperform collocated arrays for future wireless communications?" 2023, *arXiv:2307.07925*.

[35] P. P. Vaidyanathan and P. Pal, "Sparse sensing with co-prime samplers and arrays," *IEEE Trans. Signal Process.*, vol. 59, no. 2, pp. 573–586, Feb. 2011.

[36] W. L. Stutzman and G. A. Thiele, *Antenna Theory and Design*. Hoboken, NJ, USA: Wiley, 2012.

[37] C. A. Balanis, *Antenna Theory: Analysis and Design*. Hoboken, NJ, USA: Wiley, 2016.

[38] X. Li, H. Lu, Y. Zeng, S. Jin, and R. Zhang, "Modular extremely large-scale array communication: Near-field modelling and performance analysis," *China Commun.*, vol. 20, no. 4, pp. 132–152, Apr. 2023.

[39] X. Li, H. Lu, Y. Zeng, S. Jin, and R. Zhang, "Near-field modeling and performance analysis of modular extremely large-scale array communications," *IEEE Commun. Lett.*, vol. 26, no. 7, pp. 1529–1533, Jul. 2022.

[40] J. Jeon et al., "MIMO evolution toward 6G: Modular massive MIMO in low-frequency bands," *IEEE Commun. Mag.*, vol. 59, no. 11, pp. 52–58, Nov. 2021.

[41] A. Pizzo, L. Sanguinetti, and T. L. Marzetta, "Fourier plane-wave series expansion for holographic MIMO communications," *IEEE Trans. Wireless Commun.*, vol. 21, no. 9, pp. 6890–6905, Sep. 2022.

[42] L. Sanguinetti, A. A. D'Amico, and M. Debbah, "Wavenumber-division multiplexing in line-of-sight holographic MIMO communications," *IEEE Trans. Wireless Commun.*, vol. 22, no. 4, pp. 2186–2201, Apr. 2023.

[43] A. Pizzo, T. L. Marzetta, and L. Sanguinetti, "Degrees of freedom of holographic MIMO channels," in *Proc. IEEE 21st Int. Workshop Signal Process. Adv. Wireless Commun. (SPAWC)*, 2020, pp. 1–5.

[44] S. Hu, F. Rusek, and O. Edfors, "Beyond massive MIMO: The potential of data transmission with large intelligent surfaces," *IEEE Trans. Signal Process.*, vol. 66, no. 10, pp. 2746–2758, May 2018.

[45] D. Dardari, "Communicating with large intelligent surfaces: Fundamental limits and models," *IEEE J. Sel. Areas Commun.*, vol. 38, no. 11, pp. 2526–2537, Nov. 2020.

[46] N. Decarli and D. Dardari, "Communication modes with large intelligent surfaces in the near field," *IEEE Access*, vol. 9, pp. 165648–165666, 2021.

[47] S. Hu, F. Rusek, and O. Edfors, "Capacity degradation with modeling hardware impairment in large intelligent surface," in *Proc. IEEE Glob. Commun. Conf. (GLOBECOM)*, 2018, pp. 1–6.

[48] J. Yuan, H. Q. Ngo, and M. Matthaiou, "Towards large intelligent surface (LIS)-based communications," *IEEE Trans. Commun.*, vol. 68, no. 10, pp. 6568–6582, Oct. 2020.

[49] H. Lu and Y. Zeng, "Communicating with extremely large-scale array/surface: Unified modeling and performance analysis," *IEEE Trans. Wireless Commun.*, vol. 21, no. 6, pp. 4039–4053, Jun. 2022.

[50] R. J. Williams, E. De Carvalho, and T. L. Marzetta, "A communication model for large intelligent surfaces," in *Proc. IEEE Int. Conf. Commun. Workshops (ICC Workshops)*, 2020, pp. 1–6.

[51] H. Lu and Y. Zeng, "Near-field modeling and performance analysis for multi-user extremely large-scale MIMO communication," *IEEE Commun. Lett.*, vol. 26, no. 2, pp. 277–281, Feb. 2022.

[52] S. S. A. Yuan, Z. He, X. Chen, C. Huang, and W. E. I. Sha, "Electromagnetic effective degree of freedom of an MIMO system in free space," *IEEE Antennas Wireless Propag. Lett.*, vol. 21, pp. 446–450, 2022.

[53] R. Ji et al., "Extra DoF of near-field holographic MIMO communications leveraging evanescent waves," *IEEE Wireless Commun. Lett.*, vol. 12, no. 4, pp. 580–584, Apr. 2023.

[54] J. Xu, L. You, G. C. Alexandropoulos, X. Yi, W. Wang, and X. Gao, "Near-field wideband extremely large-scale MIMO transmissions with holographic metasurface-based antenna arrays," *IEEE Trans. Wireless Commun.*, vol. 23, no. 9, pp. 12054–12067, Sep. 2024.

[55] S. S. A. Yuan, Z. He, S. Sun, X. Chen, C. Huang, and W. E. I. Sha, "Electromagnetic effective-degree-of-freedom limit of a MIMO system in 2-D inhomogeneous environment," *Electronics*, vol. 11, no. 19, p. 3232, 2022.

[56] M. Cui and L. Dai, "Channel estimation for extremely large-scale MIMO: Far-field or near-field?" *IEEE Trans. Commun.*, vol. 70, no. 4, pp. 2663–2677, Apr. 2022.

[57] L. Wei et al., "Multi-user holographic MIMO surfaces: Channel modeling and spectral efficiency analysis," *IEEE J. Sel. Topics Signal Process.*, vol. 16, no. 5, pp. 1112–1124, Aug. 2022.

[58] H. Zhang, N. Shlezinger, F. Guidi, D. Dardari, M. F. Imani, and Y. C. Eldar, "Beam focusing for near-field multiuser MIMO communications," *IEEE Trans. Wireless Commun.*, vol. 21, no. 9, pp. 7476–7490, Sep. 2022.

[59] S. Willhammar, J. Flordelis, L. Van Der Perre, and F. Tufvesson, "Channel hardening in massive MIMO: Model parameters and experimental assessment," *IEEE Open J. Commun. Soc.*, vol. 1, pp. 501–512, 2020.

[60] Z. Yuan, J. Zhang, Y. Ji, G. F. Pedersen, and W. Fan, "Spatial non-stationary near-field channel modeling and validation for massive MIMO systems," *IEEE Trans. Antennas Propag.*, vol. 71, no. 1, pp. 921–933, Jan. 2023.

[61] X. Cai, W. Fan, X. Yin, and G. F. Pedersen, "Trajectory-aided maximum-likelihood algorithm for channel parameter estimation in ultrawideband large-scale arrays," *IEEE Trans. Antennas Propag.*, vol. 68, no. 10, pp. 7131–7143, Oct. 2020.

[62] W. Fan, I. Carton, J. Ø. Nielsen, K. Olesen, and G. F. Pedersen, "Measured wideband characteristics of indoor channels at centimetric and millimetric bands," *EURASIP J. Wireless Commun. Netw.*, vol. 2016, pp. 1–13, Dec. 2016.

[63] X. Zhao, S. Li, Q. Wang, M. Wang, S. Sun, and W. Hong, "Channel measurements, modeling, simulation and validation at 32 GHz in outdoor microcells for 5G radio systems," *IEEE Access*, vol. 5, pp. 1062–1072, 2017.

[64] X. Wu et al., "60-GHz millimeter-wave channel measurements and modeling for indoor office environments," *IEEE Trans. Antennas Propag.*, vol. 65, no. 4, pp. 1912–1924, Apr. 2017.

[65] T. L. Marzetta and H. Yang, *Fundamentals of Massive MIMO*. Cambridge, U.K.: Cambridge Univ. Press, 2016.

[66] E. Björnson, J. Hoydis, and L. Sanguinetti, "Massive MIMO networks: Spectral, energy, and hardware efficiency," *Found. Trends® Signal Process.*, vol. 11, nos. 3–4, pp. 154–655, 2017.

[67] H. Lu and Y. Zeng, "How does performance scale with antenna number for extremely large-scale MIMO?" in *Proc. IEEE Int. Conf. Commun. (ICC)*, 2021, pp. 1–6.

[68] Z. Zhou, X. Gao, J. Fang, and Z. Chen, "Spherical wave channel and analysis for large linear array in LoS conditions," in *Proc. IEEE Globecom Workshops (GC Wkshps)*, 2015, pp. 1–6.

[69] J. C. B. Garcia, A. Sibille, and M. Kamoun, "Reconfigurable intelligent surfaces: Bridging the gap between scattering and reflection," *IEEE J. Sel. Areas Commun.*, vol. 38, no. 11, pp. 2538–2547, Nov. 2020.

[70] S. W. Ellingson, "Path loss in reconfigurable intelligent surface-enabled channels," in *Proc. IEEE 32nd Annu. Int. Symp. Pers., Indoor Mobile Radio Commun. (PIMRC)*, 2021, pp. 829–835.

[71] W. Tang et al., "Wireless communications with reconfigurable intelligent surface: Path loss modeling and experimental measurement," *IEEE Trans. Wireless Commun.*, vol. 20, no. 1, pp. 421–439, Jan. 2021.

[72] E. Björnson and L. Sanguinetti, "Demystifying the power scaling law of intelligent reflecting surfaces and metasurfaces," in *Proc. IEEE 8th Int. Workshop Comput. Adv. Multi-Sens. Adapt. Process. (CAMSAP)*, 2019, pp. 549–553.

[73] E. Björnson and L. Sanguinetti, "Power scaling laws and near-field behaviors of massive MIMO and intelligent reflecting surfaces," *IEEE Open J. Commun. Soc.*, vol. 1, pp. 1306–1324, 2020.

[74] P. Ramezani and E. Björnson, "Near-field beamforming and multiplexing using extremely large aperture arrays," 2022, *arXiv:2209.03082*.

[75] J. Yang, Y. Zeng, S. Jin, C.-K. Wen, and P. Xu, "Communication and Localization with extremely large lens antenna array," *IEEE Trans. Wireless Commun.*, vol. 20, no. 5, pp. 3031–3048, May 2021.

[76] T. L. Marzetta, "Noncooperative cellular wireless with unlimited numbers of base station antennas," *IEEE Trans. Wireless Commun.*, vol. 9, no. 11, pp. 3590–3600, Nov. 2010.

[77] H. Yang and T. L. Marzetta, "Performance of conjugate and zero-forcing beamforming in large-scale antenna systems," *IEEE J. Sel. Areas Commun.*, vol. 31, no. 2, pp. 172–179, Feb. 2013.

[78] H. Q. Ngo, E. G. Larsson, and T. L. Marzetta, "Energy and spectral efficiency of very large multiuser MIMO systems," *IEEE Trans. Commun.*, vol. 61, no. 4, pp. 1436–1449, Apr. 2013.

[79] D. Tse and P. Viswanath, *Fundamentals of Wireless Communication*. Cambridge, U.K.: Cambridge Univ. Press, 2005.

[80] A. Paulraj, R. Nabar, and D. Gore, *Introduction to Space-Time Wireless Communications*. Cambridge, U.K.: Cambridge Univ. Press, 2003.

[81] H. Shin and J. H. Lee, "Closed-form formulas for ergodic capacity of MIMO rayleigh fading channels," in *Proc. IEEE Int. Conf. Commun. (ICC)*, 2003, pp. 2996–3000 vol.5.

[82] P. Kyosti, "WINNER II channel models," EBITG, Mumbai, India, TUI, Hanover, Germany, UOULU, Haldwani, India, CU/CRC, Boulder, CO, USA, NOKIA, Espoo, Finland, document IST-4-027756 WINNER II D1. 2 V1. 2, 2007.

[83] M. Series, *Guidelines for Evaluation of Radio Interface Technologies for IMT-Advanced*, ITU-Rec. 638, Int. Telecommun. Union, Geneva, Switzerland, 2009.

[84] S. Payami and F. Tufvesson, "Channel measurements and analysis for very large array systems at 2.6 GHz," in *Proc. 6th Eur. Conf. Antennas Propag. (EUCAP)*, 2012, pp. 433–437.

[85] X. Gao, O. Edfors, F. Tufvesson, and E. G. Larsson, "Massive MIMO in real propagation environments: Do all antennas contribute equally?" *IEEE Trans. Commun.*, vol. 63, no. 11, pp. 3917–3928, Nov. 2015.

[86] B. Ai et al., "On indoor millimeter wave massive MIMO channels: Measurement and simulation," *IEEE J. Sel. Areas Commun.*, vol. 35, no. 7, pp. 1678–1690, Jul. 2017.

[87] E. D. Carvalho, A. Ali, A. Amiri, M. Angjelichinoski, and R. W. Heath, "Non-stationarities in extra-large-scale massive MIMO," *IEEE Wireless Commun.*, vol. 27, no. 4, pp. 74–80, Aug. 2020.

[88] L. Liu et al., "The COST 2100 MIMO channel model," *IEEE Wireless Commun.*, vol. 19, no. 6, pp. 92–99, Dec. 2012.

[89] X. Gao, F. Tufvesson, and O. Edfors, "Massive MIMO channels—Measurements and models," in *Proc. Asilomar Conf. Signals, Syst. Comput.*, 2013, pp. 280–284.

[90] Y. Han, S. Jin, C.-K. Wen, and X. Ma, "Channel estimation for extremely large-scale massive MIMO systems," *IEEE Wireless Commun. Lett.*, vol. 9, no. 5, pp. 633–637, May 2020.

[91] A. Amiri, M. Angjelichinoski, E. De Carvalho, and R. W. Heath, "Extremely large aperture massive MIMO: Low complexity receiver architectures," in *Proc. IEEE Globecom Workshops (GC Wkshps)*, 2018, pp. 1–6.

[92] A. Ali, E. D. Carvalho, and R. W. Heath, "Linear receivers in non-stationary massive MIMO channels with visibility regions," *IEEE Wireless Commun. Lett.*, vol. 8, no. 3, pp. 885–888, Jun. 2019.

[93] C.-C. Chong, C.-M. Tan, D. I. Laurenson, S. McLaughlin, M. A. Beach, and A. R. Nix, "A novel wideband dynamic directional indoor channel model based on a Markov process," *IEEE Trans. Wireless Commun.*, vol. 4, no. 4, pp. 1539–1552, Jul. 2005.

[94] J. Salmi, A. Richter, and V. Koivunen, "Detection and tracking of MIMO propagation path parameters using state-space approach," *IEEE Trans. Signal Process.*, vol. 57, no. 4, pp. 1538–1550, Apr. 2009.

[95] R. Zentner and A. Katalinic, "Dynamics of multipath variations in urban environment," in *Proc. 3rd Eur. Wireless Technol. Conf.*, 2010, pp. 125–128.

[96] W. Wang, T. Jost, U.-C. Fiebig, and W. Koch, "Time-variant channel modeling with application to mobile radio based positioning," in *Proc. IEEE Glob. Commun. Conf. (GLOBECOM)*, 2012, pp. 5038–5043.

[97] M. Zhu, J. Vieira, Y. Kuang, K. Åström, A. F. Molisch, and F. Tufvesson, "Tracking and positioning using phase information from estimated multi-path components," in *Proc. IEEE Int. Conf. Commun. Workshop (ICCW)*, 2015, pp. 712–717.

[98] R. He et al., "A dynamic wideband directional channel model for vehicle-to-vehicle communications," *IEEE Trans. Ind. Electron.*, vol. 62, no. 12, pp. 7870–7882, Dec. 2015.

[99] W. Wang, T. Jost, U.-C. Fiebig, and W. Koch, "A time variant outdoor-to-indoor channel model for mobile radio based navigation applications," *Int. J. Antennas Propag.*, vol. 2015, no. 1, 2015, Art. no. 375346.

[100] K. Mahler, W. Keusgen, F. Tufvesson, T. Zemen, and G. Caire, "Measurement-based wideband analysis of dynamic multipath propagation in vehicular communication scenarios," *IEEE Trans. Veh. Technol.*, vol. 66, no. 6, pp. 4657–4667, Jun. 2017.

[101] X. Li, E. Leitinger, M. Oskarsson, K. Åström, and F. Tufvesson, "Massive MIMO-based localization and mapping exploiting phase information of multipath components," *IEEE Trans. Wireless Commun.*, vol. 18, no. 9, pp. 4254–4267, Sep. 2019.

[102] J. Flordelis, X. Li, O. Edfors, and F. Tufvesson, "Massive MIMO extensions to the COST 2100 channel model: Modeling and validation," *IEEE Trans. Wireless Commun.*, vol. 19, no. 1, pp. 380–394, Jan. 2020.

[103] E. T. Michailidis, N. Nomikos, P. Trakadas, and A. G. Kanatas, "Three-dimensional modeling of mmWave doubly massive MIMO aerial fading channels," *IEEE Trans. Veh. Technol.*, vol. 69, no. 2, pp. 1190–1202, Feb. 2020.

[104] M. Cui, Z. Wu, Y. Lu, X. Wei, and L. Dai, "Near-field MIMO communications for 6G: Fundamentals, challenges, potentials, and future directions," *IEEE Commun. Mag.*, vol. 61, no. 1, pp. 40–46, Jan. 2023.

[105] E. Björnson, O. T. Demir, and L. Sanguinetti, "A primer on near-field beamforming for arrays and reconfigurable intelligent surfaces," in *Proc. 55th Asilomar Conf. Signals, Syst., Comput.*, 2021, pp. 105–112.

[106] A. Kosasih and E. Björnson, "Finite beam depth analysis for large arrays," 2024, *arXiv:2306.12367*.

[107] P. Ramezani, A. Kosasih, A. Irshad, and E. Björnson, "Massive spatial multiplexing: Vision, foundations, and challenges," 2023, *arXiv:2307.02684*.

[108] D. Cheng, "On the simulation of Fraunhofer radiation patterns in the fresnel region," *IRE Trans. Antennas Propag.*, vol. 5, no. 4, pp. 399–402, Oct. 1957.

[109] J. Sherman, "Properties of focused apertures in the fresnel region," *IRE Trans. Antennas Propagat.*, vol. 10, no. 4, pp. 399–408, Jul. 1962.

[110] K. T. Selvan and R. Janaswamy, "Fraunhofer and fresnel distances: Unified derivation for aperture antennas," *IEEE Antennas Propag. Mag.*, vol. 59, no. 4, pp. 12–15, Aug. 2017.

[111] A. Yaghjian, "An overview of near-field antenna measurements," *IEEE Trans. Antennas Propag.*, vol. 34, no. 1, pp. 30–45, Jan. 1986.

[112] M. Franceschetti, *Wave Theory of Information*. Cambridge, U.K.: Cambridge Univ. Press, 2017.

[113] R. B. Ertel, P. Cardieri, K. W. Sowerby, T. S. Rappaport, and J. H. Reed, "Overview of spatial channel models for antenna array communication systems," *IEEE Pers. Commun.*, vol. 5, no. 1, pp. 10–22, Feb. 1998.

[114] E. Björnson and L. Sanguinetti, "Utility-based precoding optimization framework for large intelligent surfaces," in *Proc. 53rd Asilomar Conf. Signals, Syst., Comput.*, 2019, pp. 863–867.

[115] D. Starer and A. Nehorai, "Passive localization of near-field sources by path following," *IEEE Trans. Signal Process.*, vol. 42, no. 3, pp. 677–680, Mar. 1994.

[116] L. L. Magoarou, A. L. Calvez, and S. Paquelet, "Massive MIMO channel estimation taking into account spherical waves," in *Proc. IEEE 20th Int. Workshop Signal Process. Adv. Wireless Commun. (SPAWC)*, 2019, pp. 1–5.

[117] B. Friedlander, "Localization of signals in the near-field of an antenna array," *IEEE Trans. Signal Process.*, vol. 67, no. 15, pp. 3885–3893, Aug. 2019.

[118] C. Polk, "Optical fresnel-zone gain of a rectangular aperture," *IRE Trans. Antennas Propag.*, vol. 4, no. 1, pp. 65–69, Jan. 1956.

[119] R. Hansen and L. Bailin, "A new method of near field analysis," *IRE Trans. Antennas Propag.*, vol. 7, no. 5, pp. 458–467, Dec. 1959.

[120] R. Li, S. Sun, and M. Tao, "Applicable regions of spherical and plane wave models for extremely large-scale array communications," 2023, *arXiv:2301.06036*.

[121] J.-S. Jiang and M. A. Ingram, "Spherical-wave model for short-range MIMO," *IEEE Trans. Commun.*, vol. 53, no. 9, pp. 1534–1541, Sep. 2005.

[122] F. Bohagen, P. Orten, and G. E. Oien, "On spherical vs. plane wave modeling of line-of-sight MIMO channels," *IEEE Trans. Commun.*, vol. 57, no. 3, pp. 841–849, Mar. 2009.

[123] P. Wang, Y. Li, X. Yuan, L. Song, and B. Vucetic, "Tens of Gigabits wireless communications over E-band LoS MIMO channels with uniform linear antenna arrays," *IEEE Trans. Wireless Commun.*, vol. 13, no. 7, pp. 3791–3805, Jul. 2014.

[124] Z. Xie, Y. Liu, J. Xu, X. Wu, and A. Nallanathan, "Performance analysis for near-field MIMO: Discrete and continuous aperture antennas," *IEEE Wireless Commun. Lett.*, vol. 12, no. 12, pp. 2258–2262, Dec. 2023.

[125] H. Chen, A. Elzanaty, R. Ghazalian, M. F. Keskin, R. Jäntti, and H. Wymeersch, "Channel model mismatch analysis for XL-MIMO systems from a localization perspective," in *Proc. IEEE Glob. Commun. Conf.*, 2022, pp. 1588–1593.

[126] A. Chen, L. Chen, Y. Chen, N. Zhao, and C. You, "Near-field positioning and attitude sensing based on electromagnetic propagation modeling," 2023, *arXiv:2310.17327*.

[127] E. G. Larsson, O. Edfors, F. Tufvesson, and T. L. Marzetta, "Massive MIMO for next generation wireless systems," *IEEE Commun. Mag.*, vol. 52, no. 2, pp. 186–195, Feb. 2014.

[128] S. Tretyakov, "Metasurfaces for general transformations of electromagnetic fields," *Philosoph. Trans. Roy. Soc. A, Math., Phys. Eng. Sci.*, vol. 373, no. 2049, 2015, Art. no. 20140362.

[129] D. González-Ovejero, G. Minatti, G. Chattopadhyay, and S. Maci, "Multibeam by metasurface antennas," *IEEE Trans. Antennas Propag.*, vol. 65, no. 6, pp. 2923–2930, Jun. 2017.

[130] C. L. Holloway, E. F. Kuester, J. A. Gordon, J. O'Hara, J. Booth, and D. R. Smith, "An overview of the theory and applications of metasurfaces: The two-dimensional equivalents of metamaterials," *IEEE Antennas Propag. Mag.*, vol. 54, no. 2, pp. 10–35, Apr. 2012.

[131] N. Kaina, M. Dupré, G. Lerosey, and M. Fink, "Shaping complex microwave fields in reverberating media with binary tunable metasurfaces," *Sci. Rep.*, vol. 4, no. 1, p. 6693, 2014.

[132] Q. Wu, S. Zhang, B. Zheng, C. You, and R. Zhang, "Intelligent reflecting surface-aided wireless communications: A tutorial," *IEEE Trans. Commun.*, vol. 69, no. 5, pp. 3313–3351, May 2021.

[133] M. Di Renzo et al., "Smart radio environments empowered by reconfigurable intelligent surfaces: How it works, state of research, and the road ahead," *IEEE J. Sel. Areas Commun.*, vol. 38, no. 11, pp. 2450–2525, Nov. 2020.

[134] D.-S. Shiu, G. Foschini, M. Gans, and J. Kahn, "Fading correlation and its effect on the capacity of multielement antenna systems," *IEEE Trans. Commun.*, vol. 48, no. 3, pp. 502–513, Mar. 2000.

[135] T. Muharemovic, A. Sabharwal, and B. Aazhang, "Antenna packing in low-power systems: Communication limits and array design," *IEEE Trans. Inf. Theory*, vol. 54, no. 1, pp. 429–440, Jan. 2008.

[136] D. Gesbert, T. Ekman, and N. Christophersen, "Capacity limits of dense palm-sized MIMO arrays," in *Proc. Glob. Telecommun. Conf.*, 2002, pp. 1187–1191.

[137] A. Poon, R. Brodersen, and D. Tse, "Degrees of freedom in multiple-antenna channels: A signal space approach," *IEEE Trans. Inf. Theory*, vol. 51, no. 2, pp. 523–536, Feb. 2005.

[138] S. Verdu, "Spectral efficiency in the wideband regime," *IEEE Trans. Inf. Theory*, vol. 48, no. 6, pp. 1319–1343, Jun. 2002.

[139] M. Migliore, "On the role of the number of degrees of freedom of the field in MIMO channels," *IEEE Trans. Antennas Propag.*, vol. 54, no. 2, pp. 620–628, Feb. 2006.

[140] D. A. Miller, "Waves, modes, communications, and optics: A tutorial," *Adv. Opt. Photon.*, vol. 11, no. 3, pp. 679–825, 2019.

[141] C. E. Shannon, "A mathematical theory of communication," *Bell Syst. Tech. J.*, vol. 27, no. 3, pp. 379–423, 1948.

[142] M. Franceschetti, "On Landau'S Eigenvalue theorem and information cut-sets," *IEEE Trans. Inf. Theory*, vol. 61, no. 9, pp. 5042–5051, Sep. 2015.

[143] D. A. Miller, "Communicating with waves between volumes: Evaluating orthogonal spatial channels and limits on coupling strengths," *Appl. Opt.*, vol. 39, no. 11, pp. 1681–1699, 2000.

[144] J. Brady, N. Behdad, and A. M. Sayeed, "Beamspace MIMO for millimeter-wave communications: System architecture, modeling, analysis, and measurements," *IEEE Trans. Antennas Propag.*, vol. 61, no. 7, pp. 3814–3827, Jul. 2013.

[145] K. Nishimori, N. Honma, T. Seki, and K. Hiraga, "On the transmission method for short-range MIMO communication," *IEEE Trans. Veh. Technol.*, vol. 60, no. 3, pp. 1247–1251, Mar. 2011.

[146] L. Hanlen and M. Fu, "Wireless communication systems with spatial diversity: A volumetric model," *IEEE Trans. Wireless Commun.*, vol. 5, no. 1, pp. 133–142, Jan. 2006.

[147] K. Murata, N. Honma, K. Nishimori, N. Michishita, and H. Morishita, "Analog Eigenmode transmission for short-range MIMO based on orbital angular momentum," *IEEE Trans. Antennas Propag.*, vol. 65, no. 12, pp. 6687–6702, Dec. 2017.

[148] A. Trichili, K.-H. Park, M. Zghal, B. S. Ooi, and M.-S. Alouini, "Communicating using spatial mode multiplexing: Potentials, challenges, and perspectives," *IEEE Commun. Surveys Tuts.*, vol. 21, no. 4, pp. 3175–3203, 4th Quart., 2019.

[149] T. Hu, Y. Wang, X. Liao, J. Zhang, and Q. Song, "OFDM-OAM modulation for future wireless communications," *IEEE Access*, vol. 7, pp. 59114–59125, 2019.

[150] R. Chen, W.-X. Long, X. Wang, and L. Jiandong, "Multi-mode OAM radio waves: Generation, angle of arrival estimation and reception with UCAs," *IEEE Trans. Wireless Commun.*, vol. 19, no. 10, pp. 6932–6947, Oct. 2020.

[151] O. Edfors and A. J. Johansson, "Is orbital angular momentum (OAM) based radio communication an unexploited area?" *IEEE Trans. Antennas Propag.*, vol. 60, no. 2, pp. 1126–1131, Feb. 2012.

[152] W. Cheng, W. Zhang, H. Jing, S. Gao, and H. Zhang, "Orbital angular momentum for wireless communications," *IEEE Wireless Commun.*, vol. 26, no. 1, pp. 100–107, Feb. 2019.

[153] Z. Zhang and L. Dai, "Pattern-division multiplexing for continuous-aperture MIMO," in *Proc. IEEE Int. Conf. Commun.*, 2022, pp. 3287–3292.

[154] N. Honma, K. Nishimori, T. Seki, and M. Mizoguchi, "Short range MIMO communication," in *Proc. 3rd Eur. Conf. Antennas Propag.*, 2009, pp. 1763–1767.

[155] Y. Tak and S. Nam, "Mode-based computation method of channel characteristics for a near-field MIMO," *IEEE Antennas Wireless Propag. Lett.*, vol. 10, pp. 1170–1173, 2011.

[156] K. Hiraga, T. Seki, K. Nishimori, and K. Uehara, "Effectiveness of short-range MIMO using dual-polarized antenna," *IEICE Trans. Commun.*, vol. 95, no. 1, pp. 87–96, 2012.

[157] S. Biswas, C. Masouros, and T. Ratnarajah, "Performance analysis of large multiuser MIMO systems with space-constrained 2-D antenna arrays," *IEEE Trans. Wireless Commun.*, vol. 15, no. 5, pp. 3492–3505, May 2016.

[158] J. Rodríguez-Fernández, N. González-Prelcic, K. Venugopal, and R. W. Heath, "Frequency-domain compressive channel estimation for frequency-selective hybrid millimeter wave MIMO systems," *IEEE Trans. Wireless Commun.*, vol. 17, no. 5, pp. 2946–2960, May 2018.

[159] J. Lee, G.-T. Gil, and Y. H. Lee, "Channel estimation via orthogonal matching pursuit for hybrid MIMO systems in millimeter wave communications," *IEEE Trans. Commun.*, vol. 64, no. 6, pp. 2370–2386, Jun. 2016.

[160] W. U. Bajwa, J. Haupt, A. M. Sayeed, and R. Nowak, "Compressed channel sensing: A new approach to estimating sparse multipath channels," *Proc. IEEE*, vol. 98, no. 6, pp. 1058–1076, Jun. 2010.

[161] X. Rao, V. K. N. Lau, and X. Kong, "CSIT estimation and feedback for FDD multi-user massive MIMO systems," in *Proc. IEEE Int. Conf. Acoust., Speech Signal Process. (ICASSP)*, 2014, pp. 3157–3161.

[162] Z. Gao, L. Dai, Z. Wang, and S. Chen, "Spatially common sparsity based adaptive channel estimation and feedback for FDD massive MIMO," *IEEE Trans. Signal Process.*, vol. 63, no. 23, pp. 6169–6183, Dec. 2015.

[163] X. Wei, C. Hu, and L. Dai, "Deep learning for beamspace channel estimation in millimeter-wave massive MIMO systems," *IEEE Trans. Commun.*, vol. 69, no. 1, pp. 182–193, Jan. 2021.

[164] X. Gao, L. Dai, S. Zhou, A. M. Sayeed, and L. Hanzo, "Wideband beamspace channel estimation for millimeter-wave MIMO systems relying on lens antenna arrays," *IEEE Trans. Signal Process.*, vol. 67, no. 18, pp. 4809–4824, Sep. 2019.

[165] J. Rodríguez-Fernández, N. González-Prelcic, and R. W. Heath, "A compressive sensing-maximum likelihood approach for off-grid wideband channel estimation at mmWave," in *Proc. IEEE 7th Int. Workshop Comput. Adv. Multi-Sensor Adapt. Process. (CAMSAP)*, 2017, pp. 1–5.

[166] Z. Zhou, J. Fang, L. Yang, H. Li, Z. Chen, and R. S. Blum, "Low-rank tensor decomposition-aided channel estimation for millimeter wave MIMO-OFDM systems," *IEEE J. Sel. Areas Commun.*, vol. 35, no. 7, pp. 1524–1538, Jul. 2017.

[167] C. Hu, L. Dai, T. Mir, Z. Gao, and J. Fang, "Super-resolution channel estimation for mmWave massive MIMO with hybrid precoding," *IEEE Trans. Veh. Technol.*, vol. 67, no. 9, pp. 8954–8958, Sep. 2018.

[168] N. González-Prelcic, H. Xie, J. Palacios, and T. Shimizu, "Wideband channel tracking and hybrid precoding for mmWave MIMO systems," *IEEE Trans. Wireless Commun.*, vol. 20, no. 4, pp. 2161–2174, Apr. 2021.

[169] L. Lu, K. Ma, and Z. Wang, "Block-dominant compressed sensing for near-field communications: Fundamentals, solutions and future directions," 2024, *arXiv:2403.12369*.

[170] H. Wu, L. Lu, and Z. Wang, "Near-field channel estimation in dual-band XL-MIMO with side information-assisted compressed sensing," 2024, *arXiv:2403.12620*.

[171] Y. Chen, Y. Wang, Z. Wang, and Z. Han, "Angular-distance based channel estimation for holographic MIMO," *IEEE J. Sel. Areas Commun.*, vol. 42, no. 6, pp. 1684–1702, 2024.

[172] X. Guo, Y. Chen, and Y. Wang, "Compressed channel estimation for near-field XL-MIMO using triple parametric decomposition," *IEEE Trans. Veh. Technol.*, vol. 72, no. 11, pp. 15040–15045, 2023.

[173] W. Li, H. Yin, Z. Qin, and M. Debbah, "Wavefront transformation-based near-field channel prediction for extremely large antenna array with mobility," *IEEE Trans. Wireless Commun.*, vol. 23, no. 10, pp. 15613–15626, Oct. 2024.

[174] X. Wei and L. Dai, "Channel estimation for extremely large-scale massive MIMO: Far-field, near-field, or hybrid-field?" *IEEE Commun. Lett.*, vol. 26, no. 1, pp. 177–181, Jan. 2022.

[175] W. Yang, M. Li, and Q. Liu, "A practical channel estimation strategy for XL-MIMO communication systems," *IEEE Commun. Lett.*, vol. 27, no. 6, pp. 1580–1583, Jun. 2023.

[176] P. R. Singh, Y. Wang, and P. Charge, "Near field targets localization using bistatic MIMO system with spherical wavefront based model," in *Proc. 25th Eur. Signal Process. Conf. (EUSIPCO)*, 2017, pp. 2408–2412.

[177] S. Yue, S. Zeng, L. Liu, and B. Di, "Channel estimation for holographic communications in hybrid near-far field," in *Proc. IEEE Glob. Commun. Conf.*, 2023, pp. 6133–6138.

[178] X. Shi, X. Wang, J. Tan, and J. Wang, "Sparse estimation for XL-MIMO with unified LoS/NLoS representation," 2024, *arXiv:2403.12506*.

[179] Y. Chen, L. Yan, and C. Han, "Hybrid spherical- and planar-wave modeling and DCNN-powered estimation of terahertz ultra-massive MIMO channels," *IEEE Trans. Commun.*, vol. 69, no. 10, pp. 7063–7076, Oct. 2021.

[180] W. Yu, Y. Shen, H. He, X. Yu, J. Zhang, and K. B. Letaief, "Hybrid far- and near-field channel estimation for THz ultra-massive MIMO via fixed point networks," in *Proc. IEEE Glob. Commun. Conf.*, 2022, pp. 5384–5389.

[181] W. Yu et al., "An adaptive and robust deep learning framework for THz ultra-massive MIMO channel estimation," *IEEE J. Sel. Topics Signal Process.*, vol. 17, no. 4, pp. 761–776, Jul. 2023.

[182] X. Zhang, H. Zhang, and Y. C. Eldar, "Near-field sparse channel representation and estimation in 6G wireless communications," *IEEE Trans. Commun.*, vol. 72, no. 1, pp. 450–464, Jan. 2024.

[183] X. Zhang, Z. Wang, H. Zhang, and L. Yang, "Near-field channel estimation for extremely large-scale array communications: A model-based deep learning approach," *IEEE Commun. Lett.*, vol. 27, no. 4, pp. 1155–1159, Apr. 2023.

[184] H. Lei, J. Zhang, H. Xiao, X. Zhang, B. Ai, and D. W. K. Ng, "Channel estimation for XL-MIMO systems with polar-domain multi-scale residual dense network," *IEEE Trans. Veh. Technol.*, vol. 73, no. 1, pp. 1479–1484, Jan. 2024.

[185] S. Hou, Y. Wang, T. Zeng, and S. Wu, "Sparse channel estimation for spatial non-stationary massive MIMO channels," *IEEE Commun. Lett.*, vol. 24, no. 3, pp. 681–684, Mar. 2020.

[186] Y. Chen, Z. Zhang, M. Cui, and L. Dai, "Channel estimation for non-stationary extremely large-scale MIMO," in *Proc. IEEE 97th Veh. Technol. Conf.*, 2023, pp. 1–5.

[187] Y. Chen and L. Dai, "Non-stationary channel estimation for extremely large-scale MIMO," *IEEE Trans. Wireless Commun.*, vol. 23, no. 7, pp. 7683–7697, Jul. 2024.

[188] H. Iimori et al., "Grant-free access for extra-large MIMO systems subject to spatial non-stationarity," in *Proc. IEEE Int. Conf. Commun.*, 2022, pp. 1758–1762.

[189] H. Iimori, T. Takahashi, K. Ishibashi, G. T. F. de Abreu, D. González G., and O. Gonsa, "Joint activity and channel estimation for extra-large MIMO systems," *IEEE Trans. Wireless Commun.*, vol. 21, no. 9, pp. 7253–7270, Sep. 2022.

[190] Q. Shi, Y. Liu, S. Zhang, S. Xu, and V. K. N. Lau, "A unified channel estimation framework for stationary and non-stationary fading environments," *IEEE Trans. Commun.*, vol. 69, no. 7, pp. 4937–4952, Jul. 2021.

[191] X. Cheng, K. Xu, J. Sun, and S. Li, "Adaptive grouping sparse Bayesian learning for channel estimation in non-stationary uplink massive MIMO systems," *IEEE Trans. Wireless Commun.*, vol. 18, no. 8, pp. 4184–4198, Aug. 2019.

[192] P. Nepa and A. Buffi, "Near-field-focused microwave antennas: Near-field shaping and implementation," *IEEE Antennas Propag. Mag.*, vol. 59, no. 3, pp. 42–53, Jun. 2017.

[193] Z. Wu and L. Dai, "Multiple access for near-field communications: SDMA or LDMA?" *IEEE J. Sel. Areas Commun.*, vol. 41, no. 6, pp. 1918–1935, Jun. 2023.

[194] N. Deshpande, M. R. Castellanos, S. R. Khosravirad, J. Du, H. Viswanathan, and R. W. Heath, "A wideband generalization of the near-field region for extremely large phased-arrays," *IEEE Wireless Commun. Lett.*, vol. 12, no. 3, pp. 515–519, Mar. 2023.

[195] N. J. Myers and R. W. Heath, "InFocus: A spatial coding technique to mitigate misfocus in near-field LoS beamforming," *IEEE Trans. Wireless Commun.*, vol. 21, no. 4, pp. 2193–2209, Apr. 2022.

[196] A. M. Elbir, W. Shi, A. K. Papazafeiropoulos, P. Kourtessis, and S. Chatzinotas, "Terahertz-band channel and beam split estimation via array perturbation model," *IEEE Open J. Commun. Soc.*, vol. 4, pp. 892–907, 2023.

[197] F. Zheng, "Extremely large-scale array systems: Near-filed codebook design and performance analysis," 2023, *arXiv:2306.01458*.

[198] Y. Zhang, X. Wu, and C. You, "Fast near-field beam training for extremely large-scale array," *IEEE Wireless Commun. Lett.*, vol. 11, no. 12, pp. 2625–2629, Dec. 2022.

[199] X. Wu, C. You, J. Li, and Y. Zhang, "Near-field beam training: Joint angle and range estimation with DFT codebook," *IEEE Trans. Wireless Commun.*, vol. 23, no. 9, pp. 11890–11903, Sep. 2024.

[200] C. Wu, C. You, Y. Liu, L. Chen, and S. Shi, "Two-stage hierarchical beam training for near-field communications," *IEEE Trans. Veh. Technol.*, vol. 73, no. 2, pp. 2032–2044, Feb. 2024.

[201] Y. Lu, Z. Zhang, and L. Dai, "Hierarchical beam training for extremely large-scale MIMO: From far-field to near-field," *IEEE Trans. Commun.*, vol. 72, no. 4, pp. 2247–2259, Apr. 2024.

[202] X. Shi, J. Wang, Z. Sun, and J. Song, "Spatial-chirp codebook-based hierarchical beam training for extremely large-scale massive MIMO," *IEEE Trans. Wireless Commun.*, vol. 23, no. 4, pp. 2824–2838, Apr. 2024.

[203] W. Liu, H. Ren, C. Pan, and J. Wang, "Deep learning based beam training for extremely large-scale massive MIMO in near-field domain," *IEEE Commun. Lett.*, vol. 27, no. 1, pp. 170–174, Jan. 2023.

[204] M. Xiao et al., "Millimeter wave communications for future mobile networks," *IEEE J. Sel. Areas Commun.*, vol. 35, no. 9, pp. 1909–1935, Sep. 2017.

[205] I. F. Akyildiz, C. Han, Z. Hu, S. Nie, and J. M. Jornet, "Terahertz band communication: An old problem revisited and research directions for the next decade," *IEEE Trans. Commun.*, vol. 70, no. 6, pp. 4250–4285, Jun. 2022.

[206] H. Sarieddeen, M.-S. Alouini, and T. Y. Al-Naffouri, "An overview of signal processing techniques for Terahertz communications," *Proc. IEEE*, vol. 109, no. 10, pp. 1628–1665, Oct. 2021.

[207] V. Petrov, J. M. Jornet, and A. Singh, "Near-field 6G networks: Why mobile Terahertz communications MUST operate in the near field," in *Proc. IEEE Global Commun. Conf.*, 2023, pp. 3983–3989.

[208] P. Sen, J. V. Siles, N. Thawdar, and J. M. Jornet, "Multi-kilometre and multi-gigabit-per-second sub-terahertz communications for wireless backhaul applications," *Nat. Electron.*, vol. 6, no. 2, pp. 164–175, 2023.

[209] V. Petrov, M. Komarov, D. Moltchanov, J. M. Jornet, and Y. Koucheryavy, "Interference and SINR in millimeter wave and Terahertz communication systems with blocking and directional antennas," *IEEE Trans. Wireless Commun.*, vol. 16, no. 3, pp. 1791–1808, Mar. 2017.

[210] A. Singh et al., "Wavefront engineering: Realizing efficient terahertz band communications in 6G and beyond," *IEEE Wireless Commun.*, vol. 31, no. 3, pp. 133–139, Jun. 2024.

[211] D. Headland, Y. Monnai, D. Abbott, C. Fumeaux, and W. Withayachumnankul, "Tutorial: Terahertz beamforming, from concepts to realizations," *APL Photon.*, vol. 3, no. 5, 2018, Art. no. 051101.

[212] A. Singh, I. V. Reddy, D. Bodet, and J. M. Jornet, "Bessel beams for 6G—A performance analysis," in *Proc. 56th Asilomar Conf. Signals, Syst., Comput.*, 2022, pp. 658–664.

[213] A. Singh, V. Petrov, and J. M. Jornet, "Utilization of bessel beams in wideband sub terahertz communication systems to mitigate beamsplit effects in the near-field," in *Proc. IEEE Int. Conf. Acoust., Speech Signal Process. (ICASSP)*, 2023, pp. 1–5.

[214] J. Durnin, J. Miceli, and J. H. Eberly, "Comparison of bessel and Gaussian beams," *Opt. Lett.*, vol. 13, no. 2, pp. 79–80, 1988.

[215] I. V. Reddy, D. Bodet, A. Singh, V. Petrov, C. Liberale, and J. M. Jornet, "Ultrabroadband terahertz-band communications with self-healing bessel beams," *Commun. Eng.*, vol. 2, no. 1, p. 70, 2023.

[216] K. D. Paschaloudis, R. C. Pimenta, G. Soriano, and M. Ettorre, "Near-field links with obstructed line of sight via bessel beams," in *Proc. 17th Eur. Conf. Antennas Propaga. (EuCAP)*, 2023, pp. 1–3.

[217] S. Li and J. Wang, "Adaptive free-space optical communications through turbulence using self-healing bessel beams," *Sci. Rep.*, vol. 7, no. 1, 2017, Art. no. 43233.

[218] G. A. Siviloglou, J. Broky, A. Dogariu, and D. Christodoulides, "Observation of accelerating airy beams," *Phys. Rev. Lett.*, vol. 99, no. 21, 2007, Art. no. 213901.

[219] N. K. Efremidis, Z. Chen, M. Segev, and D. N. Christodoulides, "Airy beams and accelerating waves: An overview of recent advances," *Optica*, vol. 6, no. 5, pp. 686–701, 2019.

[220] H. Guerboukha, B. Zhao, Z. Fang, E. Knightly, and D. M. Mittleman, "Curving THz beams in the near field: A framework to compute link budgets," in *Proc. 18th Eur. Conf. Antennas Propag. (EuCAP)*, 2024, pp. 1–5.

[221] H. Guerboukha, B. Zhao, Z. Fang, E. Knightly, and D. M. Mittleman, "Curving THz wireless data links around obstacles," *Commun. Eng.*, vol. 3, no. 1, p. 58, 2024.

[222] S. Park, A. Alkhateeb, and R. W. Heath, "Dynamic subarrays for hybrid precoding in wideband mmWave MIMO systems," *IEEE Trans. Wireless Commun.*, vol. 16, no. 5, pp. 2907–2920, May 2017.

[223] S. Hu, K. Chitti, F. Rusek, and O. Edfors, "User assignment with distributed large intelligent surface (LIS) systems," in *Proc. IEEE 29th Annu. Int. Symp. Pers., Indoor Mobile Radio Commun. (PIMRC)*, 2018, pp. 1–6.

[224] A. K. Mishra and V. Ponnusamy, "Millimeter wave and radio stripe: A prospective wireless technology for 6G and beyond networks," in *Proc. Smart Technol., Commun. Robot. (STCR)*, 2021, pp. 1–3.

[225] E. Bertilsson, O. Gustafsson, and E. G. Larsson, "A scalable architecture for massive MIMO base stations using distributed processing," in *Proc. 50th Asilomar Conf. Signals, Syst. Comput.*, 2016, pp. 864–868.

[226] F. Conceição, C. H. Antunes, M. Gomes, V. Silva, and R. Dinis, "User fairness in radio stripes networks using Meta-heuristics optimization," in *Proc. IEEE 95th Veh. Technol. Conf.*, 2022, pp. 1–6.

[227] O. L. A. López, D. Kumar, R. D. Souza, P. Popovski, A. Tölli, and M. Latva-Aho, "Massive MIMO with radio stripes for indoor wireless energy transfer," *IEEE Trans. Wireless Commun.*, vol. 21, no. 9, pp. 7088–7104, 2022.

[228] K. W. Helmersson, P. Frenger, and A. Helmersson, "Uplink D-MIMO with Decentralized subset combining," in *Proc. IEEE Int. Conf. Commun.*, 2022, pp. 5134–5139.

[229] K. W. Helmersson, P. Frenger, and A. Helmersson, "Uplink D-MIMO processing using Kalman filter combining," in *Proc. IEEE Global Commun. Conf.*, 2022, pp. 1703–1708.

[230] G. J. Anaya-López, J. P. González-Coma, and F. J. López-Martínez, "Spatial degrees of freedom for physical layer security in XL-MIMO," in *Proc. IEEE 95th Veh. Technol. Conf.*, 2022, pp. 1–5.

[231] G. J. Anaya-López, J. P. González-Coma, and F. J. López-Martínez, "Leakage subspace precoding and scheduling for physical layer security in multi-user XL-MIMO systems," *IEEE Commun. Lett.*, vol. 27, no. 2, pp. 467–471, Feb. 2023.

[232] Z. Zhang, Y. Liu, Z. Wang, X. Mu, and J. Chen, "Physical layer security in near-field communications," *IEEE Trans. Veh. Technol.*, vol. 73, no. 7, pp. 10761–10766, Jul. 2024.

[233] J. Chen, Y. Xiao, K. Liu, Y. Zhong, X. Lei, and M. Xiao, "Physical layer security for near-field communications via directional modulation," *IEEE Trans. Veh. Technol.*, ol. 73, no. 8, pp. 12242–12246, Aug. 2024.

[234] A. Chen, L. Chen, Y. Chen, C. You, G. Wei, and F. R. Yu, "Cramér-Rao bounds of near-field positioning based on electromagnetic propagation model," *IEEE Trans. Veh. Technol.*, vol. 72, no. 11, pp. 13808–13825, Nov. 2023.

[235] *Framework and Overall Objectives of the Future Development of IMT for 2030 and Beyond*, Int. Telecommun. Union, Geneva, Switzerland, Nov. 2023.

[236] Z. Xiao and Y. Zeng, "An overview on integrated localization and communication towards 6G," *Sci. China Inf. Sci.*, vol. 65, no. 3, 2022, Art. no. 131301.

[237] F. Liu et al., "Integrated sensing and communications: Toward dual-functional wireless networks for 6G and beyond," *IEEE J. Sel. Areas Commun.*, vol. 40, no. 6, pp. 1728–1767, Jun. 2022.

[238] H. Wang and Y. Zeng, "SNR scaling laws for radio sensing with extremely large-scale MIMO," in *Proc. IEEE Int. Conf. Commun. Workshops (ICC Workshops)*, 2022, pp. 121–126.

[239] H. Wang, Z. Xiao, and Y. Zeng, "Cramér-Rao bounds for near-field sensing with extremely large-scale MIMO," *IEEE Trans. Signal Process.*, vol. 72, pp. 701–717, Jan. 2024.

[240] Z. Wang, X. Mu, and Y. Liu, "Near-field integrated sensing and communications," *IEEE Commun. Lett.*, vol. 27, no. 8, pp. 2048–2052, Aug. 2023.

[241] Y. Zhang and C. You, "SWIPT in mixed near- and far-field channels: Joint beam scheduling and power allocation," *IEEE J. Sel. Areas Commun.*, vol. 42, no. 6, pp. 1583–1597, Apr. 2024.

[242] Y. Zhang, C. You, W. Yuan, F. Liu, and R. Zhang, "Joint beam scheduling and power allocation for SWIPT in mixed near- and far-field channels," in *Proc. IEEE Global Commun. Conf.*, 2023, pp. 1604–1609.

[243] D. P. Petersen and D. Middleton, "Sampling and reconstruction of wave-number-limited functions in N-dimensional Euclidean spaces," *Inf. Control*, vol. 5, no. 4, pp. 279–323, 1962.

[244] M. D. Renzo and M. D. Migliore, "Electromagnetic signal and information theory," *IEEE BITS Inf. Theory Mag.*, early access, Jan. 29, 2024, doi: 10.4236/jsea.2016.910036.

[245] W. Yang et al., "Semantic communications for future Internet: Fundamentals, applications, and challenges," *IEEE Commun. Surveys Tuts.*, vol. 25, no. 1, pp. 213–250, 1st Quart., 2023.

[246] X. Luo, H.-H. Chen, and Q. Guo, "Semantic communications: Overview, open issues, and future research directions," *IEEE Wireless Commun.*, vol. 29, no. 1, pp. 210–219, Feb. 2022.

[247] J. Wang, H. Du, Z. Tian, D. Niyato, J. Kang, and X. Shen, "Semantic-aware sensing information transmission for metaverse: A contest theoretic approach," *IEEE Trans. Wireless Commun.*, vol. 22, no. 8, pp. 5214–5228, Aug. 2023.

[248] M. Chen, H. V. Poor, W. Saad, and S. Cui, "Wireless communications for collaborative federated learning," *IEEE Commun. Mag.*, vol. 58, no. 12, pp. 48–54, Dec. 2020.

[249] S. Niknam, H. S. Dhillon, and J. H. Reed, "Federated learning for wireless communications: Motivation, opportunities, and challenges," *IEEE Commun. Mag.*, vol. 58, no. 6, pp. 46–51, Jun. 2020.

[250] G. Charan, M. Alrabeiah, and A. Alkhateeb, "Vision-aided 6G wireless communications: Blockage prediction and proactive hand-off," *IEEE Trans. Veh. Technol.*, vol. 70, no. 10, pp. 10193–10208, Oct. 2021.

[251] E. Balevi and J. G. Andrews, "Unfolded hybrid beamforming with GAN compressed ultra-low feedback overhead," *IEEE Trans. Wireless Commun.*, vol. 20, no. 12, pp. 8381–8392, Dec. 2021.

[252] Y. Zhang, C. You, L. Chen, and B. Zheng, "Mixed near- and far-field communications for extremely large-scale array: An interference perspective," *IEEE Commun. Lett.*, vol. 27, no. 9, pp. 2496–2500, Sep. 2023.

[253] Z. Feng, Z. Wei, X. Chen, H. Yang, Q. Zhang, and P. Zhang, "Joint communication, sensing, and computation enabled 6G intelligent machine system," *IEEE Netw.*, vol. 35, no. 6, pp. 34–42, Nov./Dec. 2021.

[254] Q. Qi, X. Chen, A. Khalili, C. Zhong, Z. Zhang, and D. W. K. Ng, "Integrating sensing, computing, and communication in 6G wireless networks: Design and optimization," *IEEE Trans. Commun.*, vol. 70, no. 9, pp. 6212–6227, 2022.

[255] L. M. Taniguchi, J. H. I. de Souza, D. W. M. Guerra, and T. Abrao, "Resource efficiency and pilot decontamination in XL-MIMO double-scattering correlated channels," *Trans. Emerg. Telecommun. Technol.*, vol. 32, no. 12, 2021, Art. no. e4365.

[256] G. A. Ubiali, T. Abrão, and J. C. Marinello, "Improving spectral efficiency via pilot assignment and subarray selection under realistic XL-MIMO channels," *Phys. Commun.*, vol. 58, Jun. 2023, Art. no. 102062.
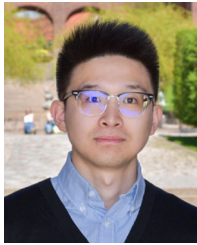
SICONG YE (Member, IEEE) received the joint B.Eng. degree from Xi'an Jiaotong-Liverpool University, China, and University of Liverpool, U.K., in 2020, and the M.S. degree from Imperial College London, U.K., in 2021. He is currently pursuing the Ph.D. degree with KTH Royal Institute of Technology, Sweden. His research interests include massive MIMO, near-field communications, integrated sensing and communications, and artificial intelligence empowered communications.
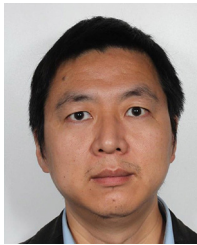
MING XIAO (Senior Member, IEEE) received the Ph.D. degree from the Chalmers University of technology, Sweden, in November 2007. Since November 2007, he has been with the Department of Information Science and Engineering, School of Electrical Engineering and Computer Science, Royal Institute of Technology, Sweden, where he is currently a Professor. He received IEEE Vehicular Technology Society Best Magazine Paper Award in 2023. He was an Editor of IEEE TRANSACTIONS ON COMMUNICATIONS from 2012 to 2017, and has been an Editor of IEEE TRANSACTIONS ON WIRELESS COMMUNICATIONS since 2018. He has been an Area Editor for IEEE OPEN JOURNAL OF THE COMMUNICATION SOCIETY since 2019.

MAN-WAI KWAN (Senior Member, IEEE) received the B.Eng. and Ph.D. degrees in electronic engineering from The Hong Kong University of Science and Technology in 2000 and 2004, respectively. He is a leading expert in 4G and 5G cellular systems design, holding over 30 patents in the field. His research interests include wireless systems design, with a focus on massive MIMO, integrated sensing and communication, and novel waveform design. He has been recognized with the Schmidt Electronics Asia Award of Excellence and the Hong Kong Telecom Institute of Information Technology Scholar. He is a member of the IEEE ComSoc and the Institution of Engineering and Technology.

ZHENG MA (Member, IEEE) received the B.Sc. and Ph.D. degrees in communications and information system from Southwest Jiaotong University in 2000 and 2006, respectively. He was a Visiting Scholar with the University of Leeds, U.K., in 2003. In 2003 and 2005, he was a Visiting Scholar with The Hong Kong University of Science and Technology. From 2008 to 2009, he was a Visiting Research Fellow with the Department of Communication Systems, Lancaster University, U.K. He is currently a Professor with Southwest Jiaotong University. He has authored over 120 research papers in high quality journals and conferences. His research interests include: Information theory and coding, signal design and applications, FPGA/DSP implementation, and professional mobile radio. He was an Area Editor of the IEEE COMMUNICATIONS LETTERS. He is also the Vice-Chairman of Information Theory Chapter in the IEEE Chengdu Section. He received the Marie Curie Individual Fellowship in 2018.

YONGMING HUANG (Senior Member, IEEE) received the B.S. and M.S. degrees from Nanjing University, Nanjing, China, in 2000 and 2003, respectively, and the Ph.D. degree in electrical engineering from Southeast University, Nanjing, China, in 2007.

Since March 2007, he has been a Faculty with the School of Information Science and Engineering, Southeast University, where he is currently a Full Professor. Since 2019, he has also been the Director of the Pervasive Communication Research Center, Purple Mountain Laboratories. From 2008 to 2009, he was visiting the Signal Processing Lab, Royal Institute of Technology (KTH), Stockholm, Sweden. He has published over 200 peer-reviewed papers, hold over 80 invention patents. He submitted around 20 technical contributions to IEEE standards, and was awarded a certificate of appreciation for outstanding contribution to the development of IEEE standard 802.11aj. His current research interests include intelligent 5G/6G mobile communications and millimeter wave wireless communications. He has served as an Associate Editor for a couple of international journals, including the IEEE TRANSACTIONS ON SIGNAL PROCESSING and the IEEE WIRELESS COMMUNICATIONS LETTERS.

GEORGE KARAGIANNIDIS (Fellow, IEEE) is currently a Professor with the Electrical and Computer Engineering Department, Aristotle University of Thessaloniki, Greece, and the Head of the Wireless Communications and Information Processing Group. He is also Faculty Fellow with the Cyber Security Systems and Applied AI Research Center, Lebanese American University. His research interests are in the areas of wireless communications systems and networks, signal processing, optical wireless communications, wireless power transfer and applications, and communications and signal processing for biomedical engineering.

Dr. Karagiannidis has received three prestigious awards: The 2021 IEEE ComSoc RCC Technical Recognition Award, the 2018 IEEE ComSoc SPCE Technical Recognition Award, and the 2023 Humboldt Semior Research Award from Alexander von Humboldt Foundation. He was the past editor in several IEEE journals and from 2012 to 2015, he was the Editor-in-Chief of IEEE COMMUNICATIONS LETTERS. In January 2024, he is the Editor-in-Chief of IEEE TRANSACTIONS ON COMMUNICATIONS. He is one of the highly-cited authors across all areas of Electrical Engineering, recognized from Clarivate Analytics as a Highly-Cited Researcher from 2015 to 2023.

PINGZHI FAN (Life Fellow, IEEE) received the M.Sc. degree in computer science from Southwest Jiaotong University, China, in 1987, and the Ph.D. degree in electronic engineering from Hull University, U.K., in 1994. He is currently a Distinguished Professor with Southwest Jiaotong University (SWJTU) and the Honorary Dean of the SWJTU-Leeds Joint School. He has been a Visiting Professor with Leeds University, U.K., in 1997. He served as the Chief Scientist of a National 973 Plan Project (MoST, 2012.1-2016.12). He is a recipient of the U.K. ORS Award in 1992, the National Science Fund for Distinguished Young Scholars (NSFC) in 1998, the IEEE VT Society Jack Neubauer Memorial Award in 2018, the IEEE SP Society SPL Best Paper Award in 2018, the IEEE VT Society Best Magazine Paper Award in 2023, and several IEEE conference best paper awards. He also served as the General Chair or the TPC Chair of a number of IEEE conferences, including VTC2016Spring, ITW2018, IWSDA2022, and PIMRC'2023, as well as coming VTC2025Fall, ISIT'2026, and ICC'2028. His research interests include high mobility wireless communications, multiple access techniques, and signal design and coding. He is an IEEE VTS Distinguished Speaker from 2019 to 2025, and a Fellow of IET, CIE, and CIC.